THE DETECTION AND CHARACTERIZATION OF URBANIZATION, INDUSTRIALIZATION, AND LONGWALL MINING IMPACTS ON FOREST ECOSYSTEMS THROUGH THE USE OF GIS AND REMOTE SENSING TECHNIQUES

by

Erin Kathleen Pfeil-McCullough

Bachelor of Science in Biology, Youngstown State University, 2007

Bachelor of Arts in Anthropology, Youngstown State University, 2007

Master of Science in Biology, Youngtown State University, 2010

Submitted to the Graduate Faculty of the

Kenneth P. Dietrich School of Arts and Sciences in partial fulfillment

of the requirements for the degree of

Doctor of Philosophy

University of Pittsburgh

2017

UNIVERSITY OF PITTSBURGH

Kenneth P. Dietrich School of Arts and Sciences

This dissertation was presented

by

Erin K. Pfeil-McCullough

It was defended on

March 17th, 2017

and approved by

Emily Elliott, Associate Professor, Geology and Environmental Science

Michael Ramsey, Professor, Geology and Environmental Science

Josef Werne, Professor, Geology and Environmental Science

Brenden McNeil, Assistant Professor, West Virginia University,

Department of Geology and Geography

Committee Chair: Daniel J. Bain, Assistant Professor,

Geology and Environmental Science

THE DETECTION AND CHARACTERIZATION OF URBANIZATION, INDUSTRIALIZATION, AND LONGWALL MINING IMPACTS ON FOREST ECOSYSTEMS THROUGH THE USE OF GIS AND REMOTE SENSING TECHNIQUES

Erin K. Pfeil-McCullough, PhD

University of Pittsburgh, 2017

Urbanization has far reaching and significant effects on forest ecosystems, directly through urban development and indirectly through supportive processes such as coal mining and agriculture. Urban processes modify the landscape leading to altered hillslope hydrology, increased disturbance, and the introduction of non-native forest pathogens. This dissertation addresses several challenges in our ability to detect these urbanization impacts on forests via geospatial analyses.

The role of forests in urban hydrological processes has been extensively studied, but the impacts of urbanized hydrology on forests remain poorly examined. This dissertation documented impacts to hydrology and forests at variety of temporal and spatial scales: 1) A geospatial comparison of the historic and contemporary forests of Allegheny County, Pennsylvania revealed substantial shifts in tree species, but less change in the species soil moisture preference. These results document additional evidence that increased heterogeneity in urban soil moisture alters forest structure. 2) To examine soil moisture changes, impacts of longwall mine subsidence were assessed by using a Landsat based canopy moisture index and hot spot analysis tools at the forest patch scale. Declines in forest canopy moisture were detected over longwall mines as mining

progressed through time, and results contradicted assumptions that the hydrological impacts overlying LMS recover within 4-5 years following subsidence of undermined land. 3) Utilizing a landslide susceptibility model (SINMAP), increases in landslide susceptibility were predicted in Pittsburgh, PA based on several scenarios of ash tree loss to the emerald ash borer (EAB), a bark beetle that rapidly kills ash trees. This model provides a tool to predict changes in landslide susceptibility following tree loss, increasing the understanding of urban forest function and its role in slope stability. Detecting how urbanized hydrology impacts forest health, function, and development is fundamental to sustaining the services forests provide. Results from this dissertation will ultimately allow improvements in the management and protection of both trees and water resources in urban systems and beyond.

TABLE OF CONTENTS

LIST OF TABLES

LIST OF FIGURES

LIST OF EQUATIONS

PREFACE

Funding for this research was provided by Tree Pittsburgh, Tree Vitalize, Heinz Foundations, The Pennsylvania Department of Environmental Protection, and The Leighton Memorial Scholarship, and the University of Pittsburgh.

Several collaborators in Pittsburgh made this research possible, including Danielle Crumrine with Tree Pittsburgh, Jeffery Bergman with Treevitalize, and Erin Copeland with the Pittsburgh Parks Conservancy. I am grateful for their support, both in the form of collaboration and through providing me with the necessary data to complete my work. I would also like to thank Melanie Ordway and Gillian Capper for their hard work in assisting me to process data for Chapter 2.

I would also like to acknowledge all of those at the University of Pittsburgh who have provided me with so much support over the years. I am grateful for the friendship and support of the geograds. There were many days where I was not sure what I would have done without them. I would also like to thank the Bain and Elliott Lab groups for their feedback, friendship, and support, including Krissy Hopkins, Rob Rossi, Sarah Lavin, Angela Mullins, Becky Tisherman, Marja Copeland, Kassia Groszewski, Lucy Rose, and Marion Divers.

I would like to thank my Committee members for their guidance and thoughtful dissertation comments. I would like to especially thank my advisor Dan Bain for his support, patience, guidance, and for giving me the freedom to pursue the science questions and opportunities that most interested me. His faith and encouragement allowed me to develop into the person and scientist I have always endeavored to become.

I want to thank my family for their love and support over the years, particularly my parents for their high expectations, encouragement, and always believing in me. Thank you to my amazing siblings for your love and support, I am lucky to have you in my life, especially my twin sister Kate who would do anything for me without complaint. I also include Janine Krippner in this list, as she was a dear freind and much like a sister to me during my time at Pitt. Finally, I am gracious for my husband Brad and his constant support. Through good times and bad, my partner of 14 years has never doubted my intelligence, my abilities, or my resolve, even when doubt was all I had for myself.

1.0 INTRODUCTION

The contemporary forests of southwestern Pennsylvania are the product of centuries of human influence through urbanization and industrialization of the landscape. Urbanization has far-reaching and significant effects on forest ecosystems, directly through urban development and indirectly through agriculture and the energy extraction activities required to power cities (e.g. coal mining). These processes result in changes to the landscape that alter hillslope hydrology, introduce forest pathogens, modify soils, and increase disturbance (Vannatta et al. 2012; Pfeil-McCullough et al. 2015; Walsh et al. 2005; Jim 1997). The consequences of these impacts vary with location, altering forest structure, function, and health (McPherson et al. 1997). Understanding how human-dominated forests function and develop is key to sustaining the ecosystem services they provide. For example, in densely populated urban areas such as Pittsburgh, Pennsylvania, urban forests provide many important services, including shade, runoff reduction by intercepting rainfall/increasing evapotranspiration (ET), stabilization of hillslopes, and removal of air pollution. These services have high ecological and economical value, increasing the health and safety of the urban environment (McPherson et al. 1994; McPherson et al. 1997).

Urban soils are highly modified from their original properties, both physically and chemically. Soil properties also vary across urban environments, but generally are often structurally degraded, contaminated, and compacted (Pouyat et al. 2007). Additionally, impervious surfaces alter surface and ground water hydrology by limiting groundwater recharge

(Bartens et al. 2008). In these conditions, storm water does not infiltrate into the soil, but is instead redirected swiftly into sewers and streams (Walsh et al. 2005). These changes alter the natural drainage patterns of soil water within cities, leading to soils that are hospitable to different communities of trees and vegetation (Bartens et al. 2009). Despite the recognition of spatial heterogeneity, urban soils are poorly characterized and it is unclear how urban soils influence urban forests (Pickett and Cadenasso 2009).

Further, human influence on contemporary forest structure, function, and evolution is not well understood. The research findings reported in this dissertation provide a spatially explicit analysis of on forest impacts following urbanization, including changes in species composition, relative soil moisture, and slope stability. The questions addressed in this research seek to fill key gaps: 1) How does urbanization alter patterns of soil moisture and therefore vegetation?, 2) How do forest losses to exotic pests impact human coupled forest systems?, and 3) How does long wall mining alter soil moisture patterns and therefore forest ecosystems?

To explores how urban hydrology, management intensity, and forest life history intersect to influence urban forest evolution, chapter 2 uses historic witness tree data derived from European settlement-era surveys of Allegheny County, PA (Figure 1-1). Witness tree data have been used to reconstruct pre-settlement forests in parts of the eastern U.S. and the resulting studies have provided fundamental reconstructions of historic forest species composition and distribution (Black et al. 2002; Whitney 1984; Whitney 1986; Whitney and Adams 1980; Whitney and DeCant 2003; Hall et al. 2002). However, these studies generally do not focus on urban forests (i.e. human-dominated forest systems) and therefore the literature on the evolution of urban forests from the early forest is poorly documented. Chapter 2 also examines changes in urban soil moisture through shifts in species type via the soil moisture preferences of trees within a modern urban forest. This

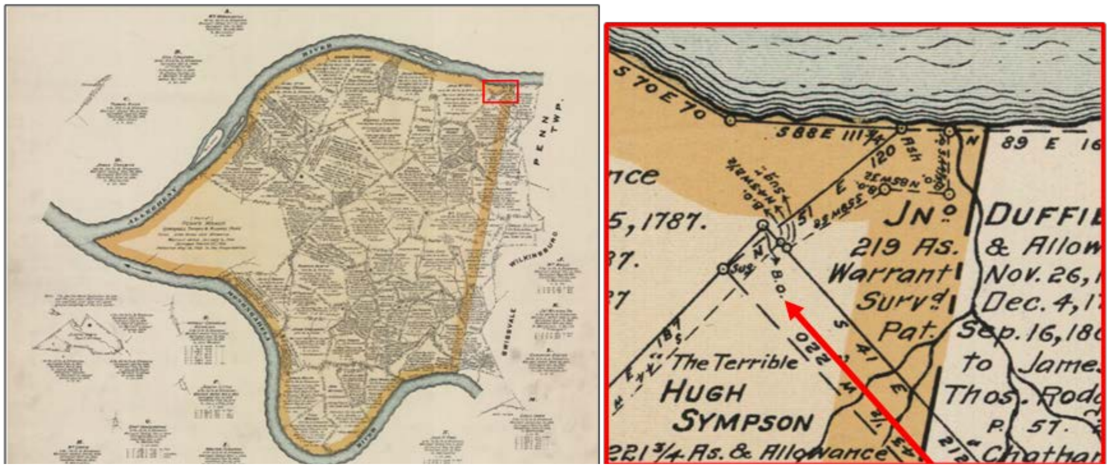

Figure 1-1: An example of historic survey maps used to record witness trees. The left image is a historic survey map of Pittsburgh, PA. The red box on the map is the location of the red bordered image on the right. Each circular vertex is a survey point, some of which indicate a tree. A black oak witness tree is identified with a red arrow.

analysis reveals shifts in tree species type within the urban datasets (i.e. soil moisture preference) assumed to arise from soil moisture preferences. importantly, this analysis revealed that proportion of upland species increased from historical forests in all the urban forest datasets we considered. This suggests landscape-scale changes in soil moisture patterns following European settlement.

Chapter 3 examines how urbanization can also drive local geomorphic processes. Southwestern Pennsylvania is an area prone to landslides due to underlying layers of shale and sandstone characteristic of the region (Pomeroy 1982). While vegetation is a primary control on slope stability (Nilaweera and Nutalaya 1999; Ekanayake and Phillips 2002), efforts to characterize patterns of urban slope stability following pathogen induced tree mortality are rare (Pfeil-McCullough et al. 2015). Loss of forests due to deforestation, construction projects, and introduced pests often leads to hillslope instability and failure in both rural and urban settings,

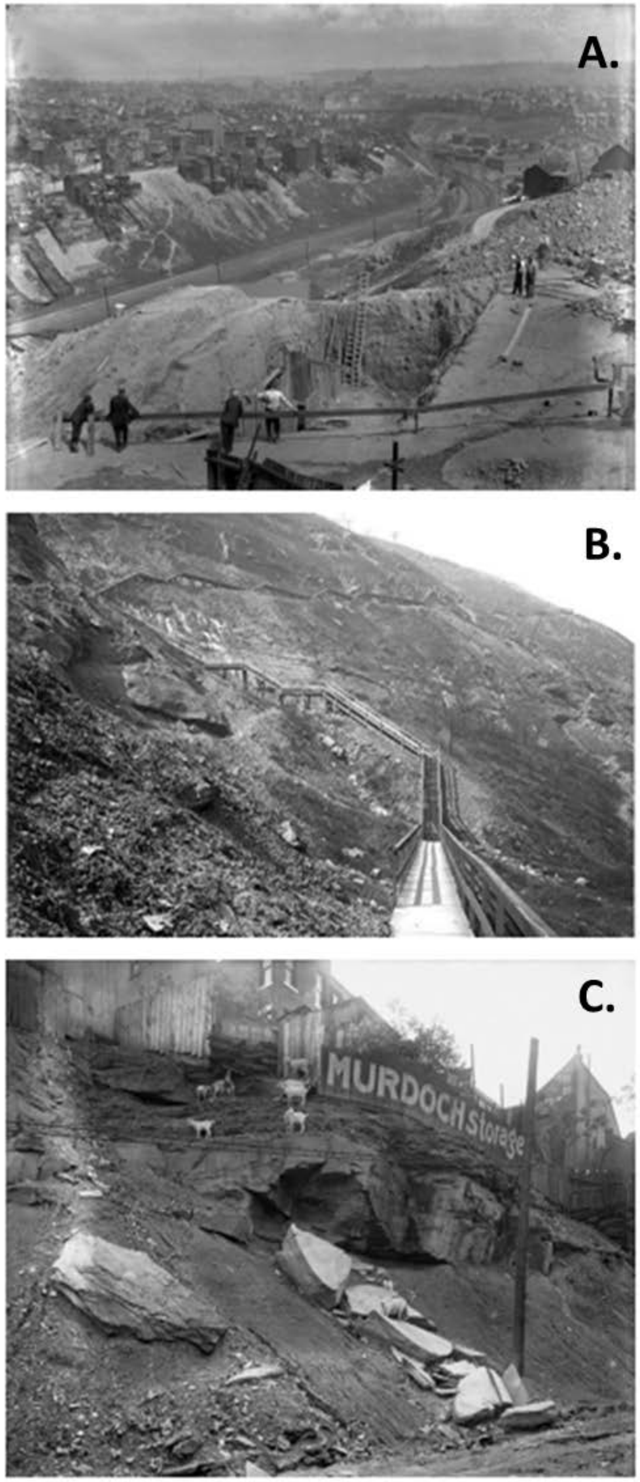

Figure 1-2: Historic photos of Pittsburgh, PA in the late 1800s, depicting erosion issues and hillslope instability due to a missing urban forest. A. View from the future site of the Bloomfield Bridge near the Bloomfield neighborhood. B and C. Mount Washington at two different locations.

costing Pennsylvania an estimated average of 10 million dollars a year in 1991 (Pomeroy 1982; DCNR 2009). The introduction of emerald ash borer (EAB) into eastern United States around 2002 has led to the loss of tens of millions of ash trees, including those within Pittsburgh's urban forest (Anulewicz et al. 2007). EAB tree mortality will likely decrease hillslope stability, as ash is an important canopy member of Pittsburgh's urban forest. Though Pittsburgh is now above the national average in canopy cover (~40% vs ~27%), historically Pittsburgh slopes were mostly bare, leading to erosion issues, rocks falls, and landslides (Figure 1-2) (Davey Resource Group 2012). Chapter 3 develops predictive models to evaluate how the loss of a major canopy member, white ash (Fraxinus spp.), impacts landslide susceptibility in Pittsburgh, PA (Pfeil-McCullough et al. 2015). This study predicted an increase in hillslope instability with increasing loss of ash, while also identifying key model parameters (soil density and soil cohesion) that strongly influence model output. This research advances knowledge of hillslope processes and urban forest function in a city with high topographic relief.

Chapter 4 explores urbanization impacts on forests that reach beyond the boundaries of a city and extend to other necessary components of the urban system such as energy production. Much of southwestern Pennsylvania, has been impacted by longwall mine subsidence (Figure 1-3) (Tonsor et al. 2013). During longwall mining, coal is removed in long panels after which the roof of the mine is collapsed into the void. This subsidence leads to damage in the overlying rock formations with impacts to surface hydrology and groundwater (Figure 1-3) (Tonsor et al. 2013). Though the more immediately detrimental surface impacts (e.g. drained streams, water bodies, and wells) are well characterized, less noticeable impacts to shallow groundwater and soil moisture are challenging to detect and poorly understood. Through detecting changes in tree canopy moisture

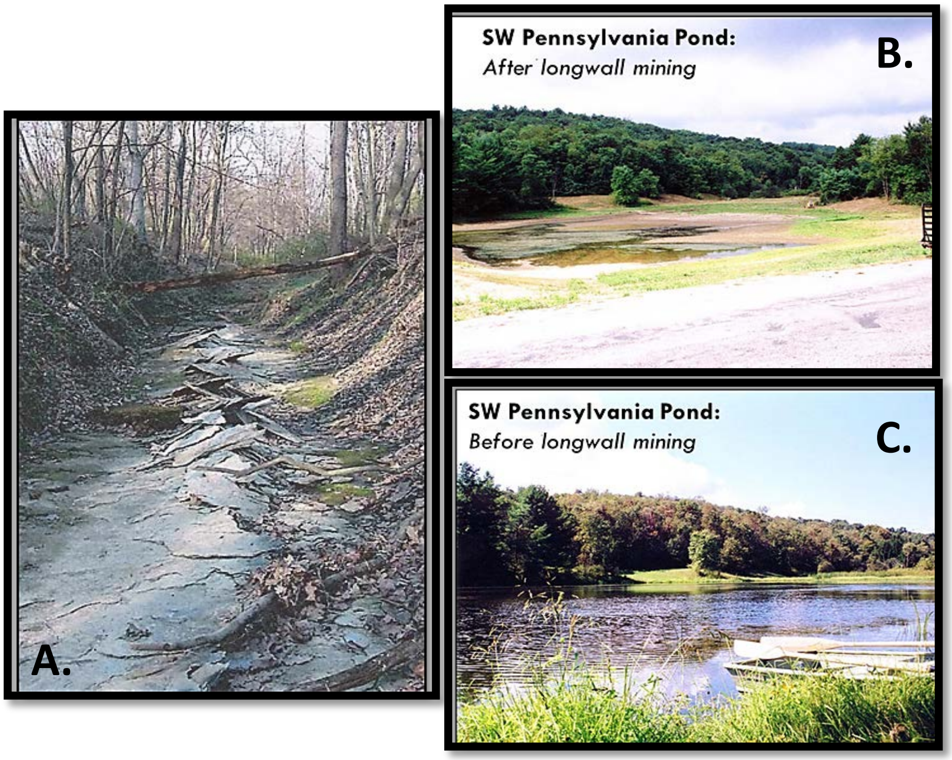

Figure 1-3: ***(A.)*** **A fractured stream bed above a longwall mine in southwestern Pennsylvania. (*B and C)* A pond in Green County, PA drained following longwall mine subsidence. (photo credit: Citizens Coal Council).**

content over time using multispectral satellite imagery, this chapter describes previously undocumented impacts of longwall coal mining to overlying tree canopy health.

Despite the potential costs and dangers of an unhealthy urban forest (e.g. landslides, increased storm runoff, high energy bills, poor air quality), human impacts on forests are not entirely understood (Dwyer, Nowak, and Noble 2003; Qi and Zhang 2010; Vannatta, Hauer, and Schuettpelz 2012). Knowledge gaps exist in how forests have developed following European settlement, specifically to original hydrology and disturbance regimes that influence forest community dynamics (Figure 1-2). These gaps limit forest protection and management efforts, as hydrology is a key factor driving forest structure, species composition, and health (Grant et al. 2013). This dissertation characterizes contemporary forests, and further ties these changes to specific human impacts on forest ecosystems at the landscape scale.

1.1 BIBLIOGRAPHY

Anulewicz, A.C., McCullough, D.G. and Cappaert, D.L. 2007. Emerald Ash Borer (Agrilus planipennis) Density and Canopy Dieback in Three North American Ash Species. Arboriculture & Urban Forestry 33(5), pp. 338–349.

Bartens, J., Day, S.D., Harris, J.R., Dove, J.E. and Wynn, T.M. 2008. Can urban tree roots improve infiltration through compacted subsoils for stormwater management? Journal of Environmental Quality 37(6), pp. 2048–2057.

Bartens, J., Day, S.D., Harris, J.R., Wynn, T.M. and Dove, J.E. 2009. Transpiration and root development of urban trees in structural soil stormwater reservoirs. Environmental Management 44(4), pp. 646–657.

Black, B.A., Foster, H.T. and Abrams, M.D. 2002. Combining environmentally dependent and independent analyses of witness tree data in east-central Alabama. Canadian Journal of Forest Research 32(11), pp. 2060–2075.

DCNR, P. 2009. Effects and Costs of Landslides [Online].

Ekanayake, J.C. and Phillips, C.J. 2002. Slope stability thresholds for vegetated hillslopes: a composite model. Canadian Geotechnical Journal 39(4), pp. 849–862.

Grant, G.E., Tague, C.L. and Allen, C.D. 2013. Watering the forest for the trees: an emerging priority for managing water in forest landscapes. Frontiers in Ecology and the Environment 11(6), pp. 314–321.

Hall, B., Motzkin, G., Foster, D.R., Syfert, M. and Burk, J. 2002. Three hundred years of forest and land-use change in Massachusetts, USA. Journal of Biogeography 29(10-11), pp. 1319–1335.

Jim, C.Y. 1997. Urban soil characteristics and limitations for landscape planting in Hong Kong. Landscape and Urban Planning 40, pp. 235–249.

McPherson, E.G., Grimmond, S. and Souch, C. 1997. Quantifying urban forest structure , function , and value : the Chicago Urban Forest Climate Project. Urban Ecosystems 1, pp. 49–61.

McPherson, E.G., Nowak, D.J., Rowntree, R.A., Gregory, E., David, J. and Rowan, A. 1994. Chicago ' s Urban Forest Ecosystem : Results of the Chicago Urban Forest Climate Project. U.S.D.A, Forest Service, Northeastern Forest Experiment Station, p. 102.

Nilaweera, N.S. and Nutalaya, P. 1999. Role of tree roots in slope stabilisation. Bulletin of Engineering Geology and the Environment 57(4), pp. 337–342.

Pfeil-McCullough, E., Bain, D.J., Bergman, J. and Crumrine, D. 2015. Emerald ash borer and the urban forest: Changes in landslide potential due to canopy loss scenarios in the City of Pittsburgh, PA. The Science of the Total Environment 536, pp. 538–545.

Pomeroy, J.S. 1982. Landslides in the Greater Pittsburgh Region, Pennsylvania.

Pouyat, R.V., Yesilonis, I.D., Russell-Anelli, J. and Neerchal, N.K. 2007. Soil Chemical and Physical Properties That Differentiate Urban Land-Use and Cover Types. Soil Science Society of America Journal 71(3), p. 1010.

Tonsor, S.J., Hale, A.N., Iannacchione, A., Bain, D.J., Keener, M., Pfeil-McCullough, E. and Garmire, K. 2013. The Effects of Subsidence Resulting from Underground Bituminous Coal Mining. pp. 2008–2013. Available at: http://www.dep.pa.gov/PublicParticipation/CitizensAdvisoryCouncil/Issue-Areas/Pages/Act54.aspx#.V0iAKPkrK70.

Vannatta, A.R., Hauer, R.H. and Schuettpelz, N.M. 2012. Economic Analysis of Emerald Ash Borer (Coleoptera : Buprestidae) Management Options. Journal of Economic Entomology 105(1), pp. 196–206.

Walsh, C.J., Roy, A.H., Feminella, J.W., Cottingham, P.D., Groffman, P.M. and Morgan, R.P. 2005. The urban stream syndrome: current knowledge and the search for a cure. Journal of the North American Benthological Society 24(3), pp. 706–723.

Whitney, G.G. 1984. Fifty Years of Change in the Arboreal Vegetation of Heart's Content , An Old-Growth Hemlock-White Pine-Northern Hardwood Stand . Ecology 65(2), pp. 403–408.

Whitney, G.G. 1986. Relation of Michigan's Presettlement Pine Forests to Substrate and Disturbance History: Published by : Ecological Society of America Stable URL : http://www.jstor.org/stable/1939085 . RELATION OF MICH. Ecology 67(6), pp. 1548–1559.

Whitney, G.G. and Adams, S.D. 1980. Man as Maker of New Plant Communities. Journal of Applied Ecology 17(2), pp. 431–448.

Whitney, G.G. and DeCant, J.P. 2003. Physical and historical determinants of the pre- and post-settlement forests of northwestern Pennsylvania. Canadian Journal of Forest Research 33(9), pp. 1683–1697.

2.0 HISTORIC FOREST TO URABAN SAVANNA: THE EVOLUTION OF CONTEMPORARY FORESTS IN PITTSBURGH, PA

2.1 INTRODUCTION

Since European settlement, the forests of Allegheny County, Pennsylvania have been heavily disturbed by human activities (e.g. timber harvesting, charcoaling, agriculture, and steel production), particularly in the City of Pittsburgh (Buck 1936; Smith and Vankat 1991; Tarr 2004). These activities have transformed the landscape, directly altering forest structure and function as well as ground and surface water flow paths that influence forest communities. Despite the dramatic changes that have taken place in southwestern Pennsylvania and Allegheny County in particular, the evolution of the region's urban and human-dominated forest systems are not well characterized. To best manage and protect forests that are coupled to human systems, it is important to understand how forests change, as elucidation of these changes reveals the influence of human activity on modern urban forest composition.

Witness trees were trees recorded in original land surveys and maps as surveying monuments, thus original surveys provide species composition data for the early to mid-18th century forest (Foster et al. 2004). For example, this method was employed to determine composition and disturbance histories of Michigan's pine forests (Whitney 1984; Whitney 1986; Whitney and Adams 1980). Here we utilize witness trees in a similar manner, to understand the evolution of contemporary forests within Allegheny County, PA.

The original survey maps (Houck 1914) are used as historical assessments of forest composition and as a baseline for evaluating modern soil moisture and forest composition.

Specifically, the relationships between soil characteristics and physiography are compared to clarify the influence of both non-human (e.g., soil and topography) and human processes. Ultimately, the distribution of trees is fundamental to built infrastructure, particularly in southwestern Pennsylvania where trees provide many services, including stability to urban hillslopes, reduction of runoff, and shade (Ekanayake and Phillips 2002; Nilaweera and Nutalaya 1999; Pomeroy 1982). This research characterizes historic forest conditions at the time of European settlement and identifies human influences on urban forest species composition and structure. Additionally, this study serves as a demonstration for how contemporary urban forests may be assessed using historic survey data.

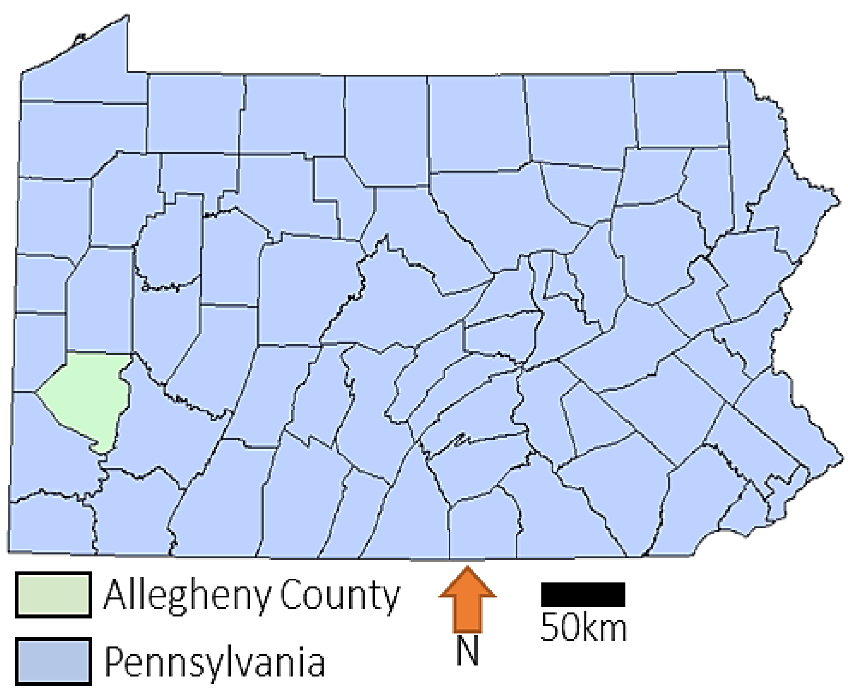

Figure 2-1: The state of Pennsylvania and location of Allegheny, County.

2.2 METHODS

2.2.1 Study Site

Allegheny County is located in southwestern Pennsylvania and its current borders were established by 1800 (Figure 2-1). Row crop agriculture (e.g., corn and wheat) was key to the economy and growth of the region during the 18th and beginning of the 19th century, before the region transformed into an energy and steel production economy (Tarr 2004). The economic growth of Allegheny County led to extensive deforestation and modification of the landscape through agricultural clearance, mining and development. Allegheny County is within the Appalachian Plateau, a region characterized by high topographic relief and deeply incised sedimentary rock.

2.2.2 Tree Data

Digital original historic survey maps of the townships of Allegheny County (Houck 1914) were georectified in ArcGIS using matching landmarks on modern township maps (e.g. roads, borders) (Anon. 2017). Once georectified, witness trees recorded on the historic maps were digitized into a point shape file, with the following attributes: species/genus, year surveyed and recorded, and surveyor name if given. Multiple trees could be represented by a single data point and data points could also represent stumps, posts, or stones instead of trees, in the same location (Figure 2-2 & Figure 2-3c). All data not representing trees was removed from the dataset. This resulted in a dataset of 8403 points, containing 9766 trees representing 36 species (Table 2-3).

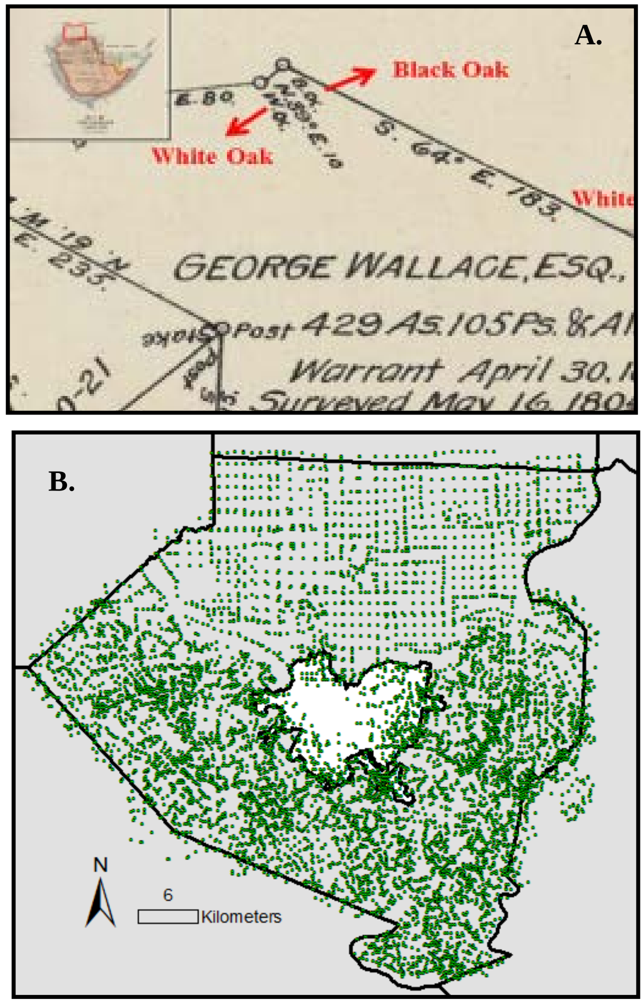

Figure 2-2: A) Original survey map (http://images.library.pitt.edu/w/warrarntee) containing tree species data that can be used to reconstruct settlement forests for Allegheny County. B) 8403 Survey points digitized from original survey maps for Allegheny County. Pittsburgh is shown in the center. The differences in surveying seen between the northern and southern parts of the county are simply due to differences in surveying methods, as the northern part of the county was surveyed by the government.

In the historic dataset twenty-five percent of trees were only identified down to the genus level, creating uncertainty in the environmental conditions preferred by those individual trees. To avoid removing 25% of the historic tree data from the analysis, assumptions were made to assign species-level designations to the genus-only tree identifications (Table 2-1). Individual tree species within a genus can vary in environmental requirements (e.g. soil moisture, sunlight, temperature), therefore when only a genus is specified and not a genus *and* a species, comparisons among datasets becomes difficult. Thus, we assumed the number of species within a genus based on the number of trees actually identified down to the species level. Specifically, the most common species was selected to represent the unidentified trees with a species. For example, trees only identified as oak were assumed to be white oak (Quercus *alba* L.), the most common species of oak.

For genera that were more evenly divided in species number, trees were assigned based on the proportion of each species with in a genus. Ash was the only genus in the dataset that required species assignment based on proportions. The trees that were only identified to ash were proportionally assigned as either black ash (Fraxinus *nigra* Marshall) or white ash (Fraxinus *americana* L.) by multiplying the number of ash trees identified to the genus-level by the proportion of ash trees identified as white ash and black ash respectively. The assumptions made are listed in Table 2-1 and this bias was considered carefully during the analyses.

No assumptions were made for two typically understory species, dogwood and hawthorn, as no species were recorded for either genus in the dataset. However, the most probable species choices for both did not vary greatly in growing requirements and thus species assumptions are likely unnecessary (Table 2-1).

Table 2-1: Trees identified only to the genus level of classification by historic surveyors with the species assumption given as a common name.

Genus	Common Name	USFS Code	Species Assumption	Count	%
Carya	Hickory	CARYA	bitternut hickory	1271	51.4
Cornus	Dogwood	CORNU	*no assumption*	224	9.1
Jugla	Walnut	JUGLA	black walnut	212	8.6
Fraxinus	Ash	FRAI	white or black ash	212	8.6
Ulmus	Elm	ULMUS	american elm	132	5.3
Castanea	Chestnut	CASTA	american chestnut	124	5.0
Acer	Maple	ACER	sugar maple	108	4.4
Pinus	Pine	PINUS	white pine	84	3.4
Prunus	Cherry	PRUNU	black cherry	48	1.9
Crataegus	Hawthorn	CRATA	*no assumption*	24	1.0
Quercus	Oak	QU	white oak	15	0.6
Betula	Birch	BETUL	yellow birch	13	0.5
Salix	Willow	SALIX	black willow	7	0.3
		TOTAL=		***2474***	***100%***

Urban forest data from Pittsburgh, PA was used for contemporary urban forest comparison (Figure 2-3). Three forest datasets were used to represent urban forests: iTree, Natural Areas Study (NAS), and Davey Street Trees (Davey Resource Group 2012; Davey Resource Group 2015, Biohabitats Inc. 2010) (Figure 2-3b-2-3d). These datasets represent three different urban forest structures: street trees, urban woodlands, and parks (Konijnendijk et al. 2013; Welch 1994). These different urban forest types experience different stressors, environments, and management practices, making it necessary to compare each separately to the historic dataset (Konijnendijk et al. 2013; Welch 1994). We define urban woodlands as patches of forests within a city that are not planted for the purpose of lining streets and they instead grow in a natural forest structure (Welch 1994). The iTree dataset is made up of 136 randomly generated sampling points based on 1/10 acre plots, representing 1435 trees and 74 species. The Pittsburgh urban woodland polygon was compared against a high-resolution base map after which a 60m buffer was applied to the woodland polygon to account for wooded areas not included within the shape file. Seventy-five of the iTree randomly generated sampling plots are located at least within 60m from the edge of

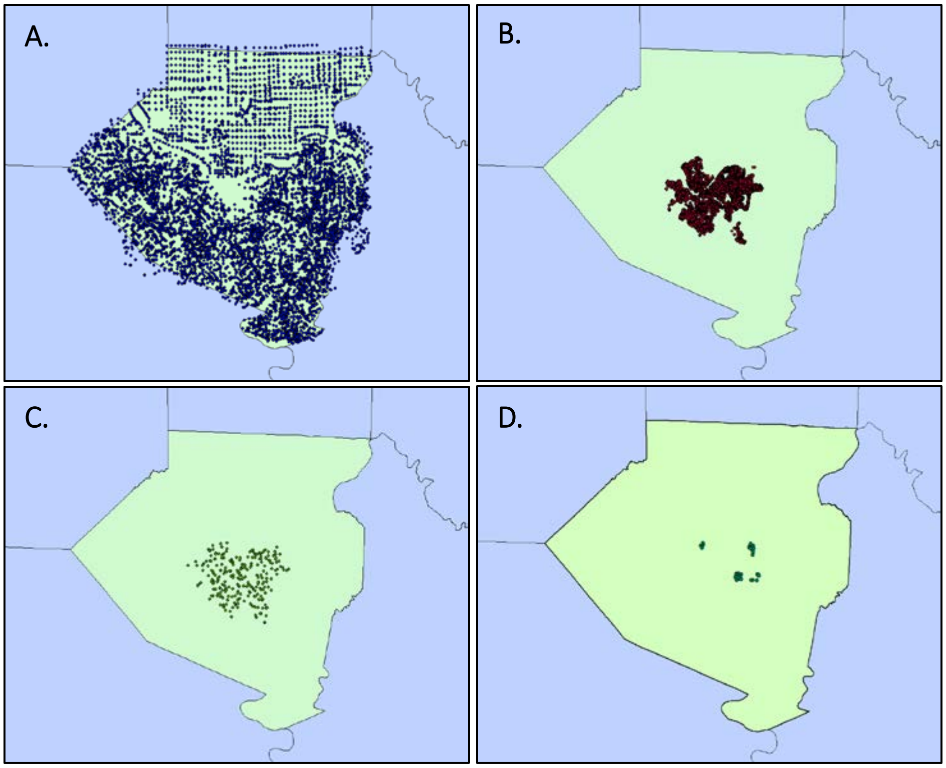

Figure 2-3: A. Historic trees B. Davey street trees C. iTree D. Natural Areas Study (NAS). The historic tree dataset was created using two different types of surveying, with a more regular method applied in the northern part of the county. The Davey tree dataset (B.) represents trees roadside in the City of Pittsburgh. The iTree and NAS dataset represent plots in which trees were recorded in urban woodland and park areas respectively.

mapped urban woodland (PASDA 2017). The 75 plots located in urban woodlands represent 77% (n=1104) of the iTree dataset and 61 species.

The Davey Street tree dataset is a collection of trees recorded roadside within the city limits of Pittsburgh. The dataset is made up of 29,144 points representing approximately 144 tree species, each point representing a single tree identified down to species-level.

2.2.3 Landscape Analysis

Landscape data representing elevation and slope derived from a 3 meter Lidar digital elevation model (DEM) were extracted to each tree point in ArcGIS (PAMAP Program 2006). Other landscape properties (e.g. aspect, concavity) were extracted and analyzed, but only analysis generated from elevation and slope data were utilized in further analysis. These site characteristics describing the position of each tree on the landscape were then compared across the 4 tree population datasets. Further, to understand landscape characteristics that drive soil moisture patterns and influence forest species composition, hillslope position was also calculated from the DEM (PAMAP Program 2006) using a topographic position index developed by (Jones et al. 2000) (Equation 2-1) . An averaged DEM was created using a round annulus neighborhood, with a 9-pixel inner diameter and a 27-pixel outer diameter. The resulting raster was used to calculate the topographic position index (TPI) (Equation 2-1). Positive TPI values indicate areas higher than surrounding areas, while negative TPI values indicate areas lower than surrounding areas. Values near zero are considered flat. The index was further classified into 6 hillslope position categories using the standard deviation of the TPI raster and slope to define the category cutoffs (Table 2-2).

Equation 2-1: Equation used to calculate the topographic position index for the study region. A 3 meter DEM was used to populate the equation, which was applied to the DEM using a moving window to calculate the focal mean in the shape of an annulus. The inner diameter of the annulus was 9 pixels, and the outer diameter was 27 pixels.

$$TPI = \left(DEM - focalmean\left(DEM,\ annulus, 9_{pixels\ inner\ diameter}, 27_{pixels\ outer\ diameter}\right)\right) + \ .5)$$

Table 2-2: Breakpoint descriptions of TPI categories.

Category	Breakpoint
1 (*Ridge*)	*TPI* > +1 standard deviation
2 (*Upper slope*)	0.5 standard deviation < *TPI* <= 1 standard deviation
3 (*Middle slope*)	-0.5 standard deviation < *TPI* < 0.5 standard deviation & slope > 5◦
4 (*Flat slope*)	-0.5 standard deviation =< *TPI* =< 0.5 standard deviation, slope <= 5◦
5 (*Lower slope*)	-1.0 standard deviation =< *TPI* < 0.5 standard deviation
6 (*Valley*)	*TPI* < -1 Standard Deviation

2.2.4 Surveyor Bias and Uncertainty

There are multiple sources of bias within each dataset, including surveyor bias, data collection methods, and data purpose (e.g. study, inventory, or boundary marking). Witness trees were not recorded for the purpose of collecting tree data, therefore there are many potential sources of bias as a result. In the historic trees dataset, property lines were drawn based on surveyor and property owner choices. This introduces potential bias in witness tree datasets. Surveyors also likely based their choice of witness trees on economic value, ease of inscription, size, health, longevity, and/or abundance (Black and Abrams 2001; Whitney 1986). Determining individual surveyor influence on historic tree identification over the historic tree dataset was assessed by finding the average number of trees identified by each surveyor. Next surveyors within the top 5% (n=64) of surveyors (those recording more than 20 trees), were assessed by their identification of the top three tree species (white oak, black oak, and bitternut hickory) for the historic dataset. Only the most active surveyors were examined for bias as it was not conceivable to assess the entire dataset due to the sample size that results for the vast majority of surveyors. Bias was assessed by comparing expected versus actual identification rates of the top three tree species. The number of trees without a surveyor name recorded were also identified (n=281).

Though the contemporary data was collected for the purpose of documenting trees, bias is still present due to data collection methods and sampling design. Bias within the iTree dataset is largely based on site accessibility. Randomly generated points occurring within city owned property (e.g. urban woodlands, city parks) were more likely to be chosen for data collection. Survey plots also had to be accessible by foot, meaning plots could not be located on dangerous slopes. The Davey Streets trees will contain bias due to being located exclusively roadside. Most roads within Pittsburgh are located on shallower slopes. For all three datasets, error may occur in tree identification. The sources of bias within each dataset were considered during data analysis and are discussed below.

2.2.5 Wetland Indicator Status

All three datasets differ widely in species composition, particularly between historic and contemporary data sets, making shifts in forest structure and composition difficult to detect over time. Therefore, wetland indicator status (WIS) was used to compare shifts in hydrological conditions at similar landscape positions across all three datasets. Soil moisture conditions differ based on landscape position. Generally, positions higher in the landscape (e.g. ridges and hilltops) tend to be drier than areas lower in the landscape (e.g. valleys and toe slopes). The difference in moisture accumulation influences species composition. In addition, the geohydrology of the Appalachian plateau can lead to relatively wet hillslopes in Allegheny County due to the discharge of perched aquifers as springs at high hillslope positions (Sheets and Kozar 2000). Further, urbanization and human modification of the landscape change soil moisture regimes, and therefore the tree species that grow in an area. For example, increased compaction and impervious cover can dry soils, whereas leaking infrastructure (e.g. sewer and water lines) and roadways can increase wetness in other areas (Pfeil-McCullough et al. 2015). WIS categories range from obligate wetland species occurring only within a wetland (OBL) to species that occur on uplands only (UPL) (Table 2-2). WIS for each species was acquired using the USDA PLANTS database (https://plants.usda.gov). All tree species, whether native or introduced/exotic, that were assigned a wetland indicator status in the PLANTS database were assigned the corresponding WIS category. Trees that are native to the region but lacked a WIS in the PLANTS database were categorized as "none" (Table 2-2). Non-native trees species lacking a WIS were labeled as "EXO". The WIS

Table 2-3: Wetland indicator state and description

#	Wetland indicator status	% Occurrence in wetlands	Description
1	OBL (obligate wetland)	99	Almost always occurs in wetlands
2	FACW (facultative wetland)	67-99	Usually occurs in wetlands, but may occur in non-wetlands.
3	FAC (facultative)	34-66	Occurs in wetlands and non-wetlands.
4	FACU (facultative upland)	1-33	Usually occurs in non-wetlands but may occur in wetlands
5	UPL (obligate upland)	1	Almost always occurs in uplands.
6	None (no WIS indicated)	N/A	Native species lacking a WIS in the PLANTS database.
7	EXO (exotic)	N/A	Introduced species lacking a WIS in the PLANTS database.

categories are being applied in this study to infer changes between settlement-era forest and modern urban forests.

2.3 RESULTS AND DISCUSSION

2.3.1 Scale Differences Between Historic and Urban Datasets

Comparison of the contemporary and historic datasets is limited by the contrasting sampled spatial extents of the data sets. The historic dataset was collected countywide (though there are few witness trees recorded inside city limits), whereas all three contemporary datasets are confined to the city boundaries of Pittsburgh. Despite the difference in analysis footprint, the Allegheny County landscape is relatively consistent across the county. The entire county is within the unglaciated portion of the Allegheny plateau ecoregion, of the Appalachian Plateau physiographic province (Bailey 2004). Further, the historic trees dataset has a much lower sampling density compared to the contemporary datasets, as the 9,766 tree points used in the analysis are spread out

Table 2-4: Species list for each tree point dataset with the count for each species (#) Species are listed by common name

A. NAS		B. iTree		C. Street Trees				D. Historic	
#	Species	#	Species (common name)	#	Species	#	Species (cont.)	#	Species
4	American beech	9	American basswood	135	American Basswood	2	Mugo Pine	42	American Basswood
1	American chestnut	118	American elm	4	American Beech	57	Northern Catalpa	152	American Beech
27	American Elm	2	American sycamore	1	American Chestnut	4792	Norway Maple	124	American Chestnut
1	American sycamore	10	Apple	320	American Elm	143	Norway Spruce	132	American Elm
44	Black cherry	1	Baldcypress	5	American Holly	9	Ohio Buckeye	182	American Hornbeam
22	Black locust	1	Balsam fir	38	American Hornbeam	2	Overcup Oak	75	American Sycamore
1	Black oak	19	Bitternut hickory	2	American Mountain Ash	1	Paper Bark Maple	1	Apple
1	Black walnut	154	Black cherry	13	American Plum	15	Paper Birch	13	Birch
2	Box elder	187	Black locust	137	American Sycamore	2	Paw Paw	1325	Bitternut Hickory
1	Callery pear	3	Black maple	143	Amur Maple	5	Peach	181	Black Ash
5	Common linden	12	Black walnut	167	Arborvitea	1	Pignut Hickory	48	Black Cherry
1	Gingko	16	Blue spruce	2	Asian White Birch	1	Pin Cherry	1125	Black Oak
3	Green ash	71	Boxelder	7	Atlantic White Cedar	1029	Pin Oak	220	Black Walnut
16	Hawthorn	6	Butternut	23	Austrian Pine	6	Port Ortford Cedar	7	Black Willow
1	Honey locust	1	Callery pear	107	Autumn Blaze Maple	5	Pussy Willow	92	Blackgum
6	hophornbeam	4	Chinese elm	5	Bald Cypress	2	Quaking Aspen	11	Blackjack Oak
4	Northern pin oak	10	Common chokecherry	3	Balsam Fir	3412	Red Maple	33	Chestnut Oak
83	Norway maple	1	Common pear	1	Bigleaf Magnolia	5	Red Mulberry	224	Dogwood
3	Pignut hickory	1	Corkscrew willow	7	Bitternut Hickory	770	Red Oak	12	Eastern Cottonwood
8	Pin oak	10	Crabapple	14	Black Ash	6	Red Pine	2	Eastern Red Cedar
1	Princess tree	15	Eastern hemlock	104	Black Cherry	12	Red Spruce	2	Eastern Redbud
1	Red bud	3	Eastern hophornbeam	1	Black Gum	22	River Birch	24	Hawthorn
3	Red maple	13	Eastern white pine	491	Black Locust	1	Rock Elm	81	Honey Locust
23	Red oak	3	Elm	66	Black Oak	2	Sawtooth Oak	7	Mulberry Sp.
1	Sassafras	11	European bird cherry	10	Black Walnut	28	Scarlet Oak	1	Peach*
1	Silver maple	3	Flowering dogwood	406	Blue Spruce	13	Scots Pine	152	Red Oak
4	Spicebush	4	Ginkgo	3340	Callery Pear	111	Siberian Elm	6	Red Spruce
46	Sugar maple	1	Gray birch	2	Carolina Silverbell	3	Silver Linden	16	Scarlet Oak
1	Sweet gum	19	Hawthorn	2	Cherry Plum	960	Silver Maple	3	Serviceberry
31	Tree of heaven	1	Hedge maple	30	Cherry Sp.	2	Slippery Elm	1	Staghorn Sumac
1	walking stick	8	Honeylocust	7	Chinese Elm	2	Southern Magnolia	562	Sugar Maple
71	White ash	1	Horsechestnut	8	Chinese Magnolia	3	Star Magnolia*	273	Swamp White Oak
10	White oak	2	Japanese maple	1	Common Buckthorn	1	Stripped Maple	7	Which Hazel
1	Willow oak	4	Japanese zelkova	24	Common Hackberry	1090	Sugar Maple	41	White Ash
5	Witch hazel	1	Kwanzan cherry	7	Common Lilac	5	Swamp White Oak	4530	White Oak
5	Yellow buckeye	6	Littleleaf linden	16	Common Pear	1	Sweet Cherry	85	White Pine
		1	Mimosa	1	Cornelian Cherry	873	Sweetgum		
		2	Northern catalpa	8	Cucumber Magnolia	13	Sycamore Maple		
		33	Northern hackberry	4	Dawn Redwood	1	Tamarack		
		20	Northern red oak	1	Eastern Cottonwood	81	Tartarian Maple		
		20	Northern white cedar	143	Eastern Hemlock	13	Trident Maple		
		174	Norway maple	19	Eastern Red Cedar	1	Virginia Pine		
		12	Norway spruce	23	Eastern Redbud	1	Washington Hawthorn		
		1	Ohio buckeye	72	Eastern White Pine	2	Weeping Willow		
		7	Pignut hickory	1	Englemann Spruce	4	Western Redcedar*		
		4	Pin cherry	1	English Oak	137	White Ash		
		4	Pin oak	1	European alder	72	White Mulberry		
		24	Plum	2	European Beech	5	White Oak		
		23	Red maple	5	European Hornbeam	12	White Spruce		
		22	Red mulberry	4	European mountain ash	2	Willow Oak		
		1	Red pine	2	European Smoketree	3	Winged Elm		
		1	River birch	12	European White Birch				
		4	Royal paulownia	61	Flowering Dogwood				
		7	Sassafras	272	Green Ash				
		2	Scotch pine	2	Grey Dogwood				
		11	Siberian elm	266	Hedge Maple				
		2	Silver linden	1417	Honey Locust				
		12	Silver maple	7	Hop Hornbeam				
		46	Sugar maple	33	Japanese Cherry				
		3	Swamp white oak	2	Japanese Hill Cherry				
		15	Sweet cherry	33	Japanese Lilac				
		2	Sweetgum	60	Japanese Maple				
		8	Sycamore maple	14	Japanese Pagoda				
		77	Tree of heaven	221	Japanese Zelkova				
		3	Tulip tree	6	Kentucky Coffee Tree				
		1	Washington hawthorn	1	Kentucky Yellowwood				
		132	White ash	11	Kousa Dogwood				
		27	White mulberry	3194	Linden				
		1	White oak	1	Lombardy Poplar				
		1	Winged elm	2656	London Plane				
		1	Yellow birch	1	Mockernut Hickory				

over the entire county whereas the Pittsburgh points are confined to a much smaller area (1930 Km^2 vs 150 Km^2).

As a result, the modern data likely reflects physiography within the city of Pittsburgh more strongly, such as a close proximity to the large rivers. However, given the consistency in the local landscape, it is a reasonable assumption that the natural process and forests located within city boundaries did not vary significantly from the rest of the county and the historical conditions recorded in the county were representative of pre-European conditions in the city.

2.3.2 Uncertainty and Bias in the Historic Trees Dataset

The identification of historic trees as witness tree markers in Allegheny County was carried out by 1,296 individual surveyors (or surveying pairs). Of the 1,296 surveyors, 1,219 (95%) recorded 20 trees or less, with 8 as the median number of trees identified per surveyor. The maximum number of trees recorded by a single person was 84, with only one other surveyor coming close with 77. Two-hundred and eighty-one of the identified historic trees were not credited to any surveyors. Considering most tree identification was divided among 1,219 people, it is unlikely that a single surveyor had a strong influence on the composition of the dataset.

To assess bias within the historic trees dataset, the top 5% of surveyors (those recording more than 20 trees) were evaluated by comparing identification rates for the top three species: white oak (n=4,530), bitternut hickory (n=1,298), and black oak (n=1,125) *(numbers are the total of each species in the entire dataset)* (Table 2-4). The expected identification rate is the proportion of each species within the entire dataset (e.g. # of white oak / # of trees in dataset). The expected rates were compared to the identification rates of each species within the top 5% of surveyors (e.g. # of white oaks $_{\text{top 5\%}}$ / # of all trees $_{\text{top 5\%}}$). White oak ID rates varied the most with an expected rate of 46% and an actual rate of 49% for the top surveyors. Black oak and bitternut hickory had expected rates of 13% and 12% respectively compared to a 14% actual rate for both species. Though there are slightly higher rates of identification in the top 5% of surveyors, overall the differences are minor and likely do not impact the interpretation of results. Even though there does not appear to be strong individual bias when considering the top 5% of surveyors, it is harder to estimate the bias of the entire group of surveyors. It is likely there were some biases common to the entire group of surveyors, likely reflecting the culture of the historical period in which the surveys took place (1700-1800s). It is not possible to know the individual priorities or circumstances of each surveyor or each surveying project, therefore this possibility cannot be ruled out and must be considered when evaluating the results.

2.3.3 Changes to Species Composition and WIS Groups

The species composition of forests in Allegheny County has changed dramatically since European settlement of the region. All three contemporary datasets contained more non-native species (exotic to the study region) than the historic dataset, which only has one exotic tree species (2.8% of the population) (Figure 2-4, Table 2-4). In contrast, the iTree data set had 31% and the Davey street tree dataset had 41% non-native species (Figure 2-4). However, each component of the urban forest (e.g. street trees, park forests, and urban woodlands) develops and is managed differently and must be considered separately when making comparisons to historic forests.

Tree species that can tolerate a broad range of light and soil moisture conditions are typically chosen for street tree plantings. This choice has led to more urban tolerant non-native selections for street trees in the urban environment as opposed to native tree species (Bassuk et al. 2009; Welch 1994). Though approximately 137 species make up Pittsburgh street trees, eight

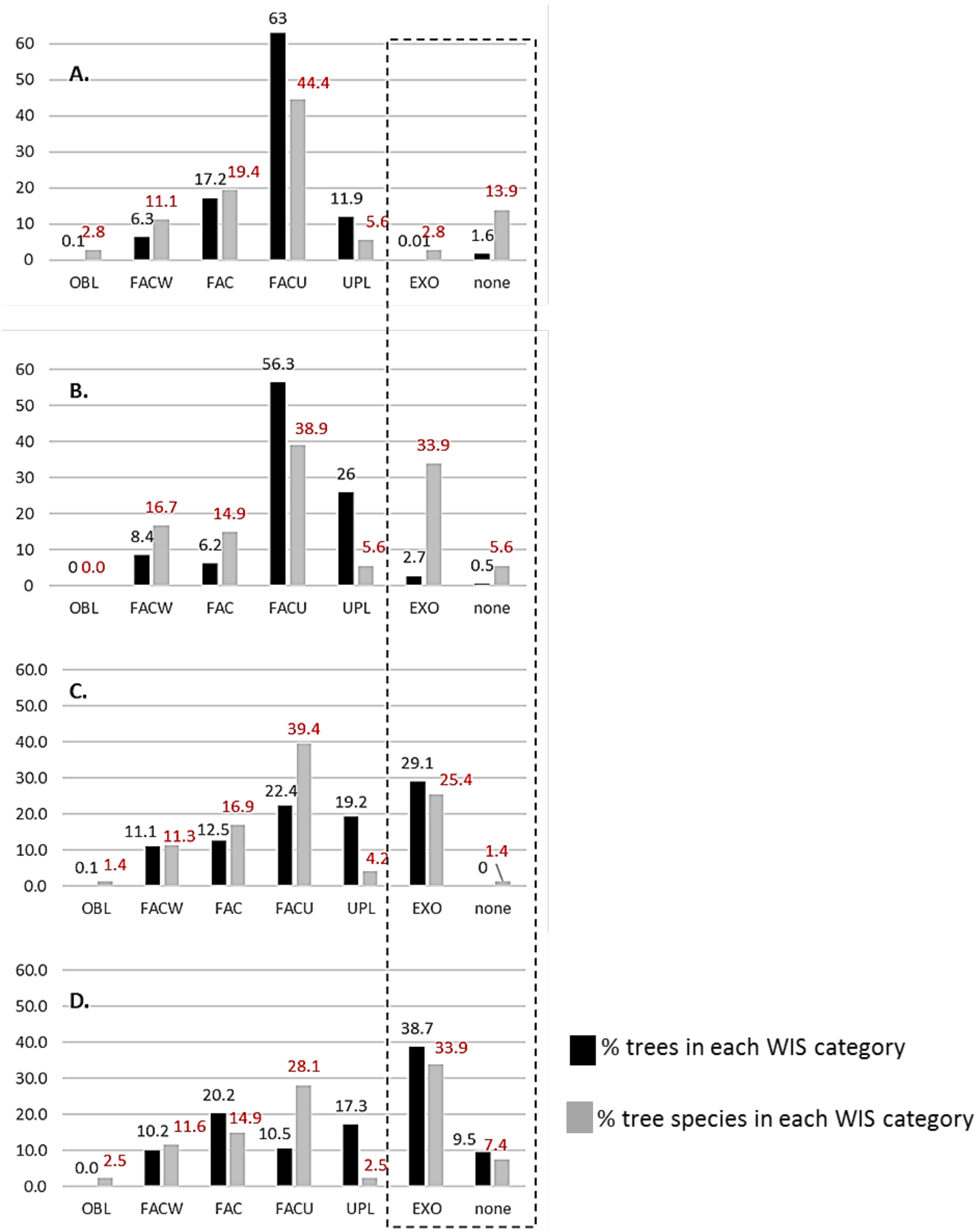

Figure 2-4: Black bars represent the percentage of trees within each WIS category per tree dataset. The grey bars represent the percentage of tree species within each tree dataset that fall with each WIS category. Red numbers are for the columns indicating percentage of each tree species in each WIS category. The dashed box contains the non-WIS categories. A. Historic Trees B. NAS C. iTree D. Davey street trees

species dominate 71.6% of the population with Norway maple (*Acer platanoides*) as the most common street tree species. Four of the eight species are non-natives from Europe and China (Table 2-4). All eight species are listed as recommended street trees that tolerate persistently wet soils to persistently dry soils and grow adequately in shaded areas (Welch 1994). In comparison, the dominant settlement-era tree species of white oak (*Quercus alba*) that makes up 46.2% of the historic tree dataset, requires full sun with maturity and well drained soils (Moore 2002). Additionally, white oak will not tolerate urban soils (compaction and high fill content) or disturbance to its root system and is not recommended as an urban tree (Bassuk et al. 2009; Moore 2002). Only five white oaks are recorded in the Davey street tree dataset out of nearly 31,000 recorded trees. Furthermore, whereas the historic forests of the region were predominantly (71.2%) white oak, black oak, and bitternut hickory (Table 2-4), urban street trees are selected for species diversity to safe guard against disease and pests (e.g. Asian longhorn beetle, emerald ash borer) and increase resilience against large mortality losses (Abrams 2005; Bassuk et al. 2009; Welch 1994). In Pittsburgh, urban forest diversity is a management priority and likely contributes to the high diversity found in the street tree dataset (Davey Resource Group 2012; Welch 1994). The species compositions of the street tree component of the urban forest evolved differently from historic forests due to urban environmental conditions, with humans driving species selection and management.

The urban woodland component of Pittsburgh's urban forest may be more similar to the historic forests of the region in structure than the street trees, but the similarities remain limited. Nine species make up 69.1% of the entire iTree dataset, with seven of those species being native to the region (Table 2-4). The two-non-native species are Norway maple (Acer platanoides) and tree of heaven (Ailanthus altissima), both species known to be highly invasive (Whitney and

Adams 1980). Black locust (Robinia psuedoacacia) is the most common tree in the iTree dataset as it grows well in poor soils and spreads easy through its roots, while Norway maple is the second most common tree in the iTree dataset (Table 2-4). The most common species of the iTree survey establish and spread easily either through wind or bird dispersal, in contrast to the historic trees in which the most common species (oaks and hickory) are heavy seeded trees that require animals such as squirrels for propagation (Anon. 2009; Welch 1994). Urban woodlands in Pittsburgh, particularly those not on park property, rely primarily on natural succession instead of planned plantings when it comes to the recruitment of new trees. Therefore, species composition in urban woodlands will represent tree species most competitive in the urban environment (i.e. able to tolerate poor soil, salt, pollution, and varying hydrological conditions) and will draw from both existing soil seedbanks as well as introduced street and yard species.

2.3.4 Comparison of WIS Landscape Position between Historic and Contemporary Forests

Though the distribution of trees among WIS functional groups is similar across the four datasets, urbanization has led to divergences in landscape position of WIS functional groups from settlement period forests, particularly with street trees. Davey street trees which are located only adjacent to roads, have higher densities of trees occurring in three distinct clusters of elevation in all four WIS categories (Figure 2-5 and 2-6). Most Davey street trees are located in either the lowest neighborhoods (e.g. the Southside Flats, the North Shore) adjacent to the rivers (~700'-900' above MSL) or neighborhoods within the paleochannel (~900-1000' above MSL) (Figure 2-5 & 2-7). These neighborhoods represent the flattest and least steep areas of the city, where dense development and thus the most roads have been placed. In contrast, the hill neighborhoods located in the blue areas of Figure 2-7 have the lowest density of streets and thus street trees in the city.

The street trees are a clear example of how urbanization can direct forest development, as human development and planning of the landscape has directly determined the species selection and distribution of the street tree urban forest component.

The iTree dataset more closely resembles the historic dataset in tree distribution on the landscape by soil moisture preference (Figure 2-6). This may be due to the more natural development of urban woodlands (iTree) as opposed to urban street trees. Both the iTree and historic datasets show the highest density of trees for each WIS group between 1000’ and 1200’ and on similarly steep slopes (Figure 2-6). However, the historic dataset shows a broader range of elevation for the UPL WIS category then the iTree dataset. The more restricted elevation range of the UPL species in urban woodlands may be due to human constraints on urban woodlands

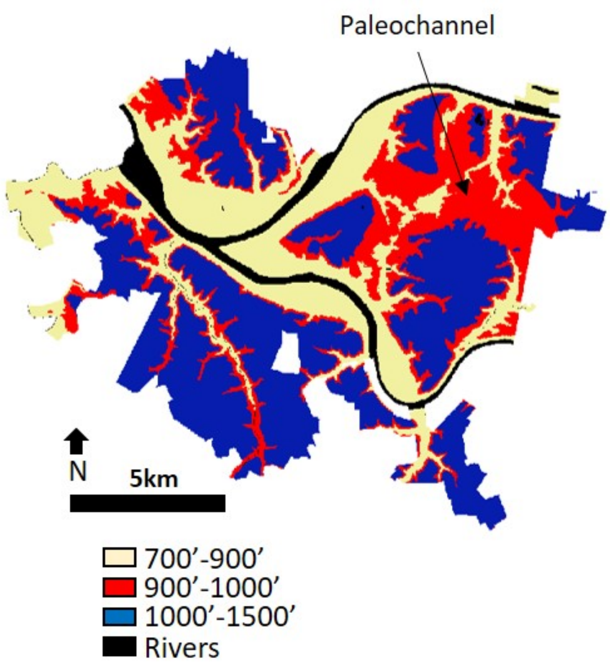

Figure 2-5: Elevation categories in the city of Pittsburgh at which Davey street trees cluster. Black pixels do not denote elevation values, but instead indicate rivers and streams within the city.

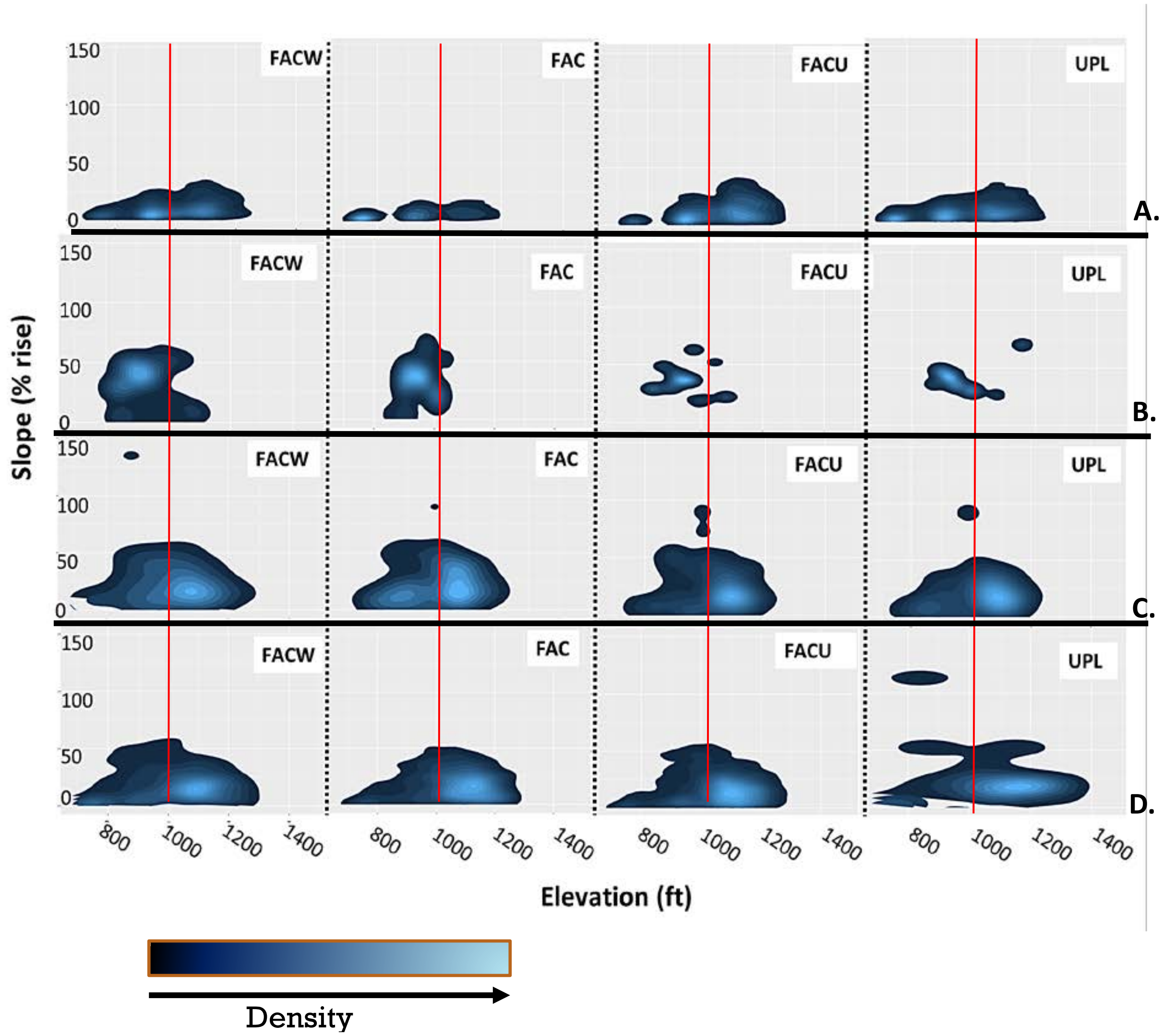

Figure 2-6: A. Davey Street Trees B. NAS C. iTree and D. Historic. Density plots with slope (% rise) and elevation. Blue gradient indicates increasing tree point density of the 4 WIS categories within each tree dataset, with lighter blue indicating the highest point densities. Plots are ordered by WIS category with the wettest category (FACW) on the left and the driest category (UPL) on the right. The red line is a reference point set at 1000' to aid in visual comparison of the plots.

and where they are permitted to exist within the city. Therefore, urban woodlands may only occur in the cityscape where a specific range of slope and elevation intersect. Overall, urban woodlands occur through succession, likely driving more natural patterns that resemble historic forests in the landscape location of WIS functional groups.

The parks trees (NAS) are more similar to both the historic trees and urban woodlands, but exhibit some clear differences. The NAS, historic, and iTree datasets occur over a similar range of slope and all extend beyond 50 percent rise (Figure 2-6). However, the NAS trees occur in narrower ranges of elevation and slope (Figure 2-6). The NAS UPL and FACU trees only occur on slopes greater than 25% rise, while the FACW and FAC trees occur at shallower slopes similar to the iTree and historic data. The NAS trees also cluster more densely on steeper slope positions, whereas historic and NAS trees cluster more densely on shallower slopes. The NAS trees occur primarily between 800’ and 1000’, as opposed to the iTree and historic datasets with elevation ranges up to 1200’ (Figure 2-6). Much like Pittsburgh’s urban woodlands, the city’s parks are also restricted to specific locations within the city. Pittsburgh parks were established in areas that were too steep to develop, which may be influencing the distribution of WIS categories within the parks (Figure 2-6). Despite clear differences among the NAS, iTree and historic datasets due to human imposed limitations (and small sample size, n=437), the NAS dataset is more similar to those datasets than the Davey street trees. Like the urban woodlands, the park trees are more influenced by natural processes than human management, leading a similar distribution of species types to historic forests.

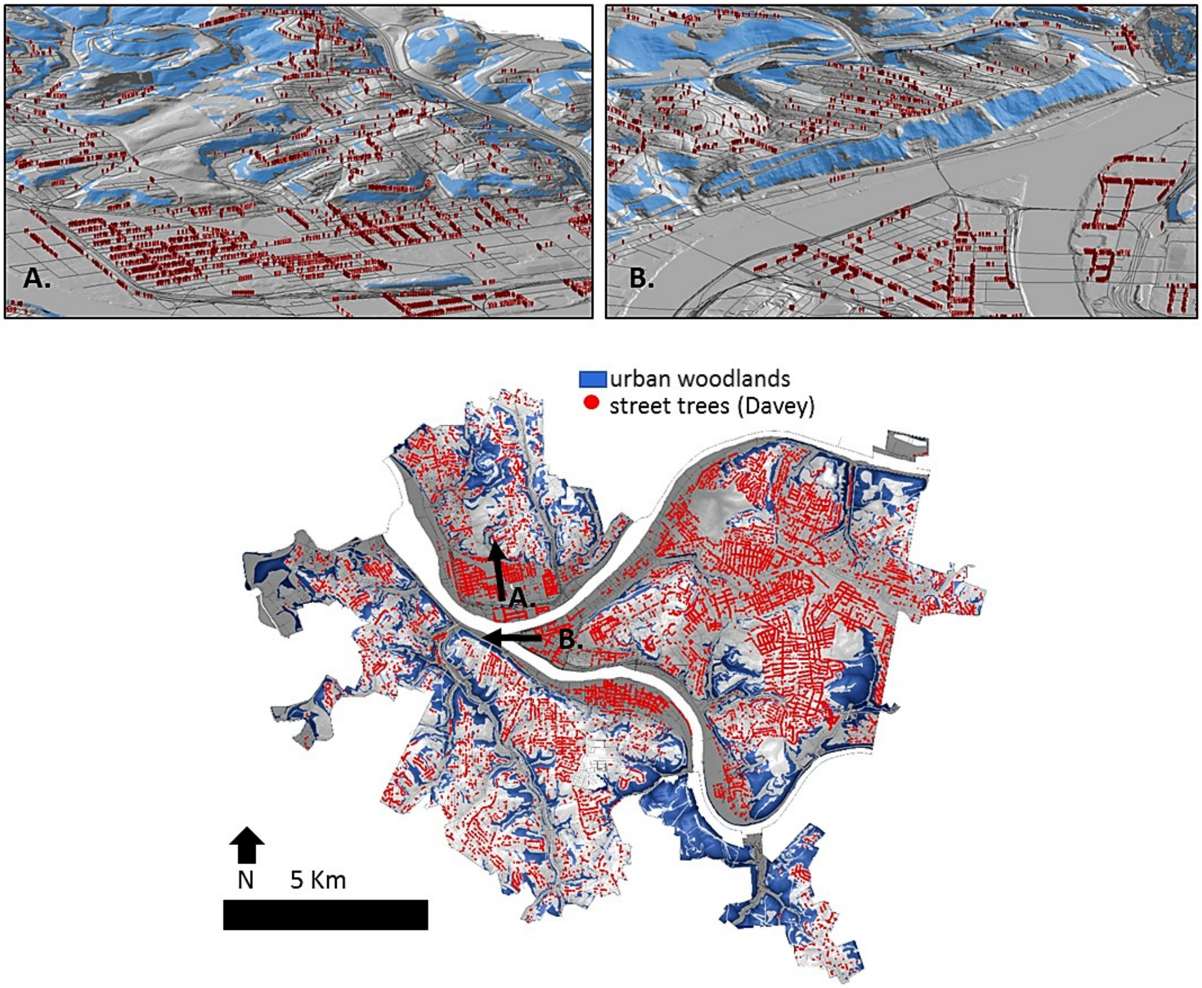

Figure 2-7: Pittsburgh's urban forest depicted as two components: streets trees (red) and urban woodlands (blue). 3D panels show detail of separation between street trees and woodlands. A) an example of Davey Street tree and urban woodland distribution from the North Shore toward the North Hills region of the city. B) an example of Davey Street tree and urban woodland distribution from downtown Pittsburgh toward the South Hills region of the city.

2.3.5 WIS Category VS Hillslope Position

Urbanization has restricted forest growth and altered the hydrology of Allegheny County, especially in the City of Pittsburgh. The differences between historical and modern tree species, particularly the differences among distributions of WIS category locations on hillslope positions (e.g. ridge vs valley) can allow evaluation of these hydrologic changes. The historic trees dataset is surprisingly consistent in the distribution of trees among various WIS categories across hillslope positions (Figure 2-8). The FACU WIS category is the most commonly occurring WIS classification and makes up the highest proportion of trees across hillslope positions in the historic dataset. Similarly, OBL and UPL are the least common WIS across landscape positions (Figure 2-8). The nearly identical WIS distributions among hillslope positions in the historic dataset may arise from either bias in witness tree selection (for white oak) or due to a strong historical dominance of white oak (nearly half the trees within the dataset are white oak (FACU)).

The dominance of facultative upland species persists in the iTree and NAS datasets despite the strong contrasts in species composition (Figure 2-9 & 2-10; Table 2-4). Facultative species are the most common in both the iTree dataset and NAS datasets (with the exception of the lower slope and flat hillslope positions in the NAS data (Figure 2-10)). Both the iTree and NAS dataset were gathered to sample forests as they grow naturally (e.g. minimally managed compared to street trees) and therefore have a structure more similar to the original settlement-era forests where human processes were less dominant. This may explain the similarities in WIS category distribution between the woodlands/parks and the historic forests, as they are both driven more by natural processes.

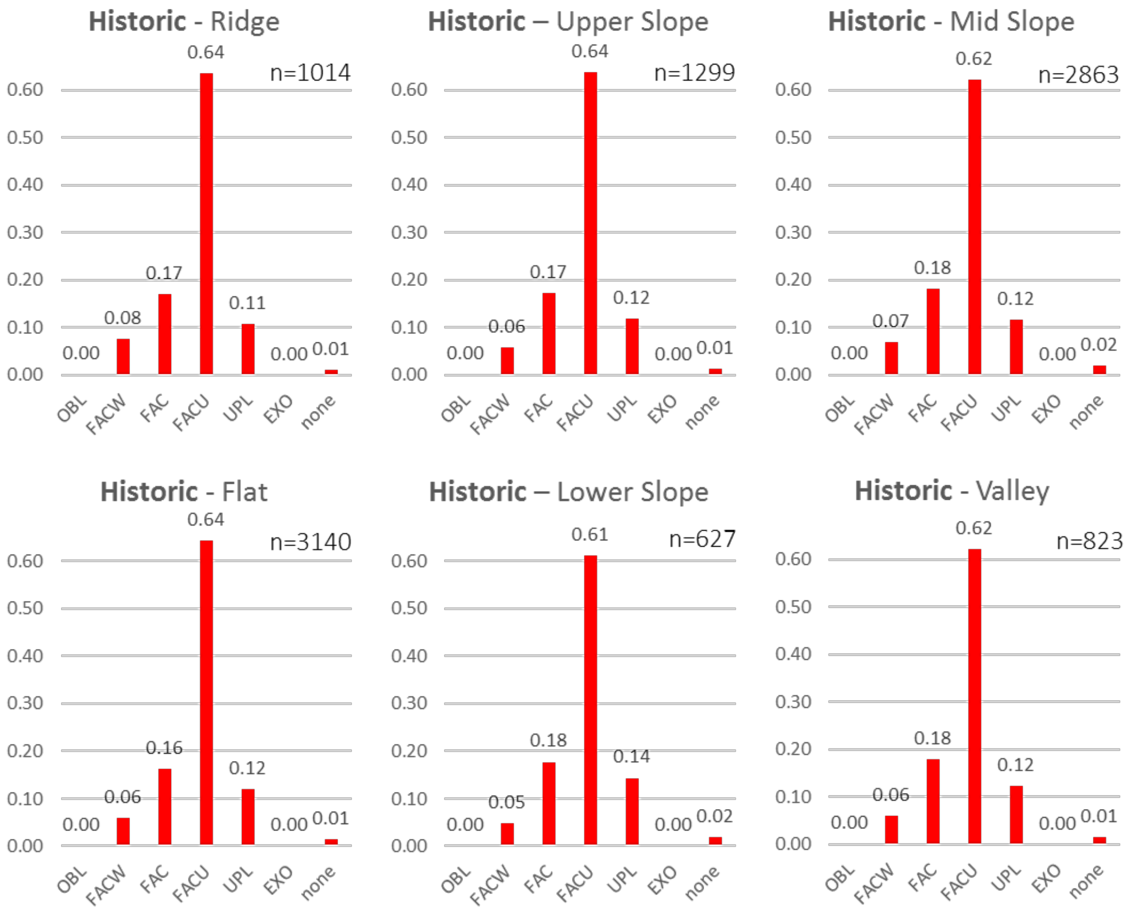

Figure 2-8: Proportion of each WIS category for each hillslope category within the historic trees dataset.

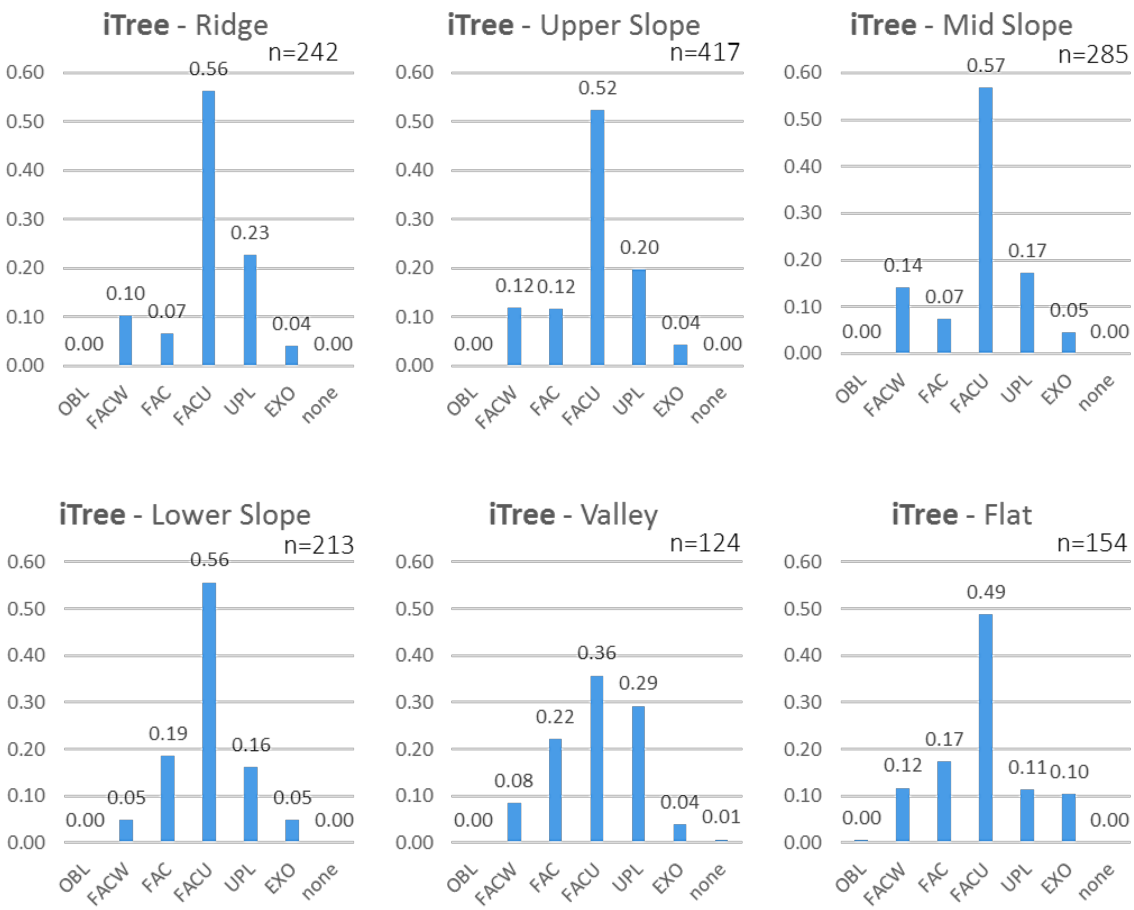

Figure 2-9: Proportion of each WIS category for each TPI category within the iTree dataset.

Drier urban soils resulting from human processes seem to have altered species composition in contemporary forests. All three contemporary datasets (Figures 2-9-2-11) have proportionally as much as triple the UPL trees relative to the historic dataset. Trees classified as UPL almost never occur in wetlands/wet areas (Lichvar et al. 2012; Anon n.d.). Soils in urban areas are often drier due to a highly fragmented or missing urban canopy, compaction and impervious surfaces, and interrupted drainage regimes (Pfeil-McCullough et al. 2015; Edmondson et al. 2011; Pavao-Zuckerman 2008). The observed shift toward UPL species prevalence in contemporary forests likely indicates human disturbance to original soil moisture regimes that influence urban forest evolution and the active planting of species that can survive in these altered conditions.

Roads alter urban hillslope hydrology and may explain changes in WIS distribution, particularly in the Davey street tree dataset. Overall, the relative proportions of various WIS species in the Davey street trees are evenly distributed among WIS categories across all hillslope positions (Figure 2-11) Further, in Davey data the FACU category is no longer dominant. (Figure 2-11). This contrast with the other datasets is likely due in part to sampling from a highly-managed and highly disturbed environment. FACW is more common in the upper slope positions than in the presumably wetter lower slope positions, whereas UPL is more common in lower slope positions despite being typically found on ridges and upper slopes (Figure 2-11). This may be caused by streets rerouting water away from natural flow paths and quickly into streams (Walsh et al. 2005). Depending on road location, they may inhibit drainage and cause water to accumulate in upper hillslope positions and lead to drier soils further downslope. Roads also reroute storm water quickly down slope, sending potential soil and ground water into sewers (Hopkins et al. 2014; Walsh et al. 2005). Street trees are selected and planted for specific sites within the city. However human selection cannot entirely explain WIS category distribution in the Davey street

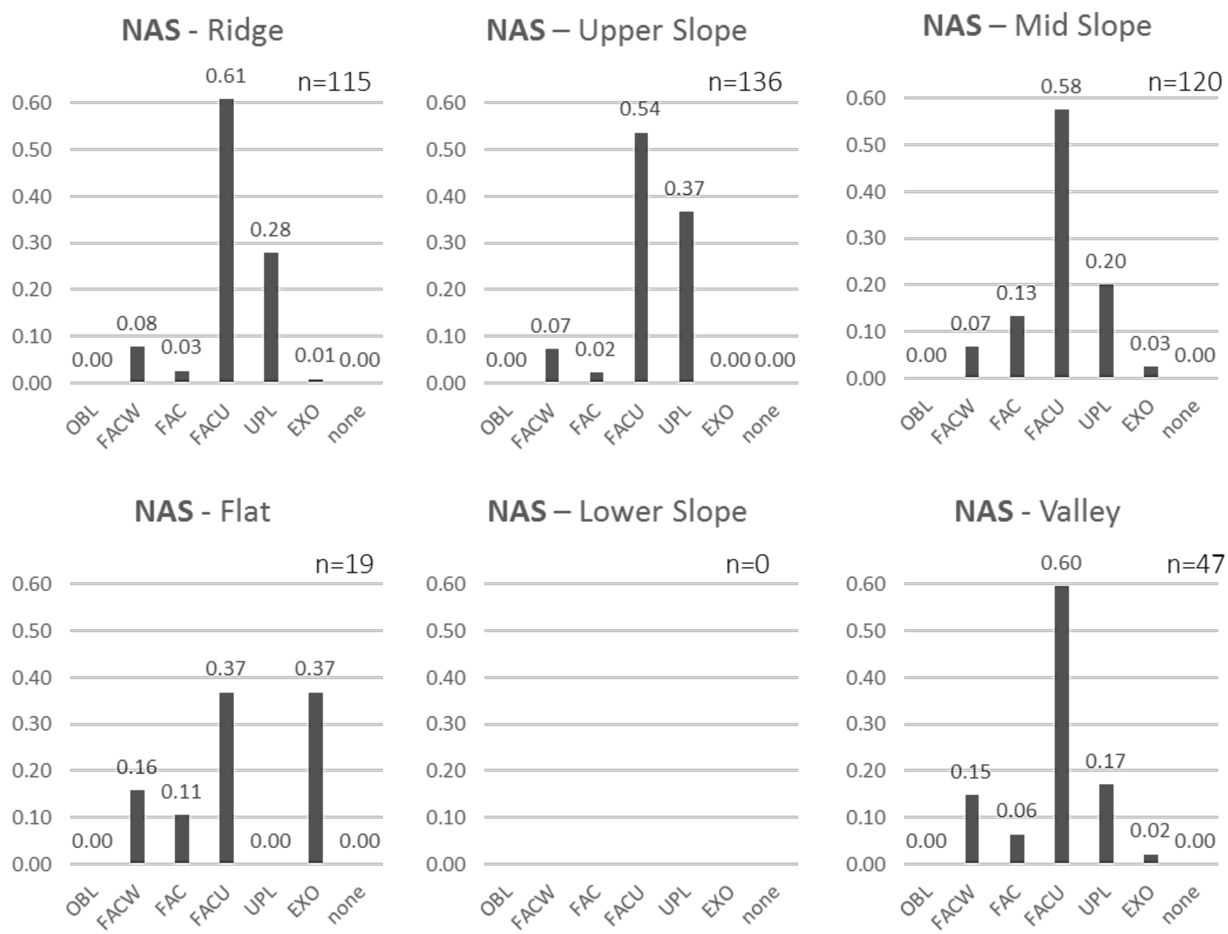

Figure 2-10: Proportion of each WIS category for each TPI category within the NAS trees dataset.

trees dataset, as a similar pattern in FACW and UPL is also seen in the urban woodlands (iTree) dataset for the valley hillslope category (Figure 2-9). These results suggest that hillslope hydrology influences urban forest evolution, despite heavy management of the street trees.

Though there is a shift across all three contemporary datasets to more upland species (e.g. prevalence of UPL and FACU), there is also a higher proportion of FACW species compared to the historic dataset, particularly in the woodland (iTree) dataset (Figure 2-9). The park and urban woodlands of Pittsburgh are mostly located in areas of the city that are too steep for building (Pfeil-McCullough et al. 2015), which may influence the distribution of WIS categories within those datasets. In the iTree dataset, the FACW category occurs in higher proportions relative to the historic and NAS datasets within the ridge, upper slope, and mid slope hillslope positions (Figure 2-9). The FACW proportions of the iTree dataset are half in the lower slope and valley categories relative to upper slope positions, suggesting wetter conditions supportive of hydrophyte tree species are more common higher on the hillslope (Figure 2-9). Though urban conditions tend to create drier soils, the hydrogeology of the region creates an exception in particularly steep areas where springs and urban forests are both common. Unfortunately, the NAS dataset does not contain tree data for the lower slope position and a comparison cannot be made between higher and lower slope positions for FACW. However, NAS does appear to be more similar to the historic dataset in FACW and UPL (Figure 2-10). In contrast to FACW, the UPL and FACU categories occur at higher proportions near the top of the hillslope, for both the NAS and iTree dataset, and decrease proportionally at the lower hillslope positions, indicating that drier, more well-drained conditions are more common near the tops the hillslopes, with groundwater discharge from springs more localized. The NAS and iTree datasets both have similar patterns in the number of trees within the upper slope, mid-slope, and ridge positions, suggesting that if these datasets had

Figure 2-11: Proportion of each WIS category for each TPI category within the Davey street trees dataset.

captured lower slopes tree species, these patterns may be consistent in lower positions as well (Figures 2.9 & 2.10).

Despite dramatic changes to the landscape due to urbanization, there are surprising consistencies among the historic and contemporary datasets, particularly the prevalence of the FACU category in the NAS and iTree datasets across most hillslope positions. Despite heavy disturbance to drainage regimes, soil properties, and the dominance of human processes, general patterns in the structure of the urban forest persists, particularly within the iTree and NAS datasets. These results suggest that key processes controlling soil moisture have not dried soils within the woodland and parks urban forest enough to fundamentally transform contemporary forests.

2.4 CONCLUSIONS

Urban forests are often managed and analyzed using socio-political boundaries (e.g. city or neighborhood boundaries) or by gradients of urbanization (Welch 1994; Steenberg et al. 2013; Mcdonnell et al. 1997; Calfapietra et al. 2015). This study instead subdivided the urban forest components of Pittsburgh by life history (street trees, urban woodlands, and park trees), distinguishing them by origin (e.g. human planned vs natural succession) and management intensity. The analysis revealed that when compared to historical forests and to each other, there are distinct differences in WIS distribution among urban forest components, particularly between street trees and more natural urban forest structures (i.e. woodland and park trees). For example, all three contemporary datasets differ from each other in species composition (Table 2-4), with Davey street trees having as much as triple the species of the other datasets. There are also clear differences in landscape position, as patterns in contemporary forests across elevation and slope revealed more restricted ranges, particularly within the Davey street trees and NAS (park trees) datasets. These results suggest that subdividing urban forests by life history might be a better approach to understanding their structure and function, particularly in the context of urban hydrology.

The urban forest body of literature is well represented by works describing the role of urban forests in urban hydrological process (Pfeil-McCullough et al. 2015; Livesley et al. 2016), but how urban hydrology impacts urban forest development remains poorly characterized. This study revealed shifts in species type within the urban datasets (i.e. WIS designation) assumed to arise from soil moisture preferences. In particular, the proportion of upland species increased from historical proportions in all the urban forest datasets we considered. There were also deviations attributed to the life history (street trees vs park trees) and WIS categories of the urban forest datasets. For example, the Davey street trees had a more even distribution of trees across WIS categories, while the historic dataset had the highest number of trees in the FACU category. Additionally, the FACW species type (prefers wetter soils) occurred more frequently at higher and presumably drier hillslope positions than expected within the iTree dataset. These shifts in species composition suggest that urbanization driven hydrological change creates new soil moisture conditions that can influence the types of tree species that populate urban forests.

The stressors of the urban environment and their effects on urban trees are well documented, from air pollution, soil compaction and introduced pests, to the urban heat island effect (Calfapietra et al. 2015; Conway and Vander Vecht 2015; McPherson et al. 1994; Pfeil-McCullough et al. 2015). These urban environmental pressures result in species composition shifts to assemblages that are more competitive in harsher urban environments (Bassuk et al. 2009).

However, despite major differences in species composition between historic and contemporary forests (Table 2-4), the general distributions of species across WIS categories (i.e. soil moisture preference) are surprisingly similar to historic forests post-urbanization, particularly in the park and urban woodland forest components. Though it is known that urban hydrology contributes to the selection of specific tree species for planned plantings (e.g. street trees)(Bassuk et al. 2009; Conway and Vander Vecht 2015), the impacts of urban hydrology to more naturally growing urban forest components that experience low management intensities remain poorly characterized (e.g. urban woodlands and parks). These results suggest that landscape-scale hydrological processes driving soil moisture conditions that influence species composition of historic forests may persist and influence contemporary forests within Pittsburgh, PA today.

2.5 BIBLIOGRAPHY

Abrams, M.D. 2005. Prescribing Fire in Eastern Oak Forests: Is Time Running Out? Northern Journal of Applied Forestry 22(3), pp. 190–196.

Anon. 2017. Pennsylvania Spatial Data Access | Data Summary [Online]. Available at: http://www.pasda.psu.edu/uci/DataSummary.aspx?dataset=41 [Accessed: 20 February 2017].

Bailey, R.G. 2004. Identifying ecoregion boundaries. Environmental Management 34(1), pp. 14–26.

Bassuk, N., Curtis, D.F., Marranca, B. and Neal, B. 2009. RECOMMENDED URBAN TREES: Site Assessment and Tree Selection for Stress Tolerance. Ithica, NY: Urban Horticulture Institute.

Black, B.A. and Abrams, M.D. 2001. Influences of Native Americans and Surveyor Biases on Metes and Bounds Witness-Tree Distribution. Ecology 82(9), pp. 2574–2586.

Buck, S.J. 1936. Frontier Economy in Southwestern Pennsylvania. Agricultural History 10(1), pp. 14–24.

Calfapietra, C., Peñuelas, J. and Niinemets, Ü. 2015. Urban plant physiology: adaptation-mitigation strategies under permanent stress. Trends in Plant Science 20(2), pp. 72–75.

Conway, T.M. and Vander Vecht, J. 2015. Growing a diverse urban forest: Species selection decisions by practitioners planting and supplying trees. Landscape and Urban Planning 138, pp. 1–10.

Davey Resource Group 2012. Pittsburgh Urban Forest Master Plan: A Roadmap for the Effective Management of Our Urban Forest, p. 78. Available at: http://treepittsburgh.org/urban-forest-master-plan.

Davey Resource Group 2015. Street Tree Management Plan City of Pittsburgh, Pennsylvania. (July), p. 67.

Ekanayake, J.C. and Phillips, C.J. 2002. Slope stability thresholds for vegetated hillslopes: a composite model. Canadian Geotechnical Journal 39(4), pp. 849–862.

Foster, H.T., Black, B. and Abrams, M.D. 2004. A Witness Tree Analysis of the Effects of Native American Indians on the Pre-European Settlement Forests in East-Central Alabama. Human ecology 32(1), pp. 27–47.

Houck, H. 1914. Warrantee Atlas of Allegheny County, Pennsylvania, 1914. Available at: http://images.library.pitt.edu/w/warrantee/.

Jones, B., Heggem, D., Wade, T., Neale, A., Ebert, D., Nash, M., Mehaffey, M., Hermann, K., Selle, A., Augustine, S., Goodman, I., Pedersen, J., Bolgrien, D., Viger, M., Chiang, D., Lin, C., Zhong, Y., Baker, J. and Van Remortel, R. 2000. Assessing landscape condition relative to water resources in the western United States: A strategic approach. Environmental Monitoring and Assessment (64), pp. 227–245.

Konijnendijk, C.C., Nilsson, K., Randrup, T.B.R. and Schipperijn, J.S. 2013. Urban Forests and Trees. The Netherlands: Springer.

Livesley, S.J., McPherson, G.M. and Calfapietra, C. 2016. The urban forest and ecosystem services: impacts on urban water, heat, and pollution cycles at the tree, street, and city scale. Journal of Environmental Quality 45(1), pp. 119–124.

Mcdonnell, M.J., Pickett, S.T.A., Groffman, P., Bohlen, P., Parmelee, R.W., Carreiro, M.M. and Medley, K. 1997. Ecosystem processes along an urban-to-rural gradient. Urban ecosystems 1, pp. 21–36.

McPherson, E.G., Nowak, D.J., Rowntree, R.A., Gregory, E., David, J. and Rowan, A. 1994. Chicago's Urban Forest Ecosystem: Results of the Chicago Urban Forest Climate Project. U.S.D.A, Forest Service, Northeastern Forest Experiment Station, p. 102.

Moore, L. 2002. Plant Fact Sheet: White Oak (Quercus alba L.) p. 2.

Nilaweera, N.S. and Nutalaya, P. 1999. Role of tree roots in slope stabilisation. Bulletin of Engineering Geology and the Environment 57(4), pp. 337–342.

Pfeil-McCullough, E., Bain, D.J., Bergman, J. and Crumrine, D. 2015. Emerald ash borer and the urban forest: Changes in landslide potential due to canopy loss scenarios in the City of Pittsburgh, PA. The Science of the Total Environment 536, pp. 538–545.

Pomeroy, J.S. 1982. Landslides in the Greater Pittsburgh Region, Pennsylvania.

Smith, L.L. and Vankat, J.L. 1991. Forests in Southwestern Pennsylvania Communities and Tree Seedling Distribution in Quercus rubra- and Prunus serotina-dominated Forests in Southwestern Pennsylvania. American Midland naturalist 126(2), pp. 294–307.

Steenberg, J.W.N., Duinker, P.N. and Charles, J.D. 2013. The neighbourhood approach to urban forest management: The case of Halifax, Canada. Landscape and Urban Planning 117, pp. 135–144.

Tarr, J. 2004. Devastation and Renewal: An Environmental History of Pittsburgh and Its Region. Pittsburgh, PA: University of Pittsburgh Press.

Welch, J.M. 1994. Street and park trees of Boston: a comparison of urban forest structure. Landscape and Urban Planning 29(2-3), pp. 131–143.

Whitney, G.G. 1984. Fifty Years of Change in the Arboreal Vegetation of Heart's Content, An Old-Growth Hemlock-White Pine-Northern Hardwood Stand. Ecology 65(2), pp. 403–408.

Whitney, G.G. 1986. Relation of Michigan's Presettlement Pine Forests to Substrate and Disturbance History Author (s): Gordon G.Whitney Reviewed work (s): Published by: Ecological Society of America Stable UR : http://www.jstor.org/stable/1939085. Ecology 67(6), pp. 1548–1559.

Whitney, G.G. and Adams, S.D. 1980. Man as Maker of New Plant Communities. Journal of Applied Ecology 17(2), pp. 431–448.

3.0 EMERALD ASH BOREER AND THE URBAN FOREST: CHANGES IN LANDSLIDE POTENTIAL DUE TO CANOPY LOSS SCENARIOS IN THE CITY OF PITTSBURGH, PA

3.1 INTRODUCTION

Forest cover is a primary control on slope stability. Trees and plants reinforce the soil on hillslopes and remove excess water through transpiration(Ekanayake and Phillips 2002; Nilaweera and Nutalaya 1999; Pomeroy 1982; Roering et al. 2003). Environmental factors that stabilize hillslopes are particularly important in urban areas where human alterations of hillslopes and hillslope processes can lead to destabilization. Vegetation removal is a fundamental cause of landsliding in many human-dominated landscapes (Glade 2003; Tsukamoto 1990). Moreover, urban forests not only stabilize urban hillslopes, but also reduce runoff, remove pollution from the atmosphere and provide cooling (McPherson et al. 1997; Xiao and McPherson 2011). Due to local geology and topography, Pittsburgh, Pennsylvania (Figure 3-1) is a city prone to landsliding, and hundreds of landslides have been recorded within city limits (Pomeroy 1982). Pittsburgh's urban canopy cover is above the national average for urban areas, near 40% and, in some areas, has expanded over the last century (Davey Resource Group 2008; Hopkins et al. 2014). However, invading forest pathogens are currently killing large numbers of important canopy species in Pittsburgh's urban forest.

Emerald ash borer (Agrilus planipennis) (EAB) is an invasive bark beetle from Asia moving through the eastern U.S. killing ash trees (Fraxinus spp.), an important canopy genus in eastern and northeastern U.S. cities (BenDor et al. 2006; Tanis and McCullough 2012). Ash is a dominating species in many urban forests, being both large and common in eastern US. urban areas (Vannatta et al. 2012). Therefore, this research focuses on the loss of ash (Fraxinus spp.) and resulting changes in urban slope stability.

The connection between tree removal and hillslope instability is important. However, spatially explicit predictions of landslide susceptibility changes following pathogen induced tree mortality are rare. This study characterizes changes in landslide susceptibility resulting from four canopy loss scenarios in Pittsburgh using SINMAP 2.0 (Stability Index MAPping), a spatially distributed slope stability model. The results of this study not only elucidate patterns of urban hillslope stability, but also advances knowledge of urban hillslope processes and urban forest function in cities with substantial topographic relief.

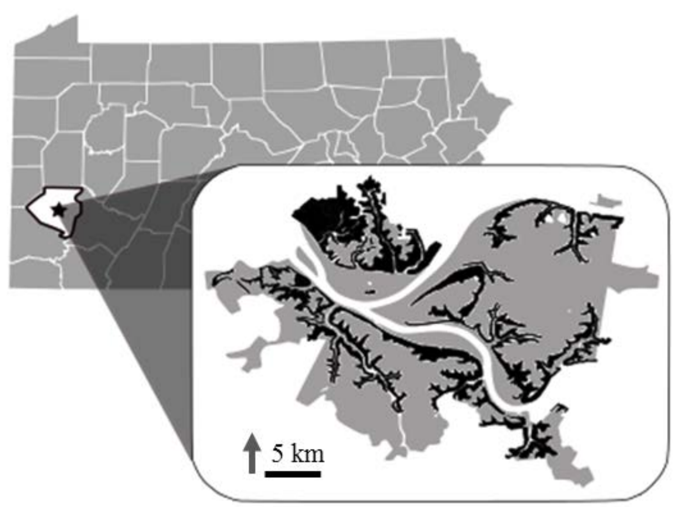

Figure 3-1: Location of Pittsburgh, Pennsylvania. Depicted in black are landslide susceptible areas based on bedrock geology (Pomeroy, 1979).

3.2 METHODS

3.2.1 Distribution of Ash

The spatial distribution of ash trees in the Pittsburgh urban forest is not well characterized. Two vegetation plot studies have sampled Pittsburgh's urban forest: iTree (U.S. Forest Service 2011) and the Natural Areas Study (NAS) (Biohabitats 2010). The iTree data were collected from 200 plots randomly placed throughout the city, while the 39 NAS plots were randomly located only in four Pittsburgh city parks. The iTree plots were 0.04 ha in size, representing 0.05% of the city's area. The NAS plot sizes differed by park; Frick contained seven 0.04 ha plots in size and the remaining 31 plots in the Highland, Riverview, and Schenley Parks were 0.016 ha (Pittsburgh Regional Parks Natural Areas Study 2010). The total NAS plot size area represents 0.0051% of the city's area (15,100 hectares). To estimate the distribution of ash trees in the City of Pittsburgh, the proportion of ash trees in each NAS and iTree sampling plot was determined. All ash species were combined in creating this proportion. There is an initial preference for green ash by the EAB, however as EAB density increases, the importance of that preference declines (Anulewicz et al. 2007). The majority of ash trees in the city were identified as white ash, however other species were also present (e.g. blue and green ash). The plots in these datasets fell within seven slope ranges (0-10, 11-20, 21-30, 31-40, 41-50, 51-60, 61-70 degrees), with slopes derived from a 10 meter resolution digital elevation model (National Elevation Dataset 2003) (Figure 3-2).

The likelihood that any particular 10m cell contained an ash tree was estimated by treating the proportions derived from the plot data and slope classes as probabilities that an ash tree occurs on a given slope. An ash proportion map was created for the city using these proportions and Monte Carlo simulation. First, a random raster with values ranging between 0 -1 was generated for all pixels with urban tree canopy and this raster divided into slope class maps by multiplying the random raster and each of 7 binary rasters representing each slope class (1=cell is in slope class, 0=otherwise). All randomly generated pixel values that were greater than the probability of an ash trees occurring in that slope class were set to zero and remaining cell values were changed to a value of 1 (i.e., the cell contains an ash). The seven resulting rasters were summed into a single raster to create a map of simulated ash distribution for the entire city. This process was repeated 100 times and these rasters summed to generate a grid of percent probability of an ash tree presence in the canopy. This process was completed for both the iTree and NAS data and the two resulting rasters were averaged to create the proportion map of ash distribution map used in this simulation.

The map of ash occurrence probabilities was then used to create four tree loss scenarios: 0%, 25%, 50%, and 75% loss. Random rasters with values from 0-1 were generated and pixels with the value ≥0.25, ≥0.50, and ≥0.75 were converted to zero, creating three rasters representing 25%, 50%, and 75% loss. These rasters were multiplied by the map of ash occurrence probabilities, to create scenarios of canopy loss, effectively zeroing out the probability an ash tree occurs when "lost".

Equation 3-1: SINMAP

$$FS = \frac{C + \cos\theta\left[1 - \min\left(\frac{R}{T} * \frac{a}{\sin\theta}, 1\right) r\right]\tan\phi}{\sin\theta}$$

3.2.2 Slope Stability

SINMAP is a landslide susceptibility model based on the "infinite slope" equation (SINMAP 2.0 User's Manual 2005). The SINMAP model predicts shallow translational landsliding phenomena controlled by shallow groundwater flow convergences and does not apply to deep-seated instability including deep earthflows and rotational slumps (Pack et al. 2011). It should be noted that although SINMAP only applies to shallow translational landslides, canopy loss can also effect these other types of landslides. A factor of safety value (FS) for each pixel in the NED (2003) 10m DEM for the City of Pittsburgh is calculated using Equation 3-1. (Other parameters in equation 1 are defined and discussed below along with relevant data sources). The FS predicts slope stability, using a range from zero to ten and was divided into three slope stability categories for this study: unstable (FS < 1), quasi-stable (FS > 1 and ≤1.5), and stable (FS > 1.5). Definition of the stability index threshold values is subjective and should be specific to the characteristics and conditions of the study area it's being applied to (Pack et al. 2011). The classification thresholds applied in this study were based on threshold values given in the SINMAP 2.0 manual. The SINMAP equation was constructed in ArcMap 9.3.1 model builder.

The tree loss scenarios were used to create SINMAP simulations predicting hillslope stability changes in Pittsburgh with the loss of ash trees. Fundamentally ash tree losses alter soil cohesion (Boerner 2011; Roering et al. 2003; Schmidt et al. 2001), although some instead attribute the increase in slope instability to friction angle changes (Graf et al. 2009). SINMAP parameters were determined from available data as follows:

Cohesion (C): C is the tendency of a soil to stick together under stress, partitioned here between root cohesion (C_r) and soil cohesion (C_s). C is dimensionless and calculated using the equation $C = (C_r + C_s)/(h*\rho_s*g)$. Thus, cohesion is also dependent on soil depth and density. Soil depth (h) and density (ρ_s) were derived from SSURGO soil data. When converting the soil polygons to rasters, pixels containing multiple values were assigned the value present at the center of the cell. g is the gravitational constant. C_{min} is used for cells not "containing" tree canopy (C_r =

0, therefore C_{min}=Cs/(h* ρs*g). Cohesion (C) is scaled to the predicted ash loss by multiplying the probability of ash presence by C_r in pixels where ash loss is predicted, i.e., C_{max} = ((C_r *proportion) + C_s) / (h* ρ_s*g)) and C_r=3000 N/m^2 and C_s=11500 N/m^2. Urban cohesion properties for roots and soils are not well characterized, therefore conservative values for cohesion were chosen from other regions and forest systems (Savigny 1990; Department of Transportation (Minnesota) 2007; Hales et al. 2009).

Effective recharge (R): This is the rainfall rate (m/hr). The 25-year storm value for Pittsburgh, PA for a storm duration of one hour was used; 0.052 m / hr (NOAA 2011). This value was applied uniformly to the entire area. Recharge was assumed to be a rainfall rate in this study, as the ratio R/T is a combination of climate and hydrological factors (Pack et al. 1998). R/T ratios are often estimated in the field (Pack et al. 1998), whereas here rasterized SSURGO soil transmissivity data was used in combination with local climate data.

Transmissivity (T): The rate (m^2/hr) at which water passes through a unit of soil. T = Soil Conductivity*Soil Depth. T was calculated for each soil type using saturated conductivity (K_{sat}) and depth values in SSURGO soil data. Transmissivity values for the city ranged from .001 m^2/hr – 0.26 m^2/hr.

Soil Density Term (r): Ratio of water density (1000 kg/m^3) and soil density (kg/m^3) values for each soil type from SSURGO soil data were used (Soil Survey Staff 2012). A horizon depth weighted average of SSURGO soil density values were used. Soil density values for the city ranged from 225 kg/m^3 – 1696 kg/m^3, with most (%99.7) soil density values >1055 kg/m^3.

Contributing area (a): The upslope area draining to each 10m pixel. Contributing area was derived using standard GIS methods from the digital elevation model (National Elevation Dataset 2003).

Land surface slope (θ) – Slope was derived from the digital elevation model.

Friction angle (ϕ, FA): The internal friction angle of soil is the angle at which shear failure occurs. The higher the FA, the more stable the slope. A value of 27° was estimated for this study using a landslide inventory map of Pittsburgh, PA (Pomeroy and Davies 1979).

SSURGO soil data used for all soil based parameters is a national soil database of synthesized soil data, including the Soil Survey of Allegheny County. This survey was conducted from 1964 – 1973 via walking surveys and sample collection for laboratory analysis. The product provides coarse soil data (at best 1:12,000 scale) for the Pittsburgh area, composed mostly of soil classified as urban.

The strength of SINMAP predictions is dependent on the quality of data used to populate the model (Michel, Kobiyama, and Goerl 2014; Wilcock et al. 2003). In some cases, data quality and resolution may be lost when applying landslide susceptibility models to regional spatial scales, due to general heterogeneity of landscape characteristics at larger scales and data availability. In particular, SINMAP is sensitive to parameter choice and will fail at the limit (Sulaiman and Rosli 2010; Thiebes 2012). That said, we are careful in our approach to utilize the best available data to understand a spatially, regional management challenge.

3.3 RESULTS AND DISCUSSION

3.3.1 Distribution of Ash Trees

Ash trees are most likely to occur on the steeper slopes of the city (Figure 3-2B and 3-2C). Given the preference for flat spaces in historical urban development (Bain and Brush 2008;

Borchert 1961) it's likely the preferential use of flat spaces during the building of Pittsburgh left predominantly steeper hillsides to more natural tree succession. The most prevalent slope classes in the city are 0-10, 11-20, and 21-30 degrees (Figure 3-2D). The 21-30 degree slope class is the third most common slope class in the city and makes up the majority of the slopes occupied by the urban forest (Figure 3-2B and 3-2C). Based on the Pittsburgh landslide inventory (Pomeroy and Davies 1979), the 21-30 degree slope class is most common slope class in the city that experiences land sliding. This slope class also contains the most ash trees, implying that EAB

3.3.2 Scenario Analysis

With increasing loss of ash (0% to 75%), landslide susceptibility increased (Figure 3-3A). The most common change in pixel factor of safety was "stable" pixels transitioning to "quasi-stable" pixels. For example, in the 75% loss scenario, 737 pixels transition from stable to "quasi-stable", while only 46 quasi-stable pixels transitioned to "unstable" (relative to 0% loss scenario) (Figure 3-3). The relatively small change from quasi-unstable to unstable results from most pixels classified as "unstable" in the 0% loss scenario being on slopes steeper than the friction angle and therefore always be predicted to be unstable under the model conditions. In general, "quasi-unstable" pixels transitioning to "unstable" following canopy loss were in steep areas where root cohesion allows the pixel to remain in the stable or quasi-stable states. The model predicts that the loss of vegetation within these critical areas is particularly important to hillslope failure risks in urban areas.

The model includes all pixels in the city, whether they are forested or not. If a pixel is not forested, then the root cohesion for the pixel was set to zero. Non-forested pixels do not change

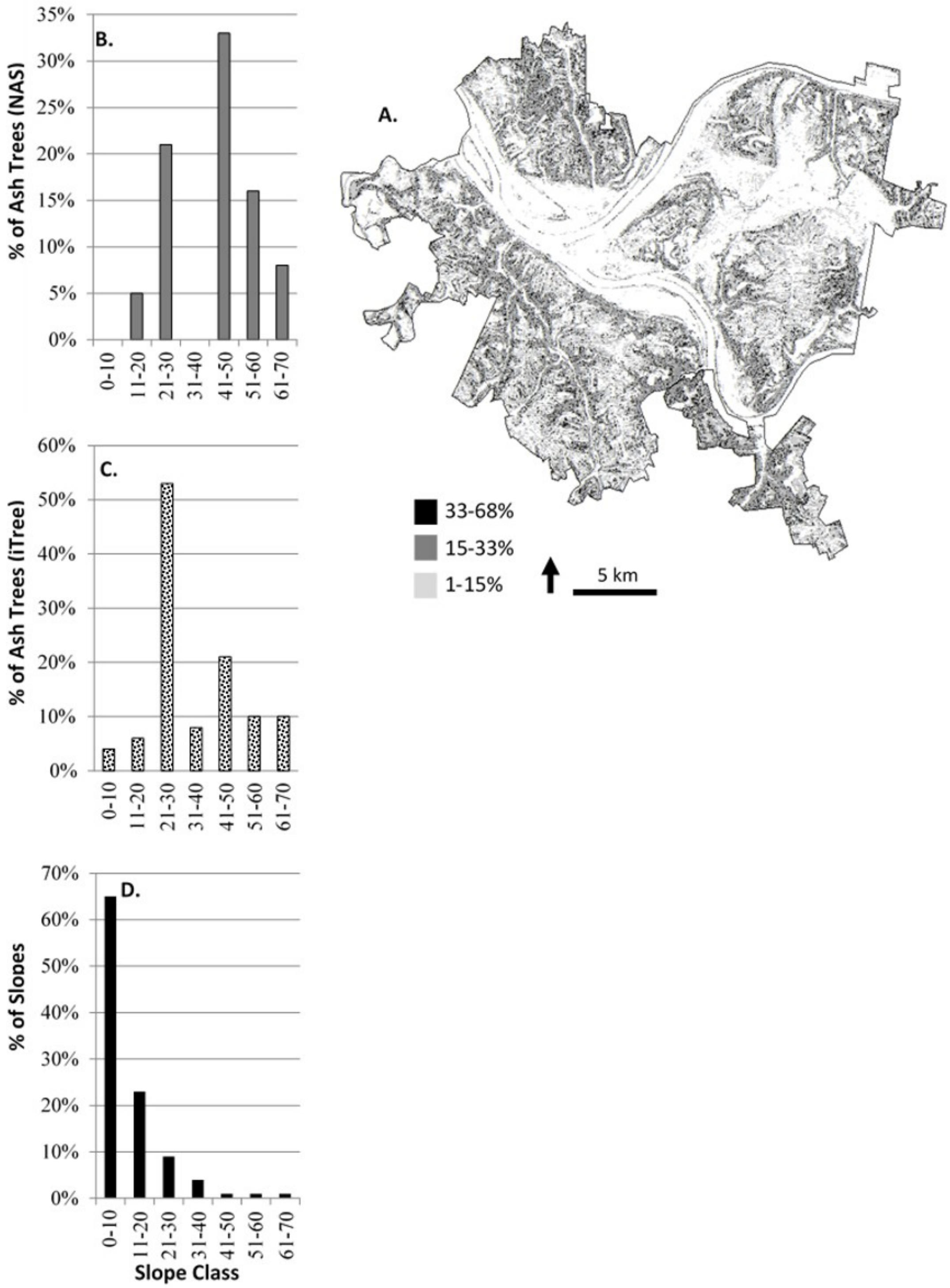

Figure 3-2: A. The average of NAS and iTree based predictions of the proportion of trees in each pixel that are ash, based on slope class. The proportion of ash tree occurrence in each slope class for B. NAS (Natural Areas Study) and C. iTree plot data. D. The distribution of slopes in Pittsburgh.

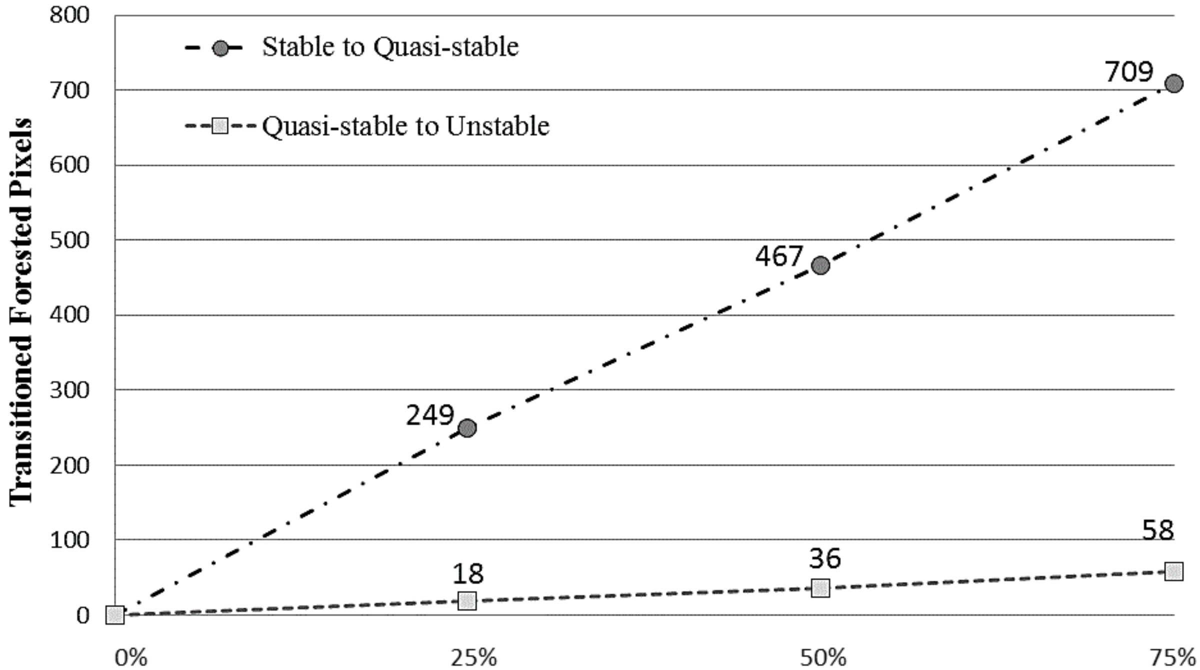

Figure 3-3: Plot depicts forested pixels that were predicted to transition from stable to quasi-stable or unstable status following the loss of ash from the pixel.

stability status as the loss scenarios are applied. The loss of ash from the model causes some of the initially forested quasi-stable pixels to transition to unstable status (Figure 3-3). Stable pixels also transitioned to quasi-stable pixels following each canopy loss scenario (Figure 3-3). The conversion of forested pixels from stable to quasi-stable is important, as these are areas that before the loss of ash were considered stable (FS > 1.5) (Figure 3-3b) and are areas where the urban forest is particularly important to maintaining stability and preventing landslides and are therefore of particular concern when considering vulnerability to tree pathogens. In addition, it is generally accepted that tree roots alter soil hydrology by changing soil properties (e.g. transmissivity) and allowing for increased infiltration of water into the soil (Bartens et al. 2009; Bramley et al. 2003; Chandler and Chappell 2008). During a precipitation event, the ratio of soil transmissivity to recharge rate (rainfall) influences if and when a column of soil reaches saturation, a factor in hillslope failure (Borga et al. 2002; Pack et al. 1998) High soil infiltration rates are linked to slope instability, as water adds weight while also reducing soil cohesion (Borga et al. 2002; Guimarães et al. 2003). During a storm event, the roots of an ash tree that remain in place will continue to facilitate infiltration of water through the soil, but no longer play a role in removing excess soil water. This may contribute to increased hillslope instability by altering the initial soil moisture status before a storm event. However, these dynamics are beyond simulations possible with the SINMAP model.

3.3.3 Model Sensitivity Analysis

Given the substantial uncertainty in some of the model parameters, the model sensitivity to these uncertainties was assessed. Sensitivity was assessed by comparing changes in counts of unstable and quasi-stable pixels relative to changes imposed on each parameter value. Rainfall rates (R) were compared with 2 year and 10 year storm rates (NOAA), soil density (r) was compared to 10% higher soil density values, cohesion (C) was compared to a much higher cohesion value derived from 23,300 N/m2 (Schmidt et al. 2001), and a low and high friction angle (ϕ) values (20° and 30° respectively) were compared to the original SINMAP results using the default values. Specifically, changes in the pixel count of both unstable (FS < 1) and quasi-stable pixels (FS values between 1 and 1.5) were tracked by comparing pixel counts between the original outputs and the sensitivity analysis outputs.

The sensitivity analysis reveals the importance of the uncertainty in soil parameters on the quality of stability predictions using SINMAP, specifically cohesion (soil and root) and soil density in predicting hillslope stability (Morrissey et al. 2001). There were also notable differences when forested pixels were analyzed separately for sensitivity (Table 3-1 and Table 3-2). Forested areas are more sensitive overall to changes in model parameters, particularly soil density and root

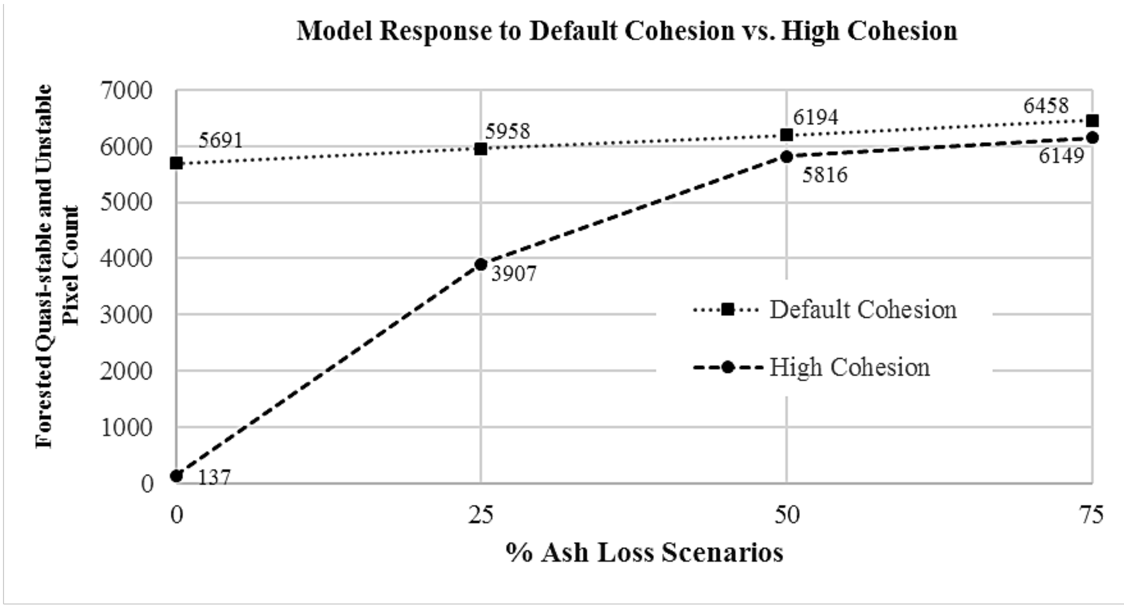

Figure 3-4: Model response following the application of high root cohesion (Cr = 23,000 N/m2) versus the default root cohesion (Cr = 3000 N/m2) value. Shown as the change in the number of forested unstable and quasi-stable pixels, with increasing loss of ash.

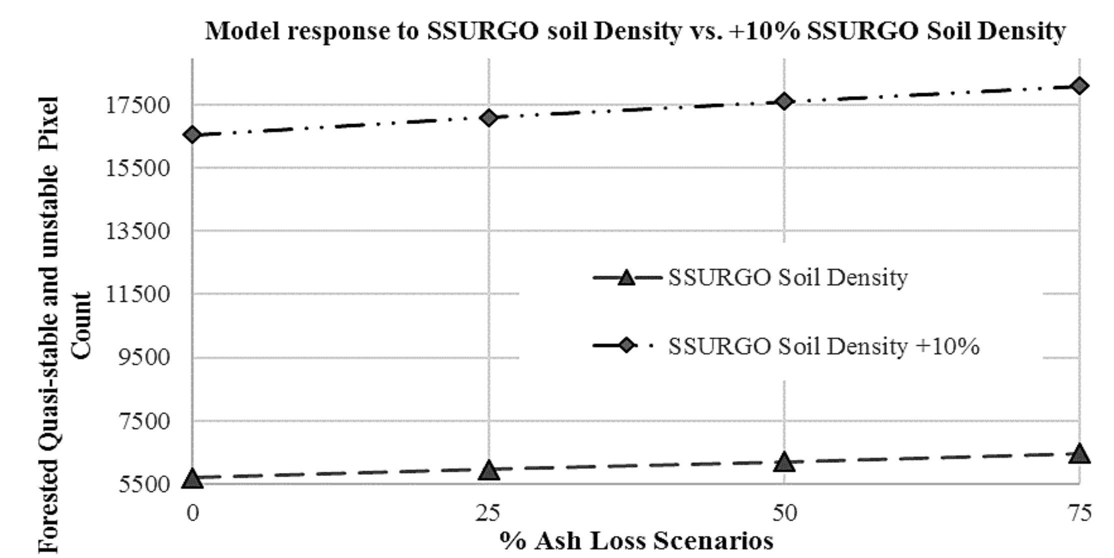

Figure 3-5: Model response following measured soil density (SSURGO) compared to 10% higher the original SSURGO soil density values. Shown as the change in the number of forested unstable and quasi-stable pixels, with increasing loss of ash.

Table 3-1: Sensitivity analysis results, all quasi-stable (QS) and unstable (UNS) pixels (combined). Default parameter model results vs. modified parameter model results, with percent increase or decrease due to modification. Pixels reflect all quasi-stable and unstable pixels combined for forested pixels only. Model modifications include: C_r = root cohesion; +10% SSURGO = soil density * 110%. A negative % change value indicates a decrease in pixel number following a change, while a positive value indicates an increase.

% Ash Loss Scenarios	Default parameter model Results *(# of QS and UNS Pixels)*	High root cohesion model results C_r = (23,000 N/m^2) *(# of QS and UNS Pixels)*	% Change between default and high root cohesion results	+10% SSURGO soil density model results *(# of QS and UNS Pixels)*	% Change between default and high soil density results	Friction Angle = 20° model results *(# of QS and UNS Pixels)*	% Change between default and FA = 20° results	Friction Angle = 30° model results *(# of QS and UNS Pixels)*	% Change between default and FA = 30° results
0	9484	3930	-58.6%	20359	114.7%	11535	21.6%	8623	-9.1%
25	9751	7700	-21%	20908	114.4%	11844	21.5%	8880	-8.9%
50	9987	9609	-3.8%	21400	114.3%	12116	21.3%	9113	-8.8%
75	10251	9942	-3%	21905	113.7%	12421	21.2%	9394	-8.4%

Table 3-2: Sensitivity analysis results, forested quasi-stable (QS) and unstable (UNS) pixels (combined). Default parameter model results are compared with modified parameter model results, with percent increase or decrease due to modification. Pixels reflect all quasi-stable and unstable pixels combined for forested pixels only. Model modifications include: Cr = root cohesion; +10% SSURGO = soil density * 110%. A negative % change value indicates a decrease in pixel number following a change, while a positive value indicates an

% Ash Loss Scenarios	Default parameter model Results *(# of QS and UNS Pixels)*	High root cohesion model results C_r = (23,000 N/m^2) *(# of QS and UNS Pixels)*	% Change between default and high root cohesion results	+10% SSURGO soil density model results *(# of QS and UNS Pixels)*	% Change between default and high soil density results	Friction Angle = 20° model results *(# of QS and UNS Pixels)*	% Change between default and FA = 20° results	Friction Angle = 30° model results *(# of QS and UNS Pixels)*	% Change between default and FA = 30° results
0	5691	137	-97.6	16566	191.1	7742	36.0	4830	-15.1
25	5958	3907	-34.4	17115	187.3	8051	35.1	5087	-14.6
50	6194	5816	-6.1	17607	184.3	8323	34.4	5320	-14.1
75	6458	6149	-4.8	18112	180.5	8628	33.6	5601	-13.3

cohesion as both saw large increases in percent change (Table 3-2, Figures 3-4 and 3-5). For example, the number of forested pixels in the 0% loss scenario classified as quasi-stable or unstable when root cohesion was increased in the model (Cr = 23,000 N/m2), decreased by 97% versus the 59% decrease when all pixels are included (Figure 3-4). With increased soil density (+10% SSURGO) there was a 190% increase in instability for forested pixels with the 0% loss scenario (Figure 3-5), compared to a 115% increase overall pixels. Forested pixels also show a modest linear increase of roughly 5% in sensitivity to modification in the friction angle value (Table 3-2). The greater sensitivity among the forested pixels is most likely due to the overrepresentation of ash on the steeper slopes of the city (Figure 3-1). These results show that SINMAP model sensitivity is relative to the spatial distribution of landscape features that drive slope stability.

At the city scale, the SINMAP model was considered most sensitive to changes in root cohesion and soil density, as the magnitude of the changes to the parameters exceeded the modification to the model parameters. By increasing root cohesion in the SINMAP model (Cr = 23,000 N/m2), instability was reduced by 59% before the loss of ash (0% scenario) (Table 3-1). Across the different scenarios, the increased cohesion results grow less sensitive with a percent difference of only 3% between changes in pixel counts with contrasting cohesion in the 75% ash loss scenario (Table 3-1) (Figure 3-4). This convergence results from the limited set of pixels that become unstable or quasi-unstable from reduced cohesion. Scenarios of increasing loss are increasingly likely to remove ash from this set of pixels and therefore differences in predicted stability changes due to cohesion values are much less important in severe tree loss scenarios. The contrast between predicted instability with high and low cohesions may also indicate that the selected default cohesion value may be too low. There is very little difference between the 0% loss and 75% loss scenarios using the default cohesion value (Cr = 3,000 N/m2), while the change is much greater between scenarios when a higher cohesion value is applied (Table 3-1). In reality, cohesion will vary spatially and most likely be represented by a range of values including those selected for this study (Hales et al. 2009; Sakals and Sidle 2004). Root cohesion will be heterogeneous laterally and vertically through the soil and will be influenced by many factors including stand age, disturbance, and forest management treatments (Sakals and Sidle 2004). Root cohesion is also not lost immediately after tree death, but generally as early as three years following mortality (Ammann et al. 2009). Regeneration would likely occur, but cohesion and evapotranspiration provided by young saplings would not equal that of the original larger tree. Minimal information in the literature is available regarding urban root and soil cohesion. A better understanding of spatial patterns in urban root and soil cohesion properties would improve stability predictions.

The number of unstable pixels increased by 115% among all pixels at 0% loss of ash when the soil density (r), derived from the SSURGO data, was increased by +10% (Table 3-1). Denser soils are heavier and more likely to fail when saturated. Urban soils are generally considered to be compacted (i.e. denser) compared to non-urban hillslopes which may reduce urban slope stability (Edmondson et al. 2011). Soil compaction can also reduce plant growth, lower transmissivity and increase erosion (Edmondson et al. 2011). These factors would also impact other model parameters, such as transmissivity. The SSURGO data does not necessarily reflect soil compaction, which may cause the SINMAP model to under-predict hillslope instability. Denser soils would result in higher slope instability.

The SINMAP model was generally insensitive to the remaining parameters, recharge and friction angle (R, FA). A 29.7% reduction in FA resulted in a 21.6% difference from the 0% loss default results, while a 10.5% increase resulted in a difference decrease of 9.1%. As ash was lost, the percent difference was reduced by less than a percent from 0% loss to 75% loss for both modified FA values (Table 3-1). Due to the importance of slope in stability predictions, changes in model response were expected. However, the magnitudes of the changes observed in model prediction are similar to the magnitude of the changes made to the FA parameter and therefore indicate a lack of model sensitivity to changes in FA. Further, altering rainfall (R) did not change the predicted outcome. This results from the threshold nature of the relative wetness (RW) component of the SINMAP equation. Relative wetness describes the depth of the perched water table and ranges in value from 0 to 1, with values over 1 representing overland flow (SINMAP 2.0 User's Manual 2005). No change was observed because the values of R (2, 10, and 25-year storm values for Pittsburgh, PA) used, all produced RW values of 1, indicating saturation of the soil during these large storm events. Complete saturation of all soils resulting in overland flow during most storm events in Pittsburgh is not likely. This model result may be due to low saturated conductivity (K_{sat}) values in the SSURGO soil data, which will result in low transmissivity estimations and thus lower SINMAP index values.

3.3.4 Sensitivity to Spatial Variability

The tree loss scenarios were created through the use of selective pixel removal from uniform random rasters. This could potentially produce dramatically different model predictions due to natural variation in the spatial distributions of slopes and soils. To assess the importance of spatial variability on model output, an additional Monte Carlo analysis was performed to evaluate uncertainty in model scenario predictions. The SINMAP model was run with 100 unique 25% loss tree scenario rasters to generate 100 sets of newly quasi-stable and unstable pixels (Figure 3-6). The random removal of pixels for the tree loss scenarios resulted in only minor changes in model prediction, with a standard deviation of only 16.1 and 4.0 from the mean for the number of quasi-stable and unstable pixels respectively (Figure 3-6). The Monte Carlo results are comparable to the original model results. The spatial distribution of landscape features may impact model results, depending on patterns of tree loss.

The spread of forests pathogens and the associated tree loss is not necessarily random and may depend on factors related to forest pathogen life cycle, transportation methods, and other related landscape and environmental factors. Ideally, data for landslide risk prediction would be representative at the grid scale of the model, but in reality parameter data often exists as field collected point data or as estimated values from the literature (Burton et al. 1998). Therefore, the true spatial variability of soil, landscape, and tree distributions of a region is unknown and these uncertainties can greatly impact model predictions. However, in Pittsburgh there seem to be enough potential landslide initiation points present, that a random removal of ash from the model consistently impacts a high number of them. Therefore, uncertainty in the model is associated primarily with the model parameters and in this case is not sensitive to spatial patterns in the geospatial data.

3.4 CONCLUSIONS

This study estimated changes in hillslope instability due to tree mortality in Pittsburgh, Pennsylvania. A slope stability investigation was carried out through the use of the SINMAP model in GIS, by manipulating the cohesion term (C) within the equation to represent the loss of ash from the urban canopy. The results demonstrate a reduction in slope stability with increasing loss of ash from the urban canopy. Moreover, the ash distribution resulted in the highest

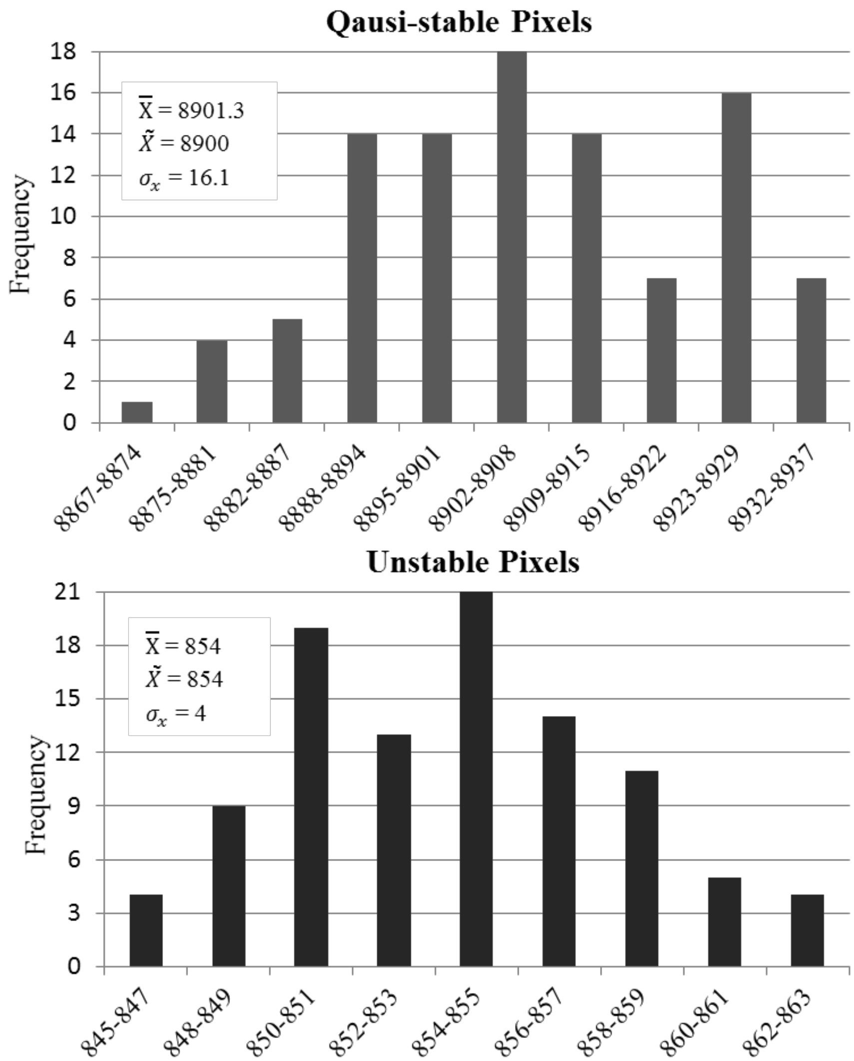

Figure 3-6: Frequency of pixel values for quasi-stable and unstable pixels resulting from a Monte Carlo analysis where the SIMAP model was run 100 times at a 25% loss scenario and the number of quasi-stable and unstable pixels were tabulated to determine uncertainty due to spatial patterns. Plot insets shows the mean, median, and standard deviation respectively.

percentage of ash presence occurring on the slopes that were steepest and also classified to be landslide prone based on bedrock geology. This emphasizes the importance of ash in Pittsburgh's urban forest, particularly to hillslope stability. Model uncertainty was associated primarily with model parameters, particularly soil properties (e.g. cohesion and density). The model was not sensitive to natural geospatial variation of model parameters and produced consistent results despite the random removal of ash from the canopy.

SINMAP is a useful tool for assessing changes to hillslope stability after the loss of ash that can complement existing strategies to increase tree species diversity and thus forest resiliency against exotic forest pathogens (Conway and Vander Vecht 2015). Further, this model can similarly be modified and applied to assess impacts from other forest pathogens or catastrophic events that result in changes the urban forests. In this way SINMAP can be utilized as a tool by urban forest managers to make more strategic urban forest management decisions as well as to increase the understanding of urban forest function and its role in slope stability.

3.5 BIBLIOGRAPHY

Ammann, Martin, Albert Böll, Christian Rickli, and Thomas Speck. 2009. "Significance of Tree Root Decomposition for Shallow Landslides." Forest, Snow and Landscape Research 82(1):79–94.

Anulewicz, Andrea C., Deborah G. McCullough, and David L. Cappaert. 2007. "Emerald Ash Borer (Agrilus Planipennis) Density and Canopy Dieback in Three North American Ash Species." Arboriculture & Urban Forestry 33(5):338–49.

Bain, Daniel J. and Grace S. Brush. 2008. "Gradients, Property Templates , and Land Use Change." The Professional Geographer 60(2):224–37.

Bartens, Julia, Susan D. Day, J. Roger Harris, Theresa M. Wynn, and Joseph E. Dove. 2009. "Transpiration and Root Development of Urban Trees in Structural Soil Stormwater Reservoirs." Environmental management 44(4):646–57. Retrieved January 18, 2014 (http://www.ncbi.nlm.nih.gov/pubmed/19707704).

BenDor, Todd K., Sara S. Metcalf, Lauren E. Fontenot, Brandi Sangunett, and Bruce Hannon. 2006. "Modeling the Spread of the Emerald Ash Borer." Ecological Modelling 197(1-2):221–36. Retrieved January 23, 2014 (http://linkinghub.elsevier.com/retrieve/pii/S030438000600113X).

Boerner, R. E. J. 2011. "Unraveling the Gordian Knot : Interactions among Vegetation , Topography , and Soil Properties in the Central and Southern Appalachians." Torrey Botanical Society 133(2):321–61.

Borchert, JR. 1961. "The Twin Cities Urbanized Area : Past , Present , Future." Geographical Review 51(1):47–70.

Borga, Marco, Giancarlo Dalla Fontana, and Federico Cazorzi. 2002. “Analysis of Topographic and Climatic Control on Rainfall-Triggered Shallow Landsliding Using a Quasi-Dynamic Wetness Index.” Journal of Hydrology 268(1-4):56–71.

Bramley, Helen, John Hutson, and Steve D. Tyerman. 2003. “Floodwater Infiltration through Root Channels on a Sodic Clay Floodplain and the Influence on a Local Tree Species Eucalyptus Largiflorens.” Plant and Soil 253(1):275–86. Retrieved (http://link.springer.com/10.1023/A:1024531325281).

Burton, A., T. J. Arkell, and J. C. Bathurst. 1998. “Field Variability of Landslide Model Parameters.” Environmental Geology 35(2-3):100–114.

Chandler, Kathy R. and Nick a. Chappell. 2008. “Influence of Individual Oak (Quercus Robur) Trees on Saturated Hydraulic Conductivity.” Forest Ecology and Management 256:1222–29.

Conway, Tenley M. and Jennifer Vander Vecht. 2015. “Growing a Diverse Urban Forest: Species Selection Decisions by Practitioners Planting and Supplying Trees.” Landscape and Urban Planning 138:1–10. Retrieved (http://linkinghub.elsevier.com/retrieve/pii/S0169204615000237).

Davey Resource Group. 2008. City of Pittsburgh, Pennsylvania, Municipal Forest Resource Analysis.

Edmondson, Jill L., Zoe G. Davies, Sarah a McCormack, Kevin J. Gaston, and Jonathan R. Leake. 2011. “Are Soils in Urban Ecosystems Compacted? A Citywide Analysis.” Biology letters 7(5):771–74. Retrieved (http://www.pubmedcentral.nih.gov/articlerender.fcgi?artid=3169067&tool=pmcentrez&rendertype=abstract).

Ekanayake, Jagath C. and Christopher J. Phillips. 2002. “Slope Stability Thresholds for Vegetated Hillslopes: A Composite Model.” Canadian Geotechnical Journal 39:849–62.

Glade, T. 2003. “Landslide Occurrence as a Response to Land Use Change: A Review of Evidence from New Zealand.” Catena 51(3-4):297–314.

Graf, Frank, Martin Frei, and Albert Böll. 2009. “Effects of Vegetation on the Angle of Internal Friction of a Moraine.” Forest, Snow and Landscape Research 82(1):61–77.

Guimarães, Renato Fontes et al. 2003. “Parameterization of Soil Properties for a Model of Topographic Controls on Shallow Landsliding: Application to Rio de Janeiro.” Engineering Geology 69(1-2):99–108. Retrieved November 10, 2014 (http://linkinghub.elsevier.com/retrieve/pii/S0013795202002636).

Hales, T. C., C. R. Ford, T. Hwang, J. M. Vose, and L. E. Band. 2009. “Topographic and Ecologic Controls on Root Reinforcement.” Journal of Geophysical Research 114:1–17. Retrieved July 31, 2014 (http://doi.wiley.com/10.1029/2008JF001168).

Hopkins, Kristina G., Daniel J. Bain, and Erin M. Copeland. 2014. “Reconstruction of a Century of Landscape Modification and Hydrologic Change in a Small Urban Watershed in Pittsburgh, PA.” Landscape Ecology 29:413–24. Retrieved June 30, 2014 (http://link.springer.com/10.1007/s10980-013-9972-z).

McPherson, E. G., S. Grimmond, and C. Souch. 1997. “Quantifying Urban Forest Structure, Function, and Value : The Chicago Urban Forest Climate Project.” Urban Ecosystems 1:49–61.

Michel, Gean Paulo, Masato Kobiyama, and Roberto Fabris Goerl. 2014. “Comparative Analysis of SHALSTAB and SINMAP for Landslide Susceptibility Mapping in the Cunha River Basin, Southern Brazil.” Journal of Soils and Sediments 14:1266–77.

Morrissey, Meghan M., Gerald F. Wieczorek, and Benjamin A. Morgan. 2001. A Comparative Analysis of Hazard Models for Predicting Debris Flows in Madison County, Virginia. Golden, CO. Retrieved (http://pubs.usgs.gov/of/2001/ofr-01-0067/ofr-01-0067.html).

Nilaweera, N. S. and P. Nutalaya. 1999. “Role of Tree Roots in Slope Stabilisation.” Bulletin of Engineering Geology and the Environment 57(4):337–42. Retrieved (http://link.springer.com/10.1007/s100640050056).

Pack, R. T., D. G. Tarboton, and C. N. Goodwin. 1998. “The SINMAP Approach to Terrain Stability Mapping.” in 8th Congress of the International Association of Engineering Geology.

Pack, R. T., D. G. Tarboton, C. P. Goodwin, and A. Rasad. 2011. “SINMAP User Manual.” Pomeroy, John S. 1982. “Landslides in the Greater Pittsburgh Region, Pennsylvania.” USGS Professional Paper 1229.

Roering, Joshua J., Kevin M. Schmidt, Jonathan D. Stock, William E. Dietrich, and David R. Montgomery. 2003. “Shallow Landsliding , Root Reinforcement , and the Range.” Canadian Geotechnical Journal 40:237–53.

Sakals, M. E. and Roy C. Sidle. 2004. “A Spatial and Temporal Model of Root Cohesion in Forest Soils.” Canadian Journal of Forest Research 34:950–58.

Schmidt, K. M. et al. 2001. “The Variability of Root Cohesion as an Influence on Shallow Landslide Susceptibility in the Oregon Coast Range.” Canadian Geotechnical Journal 38(5):995–1024. Retrieved January 18, 2014 (http://www.nrc.ca/cgi-bin/cisti/journals/rp/rp2_abst_e?cgj_t01-031_38_ns_nf_cgj38-01).

Soil Survey Staff. 2012. “(SSURGO).” Natural Resources Conservation Service, United States Department of Agriculture, Web Soil Survey. Retrieved (http://websoilsurvey.nrcs.usda.gov/.).

Sulaiman, Wan Nor Azmin and Mohd. Hafi. Rosli. 2010. “Susceptibility of Shallow Landslide in Fraser Hill Catchment, Pahang Malaysia.” Environment Asia (3):66–72.

Tanis, Sara R. and Deborah G. McCullough. 2012. “Differential Persistence of Blue Ash and White Ash Following Emerald Ash Borer Invasion.” Canadian Journal of Forest Research 42:1542–50.

Thiebes, Benni. 2012. Spring Theses: Landslide Analysis and Early Warning Systems. Springer Berlin Heidelberg.

Tsukamoto, Y. 1990. “Effect of Vegetation on Debris Slide Occurrences on Steep Forested Slopes in Japan Islands.” Pp. 183–92 in Research Needs and Applications to Reduce Erosion and Sedimentation in Tropical Steeplands (Proceedings of the Figi Symposium).

Vannatta, Author A. R., R. H. Hauer, and N. M. Schuettpelz. 2012. “Economic Analysis of Emerald Ash Borer (Coleoptera : Buprestidae) Management Options.” Journal of Economic Entomology 105(1):196–206.

Wilcock, PR et al. 2003. “When Models Meet Managers: Examples from Geomorphology.” P. (135) 27–40 in Geophysical Monograph Series.

Xiao, Qingfu and E. Gregory McPherson. 2011. “Rainfall Interception of Three Trees in Oakland, California.” Urban Ecosystems 14(4):755–69. Retrieved January 18, 2014 (http://link.springer.com/10.1007/s11252-011-0192-5).

4.0 THE DETECTION OF CHANGES TO TREE CANOPY MOISTURE FOLLOWING LONGWALL MINE SUBSIDENCE VIA A LANDSAT DERIVED MOISTURE INDEX

4.1 INTRODUCTION

The environmental impacts of high extraction coal mining methods (e.g. longwall mining, mountaintop removal) to surface processes are increasingly documented (Bernhardt and Palmer 2011; Wickham et al. 2007). Changes to surface and ground water hydrological regimes following high extraction mining disturbance can be substantial, though characterization remains incomplete (Bell, Stacey, and Genske 2000; Palmer et al. 2010; Zegre et al. 2014). In contrast to mountaintop mining, longwall mining is a form of high extraction mining that takes place underground. During longwall mining, coal is completely removed in large rectangular panels and the overlying rock collapses into the void. The degree to which the surface is impacted by longwall mine subsidence (LMS) is dependent on the depth to mining, the thickness of the mined coal seam, and the width of the mined panels (Iannacchione et al. 2008; Liu, Tan, and Ning 2015; Peng 2008). Some of the readily apparent hydrological impacts include disrupted stream and spring flow, dry domestic water wells, and drained ponds and lakes (Tonsor et al. 2013). Stretching and compression of the land surface likely impacts soil moisture and shallow groundwater, however, these impacts are challenging to detect and study (Figure 4-1).

The specific hydrological impacts following longwall mine subsidence currently cannot be accurately predicted, particularly in areas of high topographic relief (Booth 2006; Holla 1997).

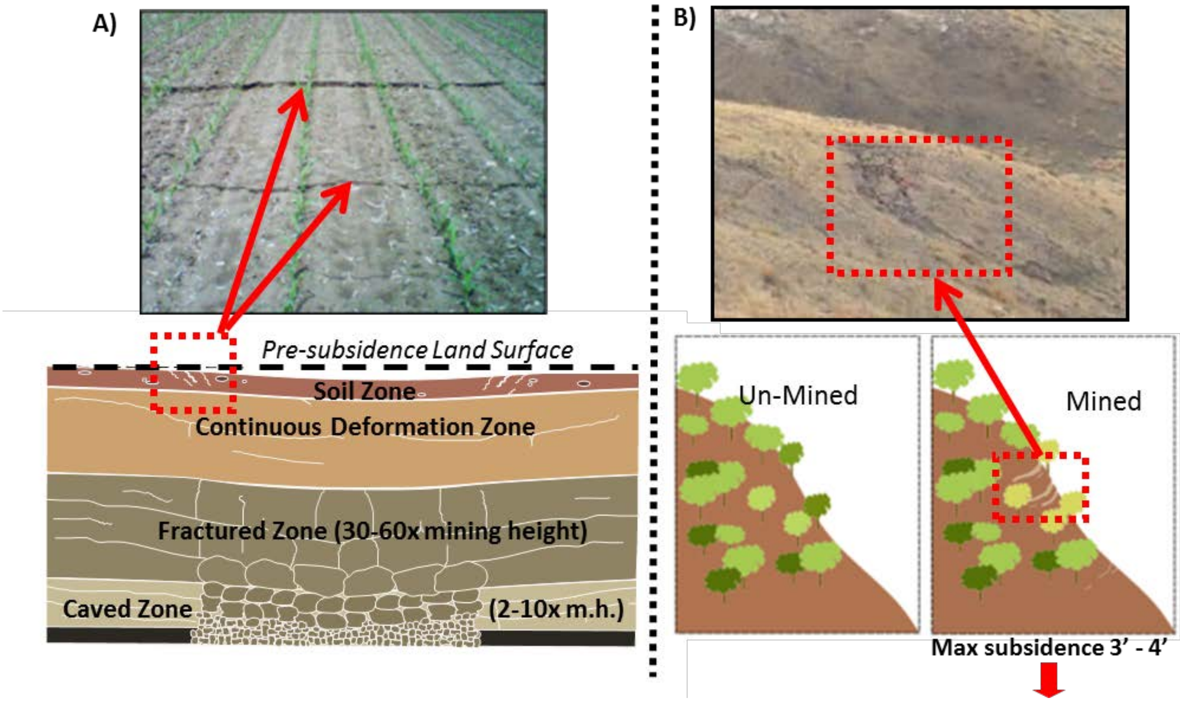

Figure 4-1: A) S.S. Peng (2008) model of zones that form following longwall mine subsidence: Caved zone: Complete disruption. Full of debris and roof material 2 – 10x mining height. Fractured zone: continuous open fractures which can be 30 -60x mining height. Continuous deformation zone: constrained with no permeability Change. Soil zone: 50 feet to surface, cracks generally considered to be temporary. The photo depicts soil impacts to an area of low relief following longwall mine subsidence. B) Less understood are potential impacts to soils and the associated vegetation in areas of high relief following longwall mine subsidence. This conceptual model depicts soil extension that can occur on undermined slopes. Picture Credits: Outlaw Partners/Joseph T. O'Connor (explorebigsky.com/coal) & Kelly Robertson Farms (krfarms.net)

Established conceptual models of subsidence are based on flat topography, with three major zones of fracture and deformation described (Peng 2008) (Figure 4-1a). However, the longwall mining impacts to hydrology in high relief regions where longwall mining often occurs remain less clear (Figure 4-1b) (Bian et al. 2008; Bian, Zhang, and Lei 2011; Li et al. 2013). LMS causes fracturing and deformation of the overlying strata, which leads to changes in fracture porosity and permeability, and ultimately changes to ground water flow (Booth 2006). Further, impacts to these high relief areas may be greater than those that occur in flatter regions (Elsworth and Liu 1995; Holla 1997; Li, Liu, and Zhao 2016). To clarify post LMS hydrological changes, studies have used ground based monitoring systems such as ground water wells and piezometers, but the resulting data are spatially and temporally limited and the monitoring wells are often destroyed following subsidence (Kelly, Luo, and Craig 2002; Tonsor et al. 2013). Here, we use spatially and temporally continuous remotely sensed data to examine subtler, landscape-scale patterns of hydrologic change.

Forests are a dominant and economically important land cover type in southwestern Pennsylvania and in many other regions across the globe. Hydrological changes to soils following LMS likely impact overlying forest ecosystems. Changes to soil moisture can be directly observed with remote sensing methods such as multispectral imagery or radar data (Wang and Qu 2009). However, due to the dense canopy cover, these techniques are generally not applied to forested areas. Given this limitation, changes in tree canopy moisture with a Landsat derived vegetation index were evaluated to infer underlying changes in soil moisture dynamics following LMS. The normalized difference moisture index (NDMI) provides an indication of relative moisture levels within the tree canopy and allows for comparison among canopies. Patterns of tree canopy water content derived from Landsat satellite imagery of southwestern Pennsylvania were analyzed over a 12-year period as mining progressed through two regions with different patterns of land use and forest patches. This study characterizes otherwise difficult to detect LMS hydrological impacts using readily available Landsat products.

4.2 METHODS

4.2.1 Study Area

The study site is located in southwestern Pennsylvania, USA, a humid temperate region of high topographic relief (up to 240 meters), in which longwall coal mining is a historical and ongoing process (Iannacchione et al. 2008; Tonsor et al. 2013). Land cover is predominantly mixed deciduous forests and mixed agricultural land use (Homer et al. 2015). The mined panels included in this study belong to two longwall mines, as defined by the mining permits, Enlow Fork to the north and Bailey Deep to the south. Panels mined between 1986 and 2013 were examined here. In these mines, the oldest mining took place near the boundary between the mines and mining moves away from this boundary in northeast/southwest directions (arrows in Figure 4-2b).

4.2.2 Data

High level Landsat surface reflectance data products from Landsat 5, 7, and 8 for the month of September were acquired, including derived products depicting the Normalized Difference Moisture Index (NDMI) from the USGS (Table 4-1). Dense cloud cover rendered most of the summer scenes (June – August) unusable for southwestern Pennsylvania. September imagery

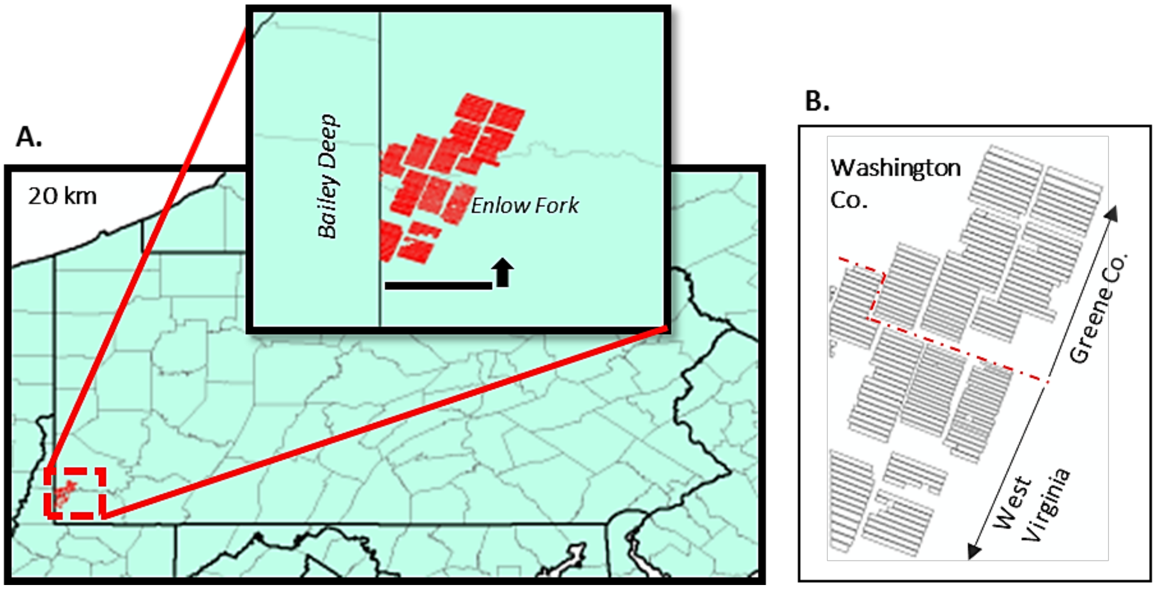

Figure 4-2: A) Study site location in southwestern Pennsylvania, in Greene and Washington Counties. Bailey mine panels present in West Virginia were excluded from this study. B) The division between the Bailey Deep and Enlow Fork mined panels.

Table 4-1: September Landsat imagery acquired for this study.

Landsat Platform & Sensor	YEAR
Landsat 5 TM	2005, 2008, 2010
Landsat 7 ETM+	2002
Landsat 8 OLI	2013, 2014

coincides with periods of maximum water deficit at the end of the growing season and thus periods sensitive to soil moisture changes. The series of September images are preprocessed, meaning they are atmospherically and topographically corrected (L1T) (Masek et al. 2006). NDMI (Equation 4-1) utilizes a water insensitive band in the near infrared region (NIR) region and a water sensitive band in the short wave infrared (SWIR) region that is sensitive to the quantity of water present within vegetation (Pechanec et al. 2014). Applied together they provide an indication of the moisture level in leaves or the entire canopy depending on the scale of application. In contrast to greenness indices utilizing visible and NIR bands such as the normalized difference vegetation index (NDVI), NDMI is sensitive to small changes in vegetation stress indicated by changes to moisture levels within the leaves. Bands used in the NDMI index differ slightly based on imagery used. For Landsat 5 and Landsat 7, bands 4 and 5 were used. For Landsat 8, bands 5 and 6 were used.

Differences in climate from year to year could influence patterns of canopy moisture so growing season precipitation and temperature trends for each year of imagery were compared. Climate data ("NOAA National Center for Environmental Information," 2016) were evaluated across the study period (Figure 4-3). Total precipitation and average temperature were determined for the growing season and over the 8 days before the imagery was acquired (Figure 4-3).

Equation 4-1: Normalized Difference Moisture Index. The spectral ranges are in micrometers.

$$NDMI = \frac{NIR_{(0.76-0.90)} - SWIR_{(1.55-1.75)}}{NIR_{(0.76-0.90)} + SWIR_{(1.55-1.75)}}$$

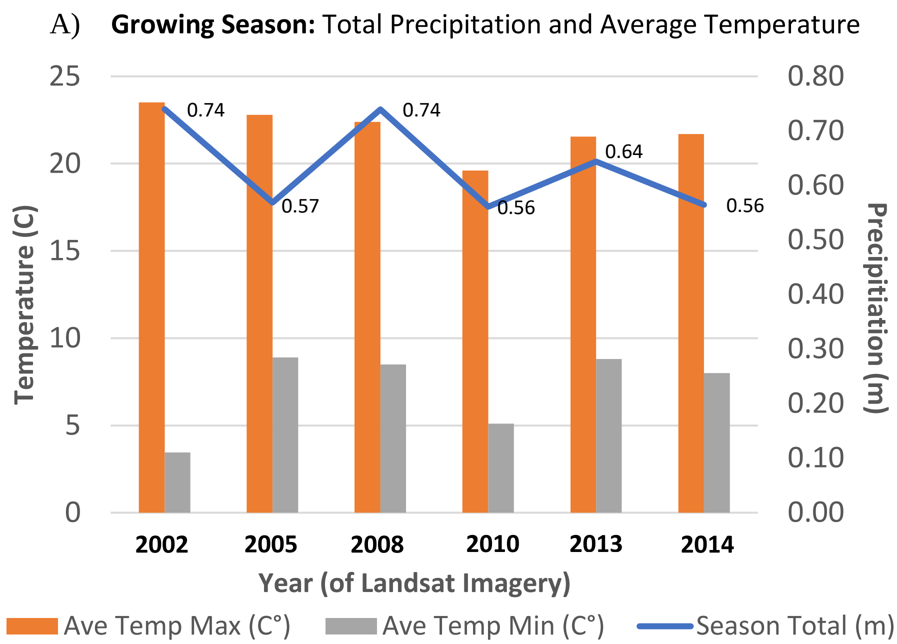

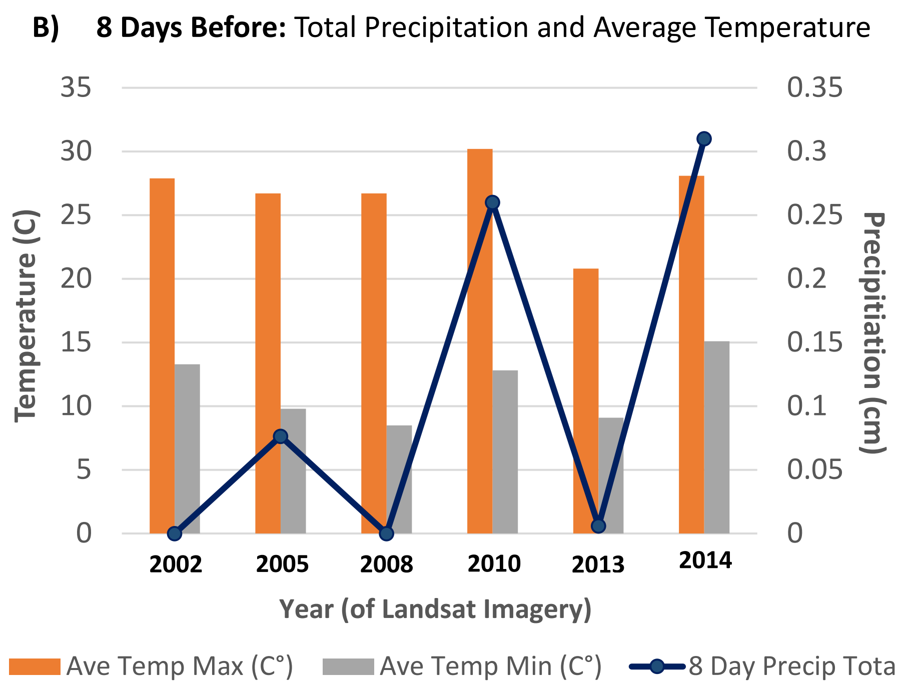

Figure 4-3: Precipitation and temperature data from the Waynesburg, PA climate data station. A) Total precipitation and average temperature from March through September of the respective year of the imagery. B) Total precipitation and average temperate for the 8 days preceding imagery acquisition.

Climate conditions were consistent year to year (Figure 4-3a). Mean total rainfall between March and September was 0.64m (±0.1) (Figure 4-3a). Average maximum temperature among all growing seasons was 21.9°C (±1.4) with an average minimum of 7.1°C (±2-3) (Figure 4-3a). However, the eight-day precipitation totals and temperature averages suggests there may have been precipitation in Waynesburg, PA on the day several of the images were acquired (2002, 2010, and 2014) (Figure 4-3b). The Waynesburg PA climate station is not located in the mined area, but approximately 20km east and may not be representative of the conditions present in the scene analyzed. NEXRAD WSR-88D and TDWR radar data from the Pittsburgh NEXRAD site was used to determine if rainfall fell on imagery acquisition dates after 2009. Light rainfall (<0.01 in/hour) was present adjacent to, but not directly over the analysis areas the day of acquisition for the 2014 image. The remaining 2010 and 2013 images did not contain rainfall the day of acquisition. It is not clear if precipitation occurred over panels mined before 2009 in the hours before the images were acquired, however the imagery was predominantly cloud free and if rainfall occurred it may have occurred later in the day. The NEXRAD data indicates that rainfall was unlikely during imagery acquisition after 2009.

The NDMI values varied little among years, with the largest deviation occurring in 2013 (Figure 4-4). The 179,572 pixels representing forest canopy were originally evaluated individually, comparing landscape features and mining activity on a pixel by pixel basis. This approach resulted in differences in average pixel canopy moisture content that were small and strongly overlapping (Figure 4-4). The range of NDMI values for 2013 are below 0.3, while the other four years are between 0.3 and 0.4. (Figure 4-4). The difference observed for 2013 is most likely due to canopy differences, as the 2013 image was acquired toward the end of the month on September 26th, while the others were all acquired on and before September 11th. Because the

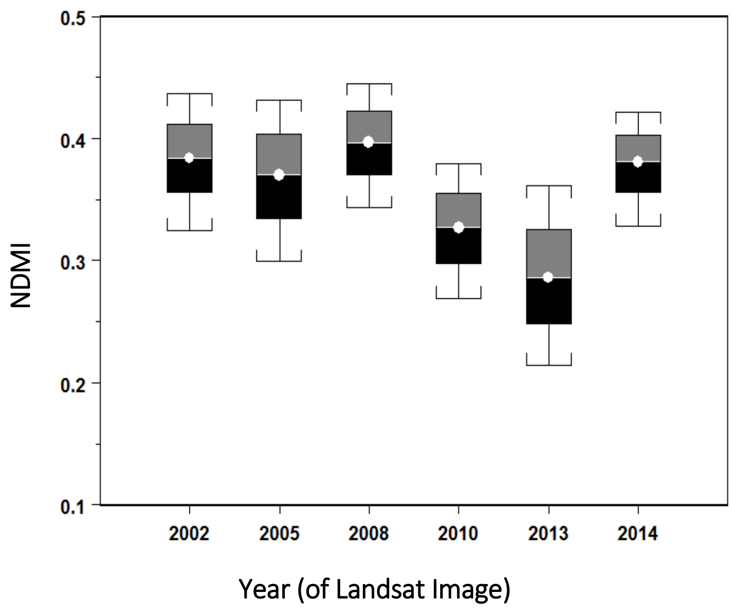

Figure 4-4: Annual data ranges of the 179,572 forest pixels utilized in this study (the top and bottom 10% of the data were excluded to remove extreme values from the plot). Most means fall between 0.3 and 0.4, while 2013 is below that range. The difference between the 2013 image and the others is most likely due to leaf senescence as it was acquired on September 26 while the others were acquired September 3 – September 11.

2013 image was acquired toward the end of the month, the beginning of autumn tree leaf senescence is likely to reduce canopy moisture. Relationships between pixel attributes (e.g. elevation, aspect, slope, topographic index, hillslope curvature, mined/unmined) and NDMI values were explored, but no patterns were found.

4.2.3 Analysis

Due to the noise in the pixel level analysis, forest patches were instead used as analysis units. Investigation of forest patches examines values in reasonable spatial areas as a unit, removing some of the noise that exists at the pixel scale as each patch represents a mean value for the population of pixels within it. The undermined and adjacent areas were divided into five groups of patches (i.e., patch analysis areas) for this study. These areas represent three distinct mining histories: unmined, Bailey and Enlow analysis areas mined 2002-2014 (Bailey and Enlow analysis areas), and the historically mined pre-2002 analysis areas. Patches were initially delineated using the 2006 National Land Cover Dataset (NLCD) (Fry et al. 2011). Pixels representing forest cover were converted into polygons. The 30m resolution of NLCD data created substantial mismatches in the extent of forest patches when compared with high resolution (< 1m) aerial imagery (Fry et al. 2011). To eliminate these mismatches and minimize edge effects, 60 meters were removed from the edge of each polygon. Finally, the NDMI raster pixels inside the delineated patches were

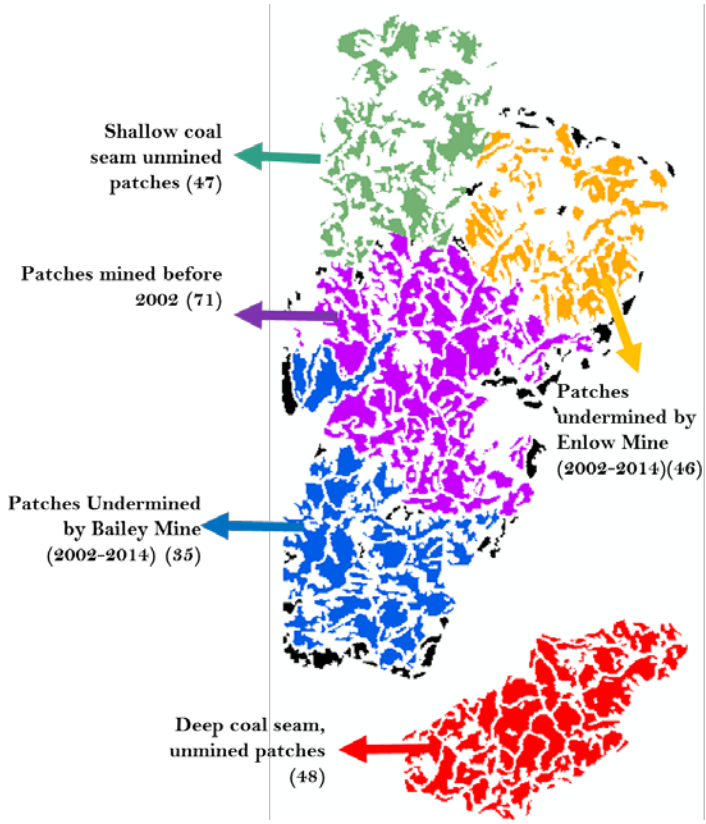

Figure 4-5: Forest patch analysis areas derived from the 2011 NLCD LULC classification. Black areas are patches adjacent to mining and were not included in this analysis.

converted to points that represented NDMI data values for each year of Landsat data included in this study (2002 – 2014) (Figure 4-5). These points were then further checked against high resolution aerial imagery and points overlying areas without mature tree cover were deleted from the dataset. Areas without sufficient canopy cover will produce a NDMI value not representative of tree canopy moisture.

Local modelling can identify spatial variations within heterogeneous spatial patterns. Here, the Getis Ord Hot Spot Analysis tool was applied to the NDMI point data in ArcMap to identify spatial clusters of high values (hot spots) and low values (cold spots) by comparing each point to its neighbors within a defined neighborhood distance (112 m in this case, the average distance to 30 nearest neighbors). All NDMI points representing forest cover that remained after the data processing described above were analyzed for "hot spots" of both relative wetness and dryness (Getis and Ord 1992). The Hot Spot tool corrects for *multiple testing* and *spatial dependency* by applying the *false discovery rate correction*. *Multiple testing* is a condition that occurs when spatial patterns appear clustered or structured and based on probability theory the patterns are assumed to be significant ($P>0.05$), when in reality the underlying spatial processes driving them are actually random. *Spatial dependency* describes the tendency of local data to be similar and therefore inflate statistical significance. *The false discovery rate correction* will estimate the number of false positives that can occur due to these two sources of error and adjust the critical P- values as a result. The Hot Spot Analysis tool outputs a shape file indicating the level of statistical significance of each point by confidence level: not significant, 99%, 95%, and 90%. For this study, only the cold and hot points within the 99% confidence level ($p <= .01$) were considered, as they represented the most significant relatively driest points and wettest points in the canopy for each forest patch. The hotspot analysis was run for each LANDSAT image year, for all of the pixels within the forest patches. Once completed, the proportion of dry (cold spots) and wet (hot spots) pixels in each forest patch were determined (Beyer 2012). Further data were extracted for each forest polygon including: depth to the top of the Pittsburgh coal seam, land surface elevation statistics (mean, min/max) of each patch, and the year the majority of each patch was undermined.

To quantify the dryness/wetness of each patch relative to the entire study region and therefore allow comparison among years, the patches were normalized for each year and each patch. The proportion of dry and wet pixels per patch were normalized by the proportion of dry and wet pixel for each scene: i.e., divide the wet/dry proportion of the patch by the wet/dry proportion of the patch analysis areas within the entire scene. The resulting normalized pixel proportion values per patch were used for both patch and patch area analysis. Areas consistently categorized as wet or dry over all six years of imagery were also identified and tracked, in order to characterize persistent canopy moisture patterns.

4.3 RESULTS

4.3.1 Dry Pixel Proportions

Many landscape characteristics can influence tree canopy moisture (e.g. aspect, slope, hillslope, and curvature) and due to high spatial correlation, these characteristic patterns can be difficult to interpret at broad spatial scales. However, certain patterns of canopy dryness across patches are apparent (Figure 4-6a). As mining progressed, dry pixel proportion of forest patches seemed to increase, particularly in the Bailey Deep Mine (BDM) region of the study area (Figure

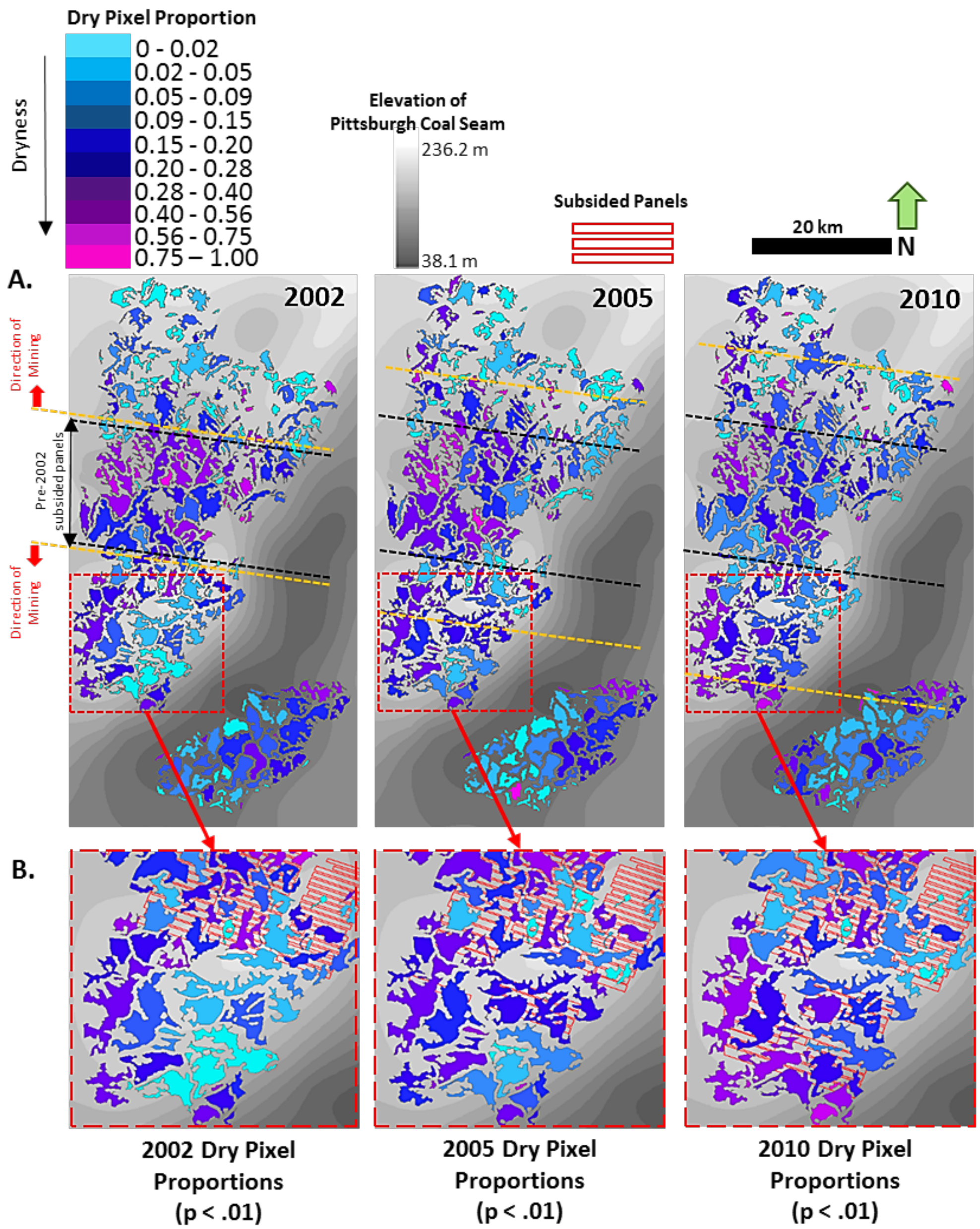

Figure 4-6: A) This panel shows the increasing proportion of dry pixels per each forest patch as mining progresses. The red dashed lines represent the progress occurring from 2002 – 2010. The Black dashed lines and the area between them represent mining that occurred before 2002. The p – values are from the Getis Ord hot spot analysis and indicate the level of statistical significance of the dry pixels used for the analysis. B) This panel is a closer look at the area indicated by the grey dashed circle in panel B. This panel shows the pattern increasing dry pixel proportion following the shallow coal seam in that area, where depth to coal is ≤ 200 meters. Mined panels are indicated in red.

4-6a & 4-6b). These increases are not apparent in the Enlow Fork Mine to the north (Figure 4-6a). When normalized mean dry pixel proportions are compared to the depth of mining, the pattern of increasing patch dryness is spatially coincident with the shallow coal contours of the mined coal seam itself, with some of the driest patches located over the shallowest parts the coal seam (Figure 4-6b).

Normalized mean proportions of dry pixels for each analysis area were compared against year of imagery (Figure 4-4). The changes in normalized mean proportion of dry pixels observed during the study period varied with mining history among the patch areas. Mean dry pixel proportions of patches mined between 2002 – 2013 were compared to unmined forest patches with similar coal depths (Bailey Deep Mine, <200m and Enlow Fork Mine, >200m). Mean dry pixel proportions for the unmined forest patches (shallow control and deep control patch areas) differed in both ranges of values and trends over time (Figure 4-7A and 4-7B). The mean dry pixel values for the shallow control forest patches increased from 2002 to 2014, with values ranging from 0.37 – 0.97 (Figure 4.7a). The shallow control and Bailey patches mean dry pixel proportion values both increased through the study period (Figure 4.7). The Bailey patches also had higher mean proportions of dry pixels than the shallow control patches, with all mean pixel proportion values for all years greater than 0.72. The shallow control patches were more variable, with proportions for 2002, 2005, and 2013 as 0.37, 0.64, and 0.38 respectively and all other values at 0.83 and higher (Figure 4-7A). Enlow Fork mine was similar to the deep control patches in that the mean pixel proportions did not increase or decrease with time (when excluding 2013). However, the Enlow patches dry pixel proportion values were notably higher than the mean proportions of the deep control patch, with values ranging from 0.63 – 0.73 (excluding 0.20 for 2013) (Figure 4-7). The deep control patches had mean dry pixel proportion values ranging from 0.34 – 0.57. The

2013 values for the deep control patches fell within that range (Figure 4-7d). Finally, the pre-2002 patches had the highest values of mean dry pixel proportions overall with a range of 0.96 – 1.3 (Figure 4-7e). There was a decreasing trend in dry hotspots over time for the pre-2002 mined patches (Figure 4-7e).

4.3.2 Wet Pixel Proportions

The normalized mean proportions of wet pixels were also compared among analysis areas, to detect changes in canopy moisture that might be associated with mining disturbance. Normalized mean wet pixel proportions in the shallow control patches decreased over time. In contrast, Bailey patches did not change over time (Figure 4-8c). The Bailey patches had the lowest values of mean wet pixel proportions of all the patch areas with values ranging from 0.27 – 0.40 (Figure 4.8c), while all of the shallow control pixel proportions tended to be higher and fell above 0.5 (0.58 – 1.21) (Figure 4-8a). The deep control patches had the highest values of mean wet pixel proportion values, ranging from 0.94 – 1.10. In comparison, the Enlow patches had a similar trend but lower mean pixel proportion values (i.e. less wet) than the deep control patches (Figure 4-8d). The pre-2002 patch areas had the second lowest mean wet pixel proportions of all the areas with values between 0.33 – 0.55 and these patches increased in mean wet pixel proportion over the study period (Figure 4-8e).

4.3.3 2013 as an Outlier

The 2013 mean NDMI value for the entire scene was lower than the other five scenes, indicating drier canopy relative to the other imagery years (Figure 4-4). However, NDMI dynamics represented in this study as normalized mean pixel proportions, varied among the patch analysis areas, as the Enlow and shallow control patch areas had normalized dry pixel proportion means lower relative to other years, indicating those regions have a relatively wetter forest canopy (Figure 4-7). The Enlow and shallow control analysis areas also have higher normalized mean wet pixel proportion values for 2013 in comparison to the other analysis areas (Figure 4-8). Differences in wet and dry pixel proportion values between the Enlow and shallow control and the other analysis areas may also be due to differences in forest patch size and distribution among the analysis areas. Overall, based on the lower mean NDMI value for the entire scene and potential differences due to leaf senescence, 2013 was considered an outlier for this study and trends in the proportion of dry and wet pixels over time were calculated both with and without 2013 (Figures 4-7&4-8).

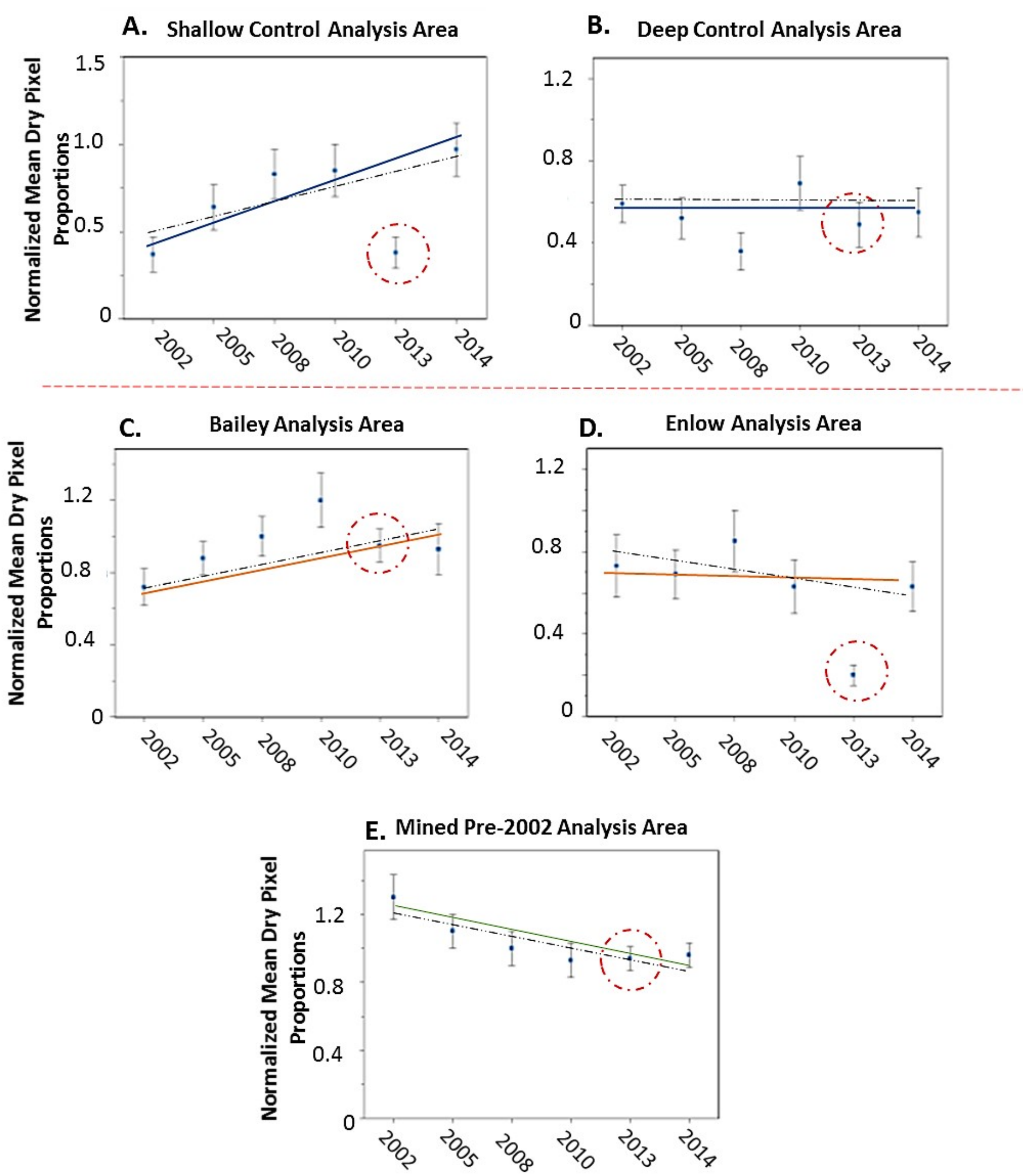

Figure 4-7: A) Normalized mean proportion of dry pixels of forest per year of imagery. B) Normalized mean proportion of dry pixels of forest patches for the deep control patch area, per year of imagery. C) Normalized mean proportion of dry pixels of forest patches for the Bailey patch area, per imagery year. D) Normalized mean proportion of dry pixels of forest patches overlying Enlow Fork Mine, per imagery year. E) Normalized mean proportion of dry pixels of forest patches for mined pre-2002 analysis area, per imagery year. Error bars represent the standard error of the mean. The solid line represents the trend calculated without 2013 and the dashed line is with 2013 included.

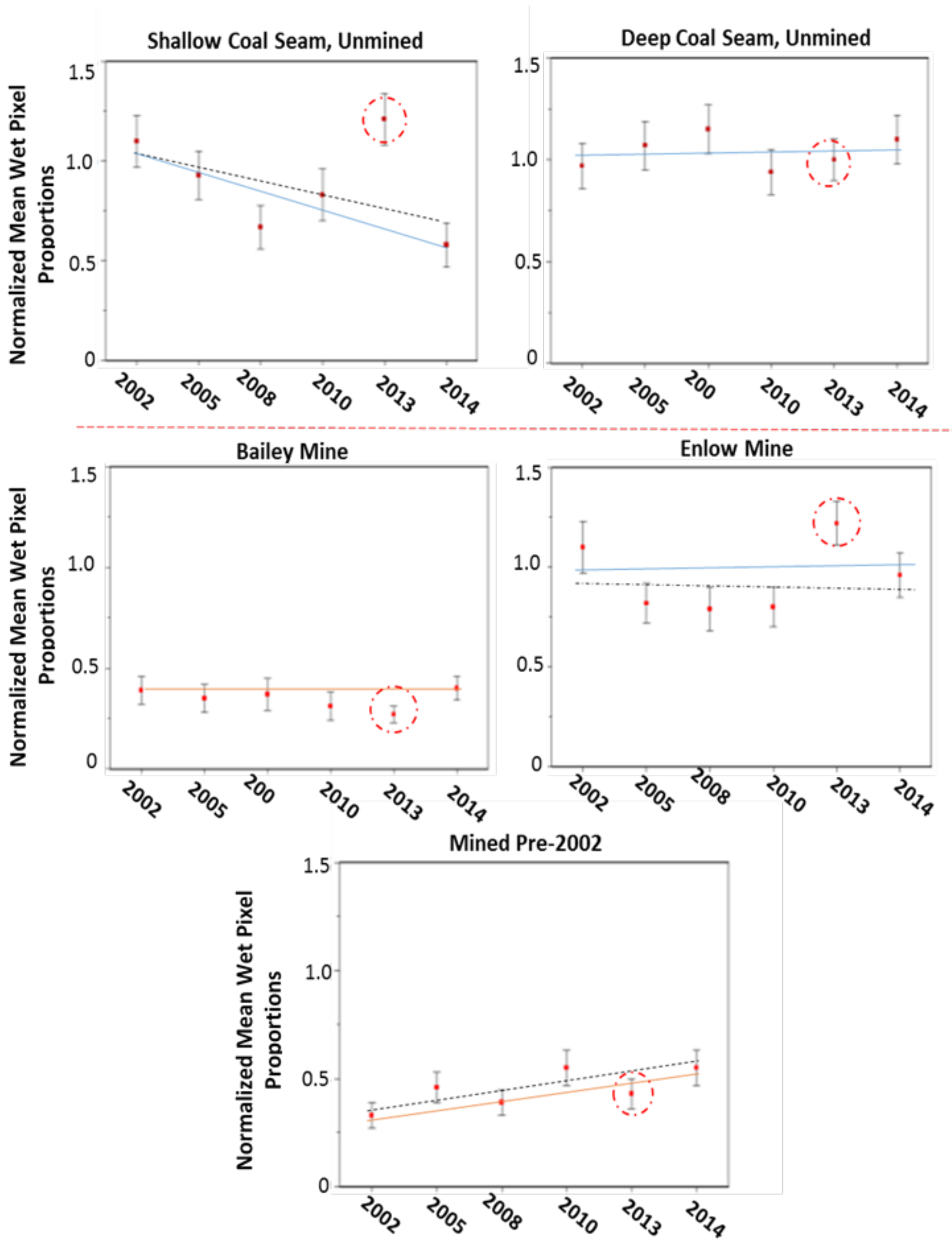

Figure 4-8: A) Mean proportion of wet pixels of forest patches overlying a shallow unmined coal seam, per year of imagery. B) Mean proportion of wet pixels of forest patches overlying a deep coal seam, per year of imagery. C) Mean proportion of wet pixels of forest patches overlying Bailey Mine, per imagery year. D) Mean proportion of wet pixels of forest patches overlying Enlow Fork Mine, per imagery year. E) Mean proportion of wet pixels of forest patches overlying coal seams mined pre-2002, per imagery year. Error bars represent the standard error of the mean. The solid line represents the trend calculated without 2013 and the dashed line is with 2013 included. The error bars represent the standard error of the mean.

4.3.4 Consistently Wet and Dry Areas

Bailey and the pre-2002 patches differed substantially from the other patch areas in the percentage of pixels consistently categorized as significantly wetter or drier over all six years of imagery (Figure 4-9). Bailey and the pre-2002 patch areas had the highest percentage of pixels consistently categorized as "dry" over all six years used for this study (Figure 4-9). The deep control and the Enlow patches were more similar to each other with 1.8% and 1.6% consistently dry pixels respectively and 15.3% and 15.4% consistently wet pixels respectively (Figure 4-9). The shallow control patches had a higher percentage of consistently wet pixels then than dry pixels as well, with 7.9% consistently wet and 2.2% consistently dry (Figure 4-9).

The average value of topographic characteristics (e.g. slope and aspect) associated with consistently wet and dry pixels did not differ between the two groups, except for elevation. Consistently dry pixels occurred at lower elevations with mean elevation values per patch area at 350 – 375 meters, while consistently wet pixels occurred at higher mean elevations ranging between 400 and 450 meters (Figure 4-10). Mean elevations of the consistently wet and consistently dry pixels were similar across analysis areas (Figure 4-10). Elevation range and patch size for consistently dry pixels revealed differences at the patch scale among the analysis areas. Specifically, consistently dry pixels in the more developed northern part of the study region (Enlow and the shallow control) tend to occur higher in elevation than consistently dry pixels in the Bailey and pre-2002 analysis areas (Figure 4-11d & 4-11e). The broadest elevation ranges of consistently dry pixels occurred in the Bailey and pre-2002 analysis areas, with patches containing the consistently dry pixel elevation minimums lower than all other patch areas (Figure 4-11a & 4-11b). The deep control patches also had relatively broader ranges of elevation for consistently dry pixels than the other patch analysis areas, but fell within a range of elevation higher than those occurring in the Bailey and pre-2002 patches, potentially due to land use and local relief (Figure 4-11a, 4-11b, & 4-11c). In contrast, the shallow control patches and Enlow patches were similar in both the size distribution of patches and the elevation of the consistently dry pixel ranges (Figure 4-11d & 4-11e). The pixel ranges for these two patch areas were narrow in comparison to the ranges of the other three patch areas, and the patches were smaller (Figure 4-11).

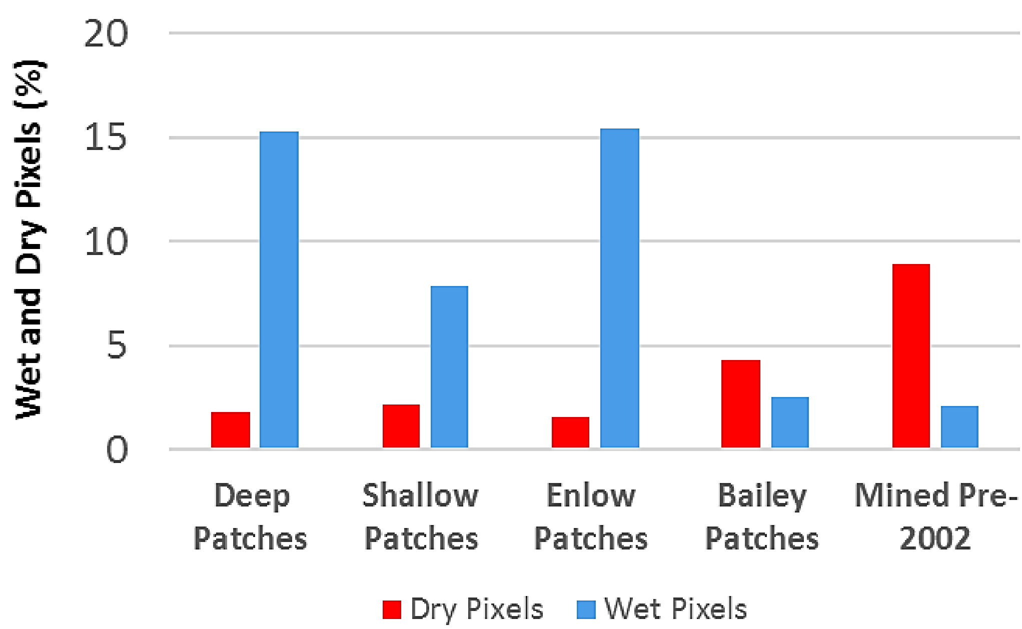

Figure 4-9: Percentage of pixels consistently categorized as wet or dry within each analysis area in all six years of imagery used. Red represents consistently dry pixels and blue represents consistently wet pixels.

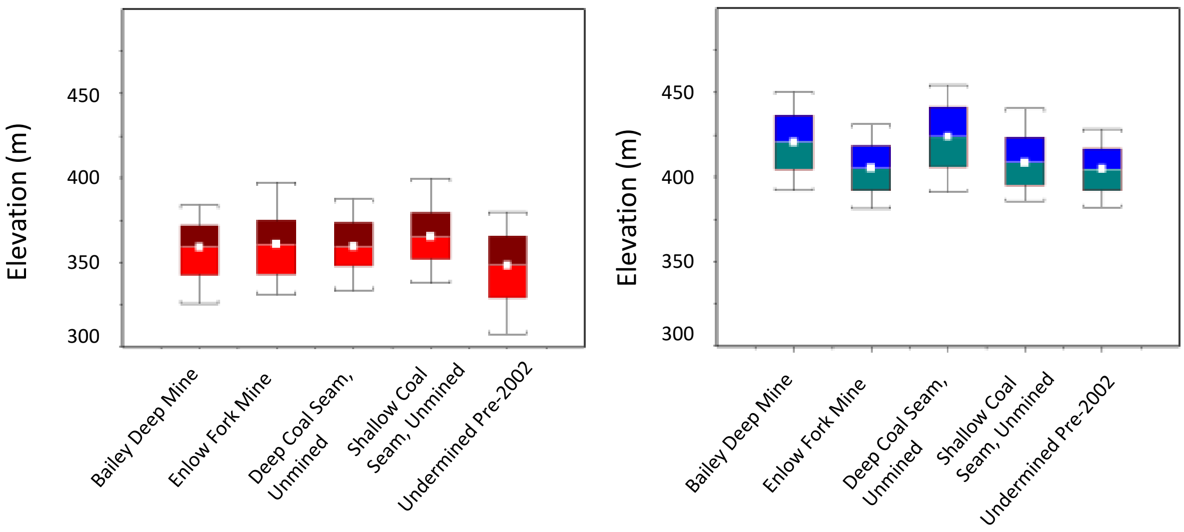

Figure 4-10: Boxplots showing elevation of the pixels consistently categorized as "wet" or "dry" for all six Landsat images. Consistently dry pixels (shown in red) occur at lower elevations then the consistently wet pixels (shown in blue).

Consistently wet pixels seem to occur relatively higher in elevation than consistently dry pixels, and the elevation range of the consistently wet pixels are more similar over all the patch analysis areas (Figure 4-12). There was also less difference in the range of elevation of the persistently wet patches between patch areas than the persistent dry areas between patch areas (Figure 4-11 & Figure 4-12). For all 5 patch analysis areas, the consistently wet pixels are located at or near the topographic highs.

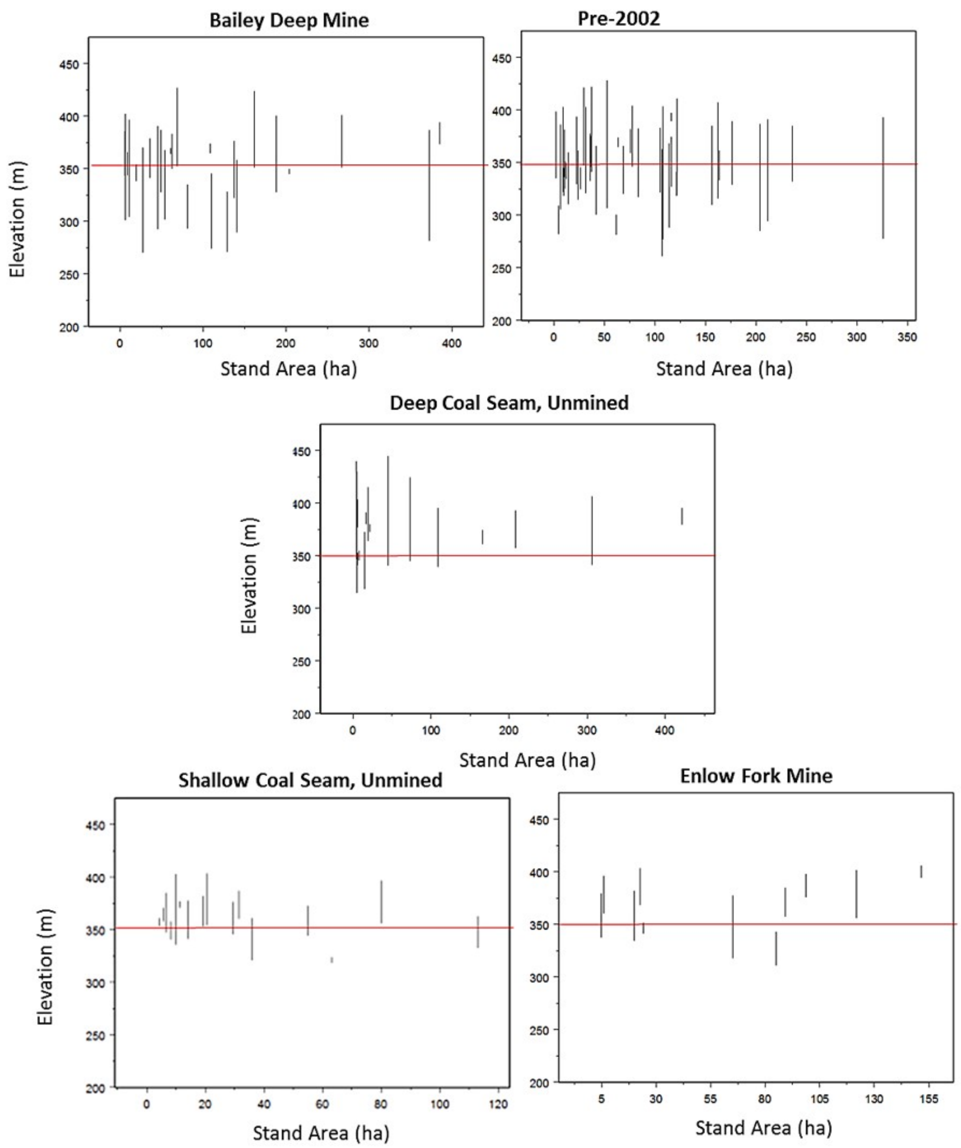

Figure 4-11: Plot depicting the elevation range of pixels consistently categorized during the Getis Ord G* hot spot analysis as significantly dry. Each elevation range line represents a forest patch containing consistently dry pixels within a given stand mosaic. The red line at 350 meters is for reference, to aid comparison. A) Elevation range of constantly dry pixels within the Bailey patch area. B) Elevation range of constantly dry pixels within stands of the pre-2002 patch area. C) Elevation range of constantly dry pixels within stands of the deep control patch area. D) Elevation range of constantly dry pixels within stands of the shallow control patch area. E) Elevation range of constantly dry pixels within stands of the Enlow patch area.

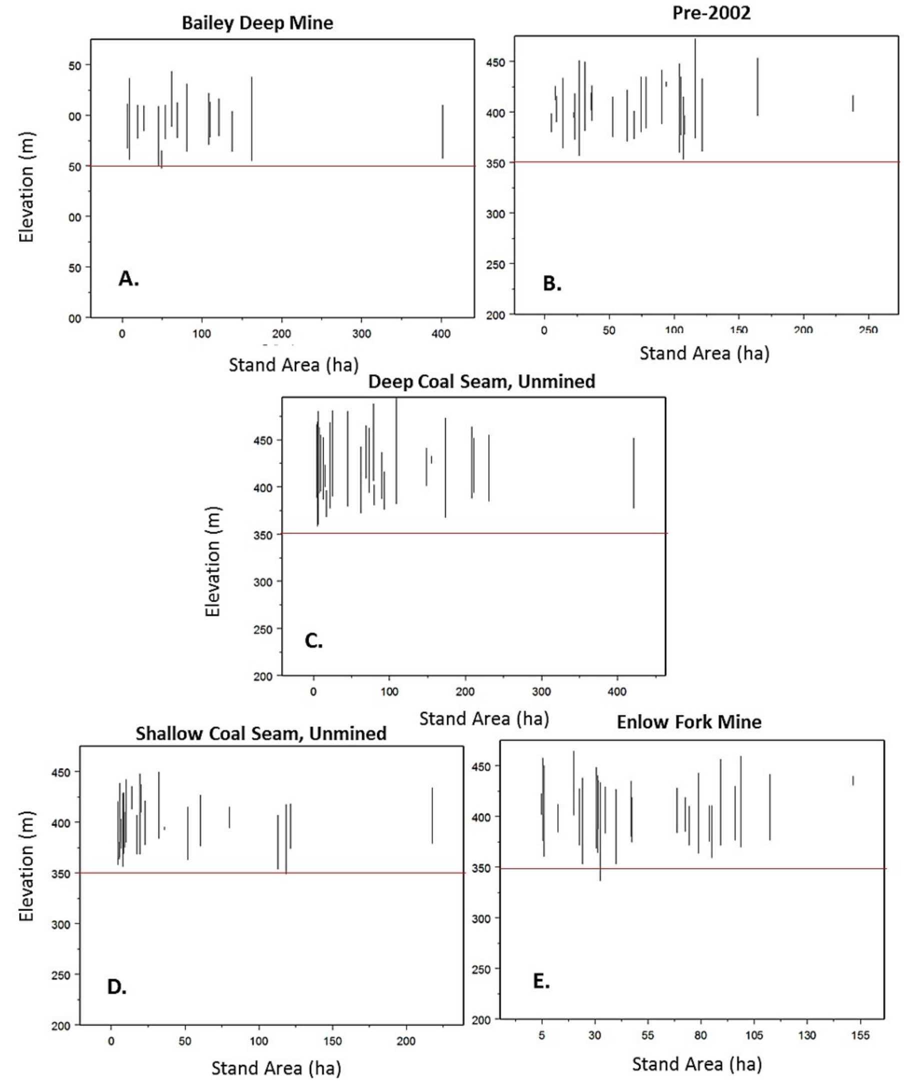

Figure 4-12: Plot depicting the elevation range of pixels consistently categorized as significantly wet during the Getis Ord G* hot spot analysis. Each elevation range line represents a stand containing consistently wet pixels with a given stand mosaic. The red line at 350 meters is for reference, to aid comparison. A) Elevation range of constantly wet pixels within stands of the Bailey patch area. B) Elevation range of constantly wet pixels within stands of the pre-2002 patch area. C) Elevation range of constantly wet pixels within stands of the deep control patch area. D) Elevation range of constantly wet pixels within stands of the shallow control patch area. E) Elevation range of constantly wet pixels within stands of the Enlow patch area.

4.4 DISCUSSION

4.4.1 Patch Fragmentation in Northern Areas

The differences in spacing and the size of the patches within each analysis area may affect canopy moisture patterns and the interpretation of the results. Increased suburban development in the northern part of the study area has led to smaller and more widely spaced patches that occur at higher elevations (i.e. hilltops) within the Enlow and shallow control patch areas (Figures 4-2,4-12, & 4-13). The smaller patch sizes may explain the low 2013 dry pixel proportions observed in the Enlow and shallow control areas, as wetter pixels tend to be located near or on hilltops, with drier pixels more commonly occurring on the hillslopes (Figure 4-8a & 4-8d). Hillslope hydrology differs from hilltop hydrology and a lack of forests on hillslopes makes changes in canopy moisture difficult or impossible to detect, particularly with respect to LMS (Figure 4-14)(Kozar et al. 2012). Changes to canopy moisture in LMS impacted regions with limited forest cover may not be comparable to regions with greater forest cover. Therefore, land use differences may have a strong influence on canopy moisture dynamics in the region that the Enlow and shallow control patches occupy, and should be considered when interpreting the results.

4.4.2 Longwall Mining Impacts to Canopy Moisture

Overall, mined areas were drier than unmined areas. The mined analysis areas had higher normalized mean dry pixel proportion values than the unmined patches, with the pre-2002 patch area having both the highest dry pixel proportion means and longest mining history out of all the patch areas. Any decreases in ground water elevation resulting from subsidence are likely to increase the efficiency of soil water drainage and thus result in drier soils. The Bailey patch area had higher dry mean pixel proportions than the Enlow, shallow control, and deep control patch areas. Hydrological impacts of longwall mine subsidence to canopy moisture may also be magnified by shallower depths to the mined coal seam, as the fractured zone can extend closer to the surface (Bian et al. 2008; Holla 1997; Iannacchione et al. 2008; Matetic, Liu, and Elsworth 1995). The Bailey patches were mined 2002 -2014, with a majority of the mining between 2002 and 2010 from a shallow coal seam. This study identified relatively higher normalized dry pixel proportions in these areas than in deeper mined areas. For example, in the Enlow patch area, over a deeper mined coal seam, dry mean pixel proportions were lower than Bailey and similar to the deep control mean dry pixel proportions (Figure 4-7). The dry normalized mean pixel proportions results indicate that a history of mining and depth to the mined coal seam influence canopy moisture patterns.

4.4.3 Distinct Landscape Position of Wet and Dry Areas

Patterns of consistently wet and dry pixels suggest that longwall mining impacts hillslope flow paths, particularly in mid to bottom slope areas. Persistently wet areas are generally on or near the hilltops for all analysis areas, while the consistently dry areas are located on the hillslopes (Figure 4-10). At the patch scale, consistently dry pixels occur at different elevation ranges dependent on mining history (Figure 4-11). For example, patches in the mined Bailey and pre-2002 areas occur over a broader range and at lower elevations than the other 3 areas (Figure 4-11). In contrast, the ranges for the Enlow patches and the shallow control patches are narrower than the ranges of Bailey, pre-2002, and deep control patches (Figure 4-11). This pattern is not likely due

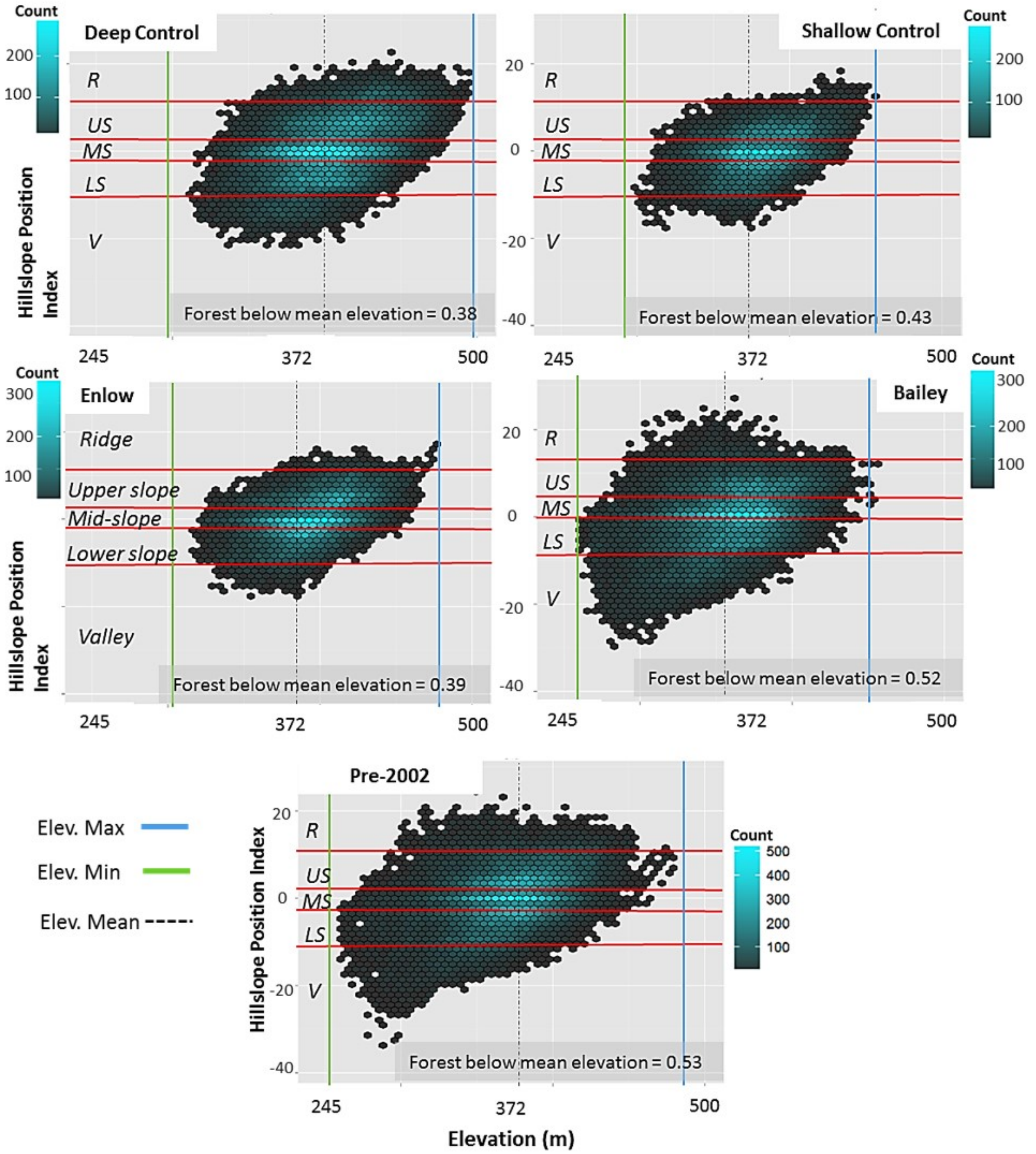

Figure 4-13: Each hexagon contains multiple points, with the point count increasing with increasing intensity in color of the pixel. The y-axis depicts hillslope position as red lines: valley (V), lower slope (LS), mid-slope (MS), upper slope (US), and ridge (R). The x-axis depict elevation above MSL in meters. Min, mean, and max) elevation of the patch area each plot represents is symbolized by a green, dashed, and blue line respectively. Each plot represents a patch area: Deep Control, Shallow Control, Enlow, Bailey, and pre-2002.

3 areas (Figure 4-11). In contrast, the ranges for the Enlow patches and the shallow control patches are narrower than the ranges of Bailey, pre-2002, and deep control patches (Figure 4-11). This pattern is not likely due to difference in response to LMS. The narrow elevation ranges eem to arise from land use differences, as clearing of forests for suburban development in the northern analysis areas results in smaller forest patches that are located relatively higher in the landscape (Figure 4-13). In addition, when comparing patches over similar mining depths (i.e. Bailey and pre-2002 patch areas to the deep control) elevation ranges of the persistently dry pixels of the deep control patches occur at higher positions on the hillslope then than the Bailey and pre-2002 patches (Figure 4-11).

In contrast to the consistently dry pixel distributions, the persistently wet pixels vary minimally in elevation ranges among all five analysis areas, regardless of mining history and land use differences (Figure 4-12). For all five patch areas, the elevation ranges at which the wet pixels occur are similar in both location and size (Figure 4-12). The contrast between consistently wet pixel vs consistently dry pixel elevation ranges suggests differences in ground water flow path characteristics cause differences in hydrologic response. For example, fracture networks that influence drainage networks and hillslope moisture conditions should react differently to subsidence than more intact bedrock.

Hillslopes of the Appalachian plateau contain networks of stress relief fractures formed by the down cutting of streams (Figure 4-14) (Kozar and Mccoy 2012; Wyrick and Borchers 1981). Recharge is thought to occur through the hilltops and then flow laterally through the shallow stress relief fractures toward the valley floors (McCoy and Kozar 2007; Sheets and Kozar 2000). Longwall mine subsidence can potentially alter these shallow subsurface flow path fracture networks through further extension or compression, changing established flow paths and disturbing shallow groundwater sources (e.g. strata aquifers, Figure 4-14). Longwall mining has been shown to cause a downslope shift in water supplies, with groundwater wells and springs located on hillslopes and on hilltops being most affected by longwall subsidence (Booth 2006; Elsworth and Liu 1995). In this data set the pre-2002 and Bailey patch areas have more consistently dry areas that are located further down slope than the control analysis areas. In summary, LMS seems to generate drier areas on hillslopes and these areas seem to be further downslope when compared to control areas.

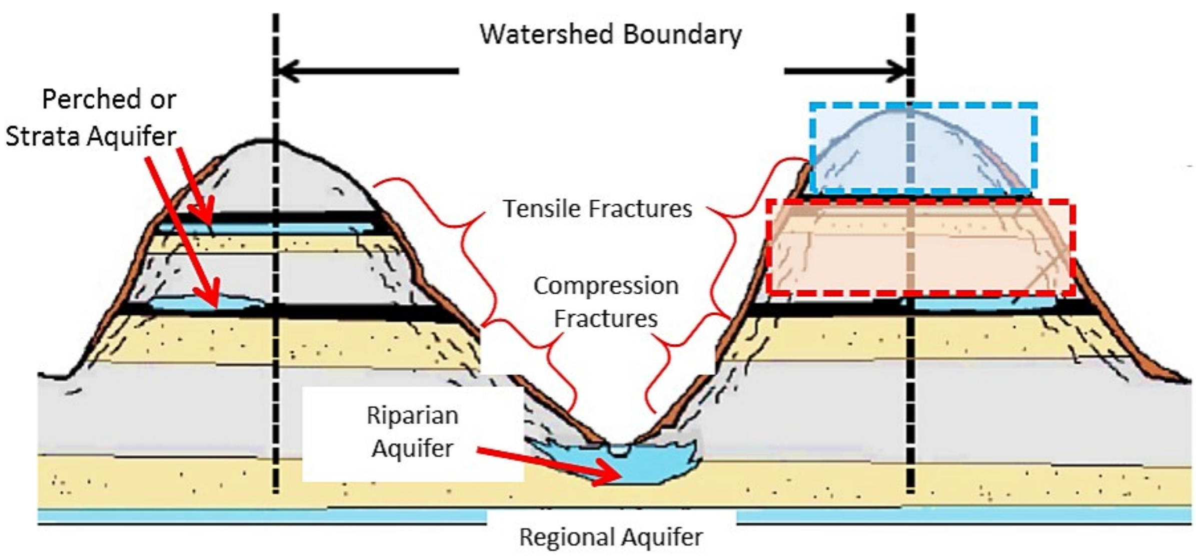

Figure 4-14: Conceptual model showing watershed boundaries and ground water aquifers of the Appalachian plateau based on Sheets and Kozar, 2000. The model also depicts tensile and compression fractures that form as a result of stream erosion. The blue box represents the spatial location of the consistently wet pixels and the red box represents the spatial location of consistently dry pixels on the landscape.

4.4.4 Hydrological Healing Not Apparent

One of the reasons that soil moisture impacts are relatively undocumented in Pennsylvania is that it is commonly assumed, though poorly established, that the hydrological impacts overlying longwall mine subsidence recover within 4-5 years following subsidence (Iannacchione et al. 2008). The presumed phenomenon of "hydrological healing", in which sediment deposition eventually reduces the increased porosity present following subsidence and re-establishes pre-existing hydrological conditions, is not consistent with our observations. This analysis indicates that longwall mining effects on hydrology can persist beyond this 5-year time frame. In particular, areas mined before 2002 have a relatively drier tree canopy than the other four patch analysis areas, some of them mined more recently. Specifically, the pre-2002 patch area had the lowest mean wet pixel proportion values and highest mean dry pixel proportion values out of all five patch analysis areas (Figure 4-7e & Figure 4-8e). The pre-2002 patch area also has the most consistently dry pixel areas and the least consistently wet pixel areas (Figure 4-10). These results suggest that changes to ground water following longwall mine subsidence are more persistent and have more of an impact to overlying ecosystems than what is currently anticipated.

4.4.5 Role of Geology in Consistently Wet/Dry Areas

The bedrock geology of the study region may influence hydrology and impacts following longwall mine subsidence. Though most of the study region's forests are underlain by the Greene formation, stream incision has exposed several other formations (Figure 4-15 & 4-16). The

Washington Formation underlies the Greene formation and is the bedrock for hillslopes in areas with deeper stream incision, particularly in the Bailey Mine and pre-2002 analysis area (Figure 4-16). Most consistently dry areas are found within the patch areas where the Washington formation bedrock is exposed (Bailey and pre-2002). A 60-meter buffer on each side of the Washington formation upper boundary was used to identify consistently dry areas that may by hydrologically connected to the Washington formation (Figure 4-17). The majority of consistently dry areas intersect sections of hillslope underlain by the Washington Formation, with 141 over the pre-2002 patch area and 75 located over the Bailey patch area. This suggests the Washington Formation, particularly strata near the formation top, may have properties that can disproportionally increase groundwater drainage (and therefore soil water drainage), following

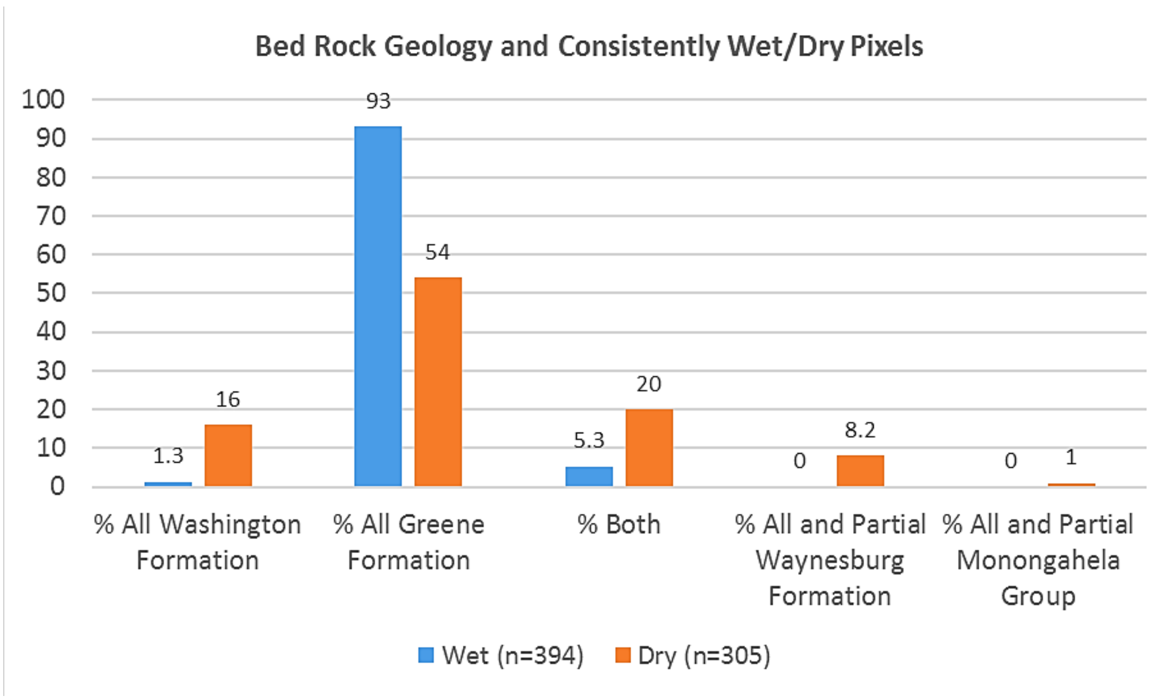

Figure 4-15: Percentage of bedrock geology type underlying consistently wet and dry areas. Twelve consistently dry areas and 5 consistently wet areas were not included in the percentage calculations due to missing geology data.

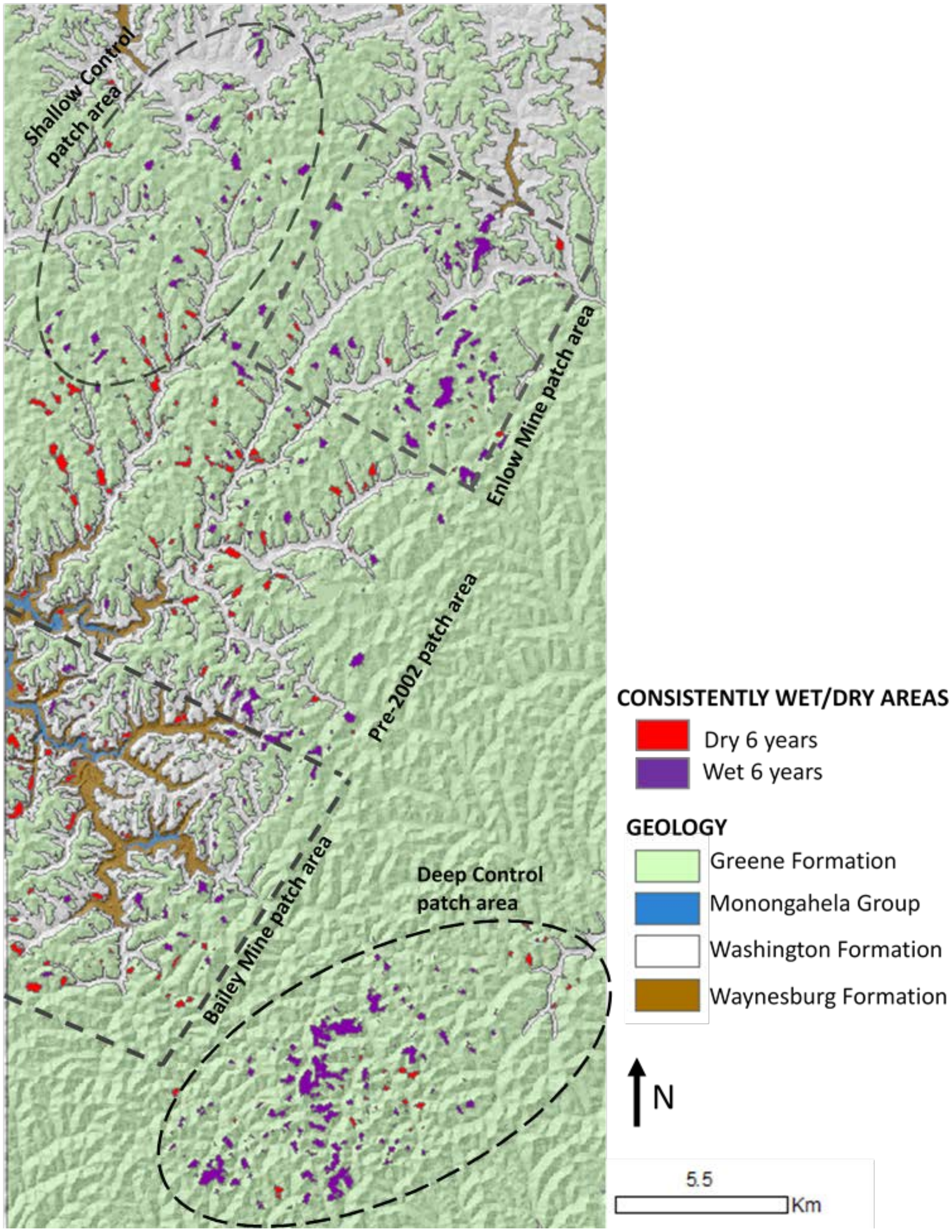

Figure 4-16: Map depicting bedrock geology of the study region. The red polygons represent areas that have been consistently categorized as "dry" for all six years and the purple polygons represent areas that have been categorized as "wet" for all six years. The Bailey, Enlow, shallow control and deep control patch areas are outlined in black dashed lines for reference. The pre-2002 patch area is not outlined.

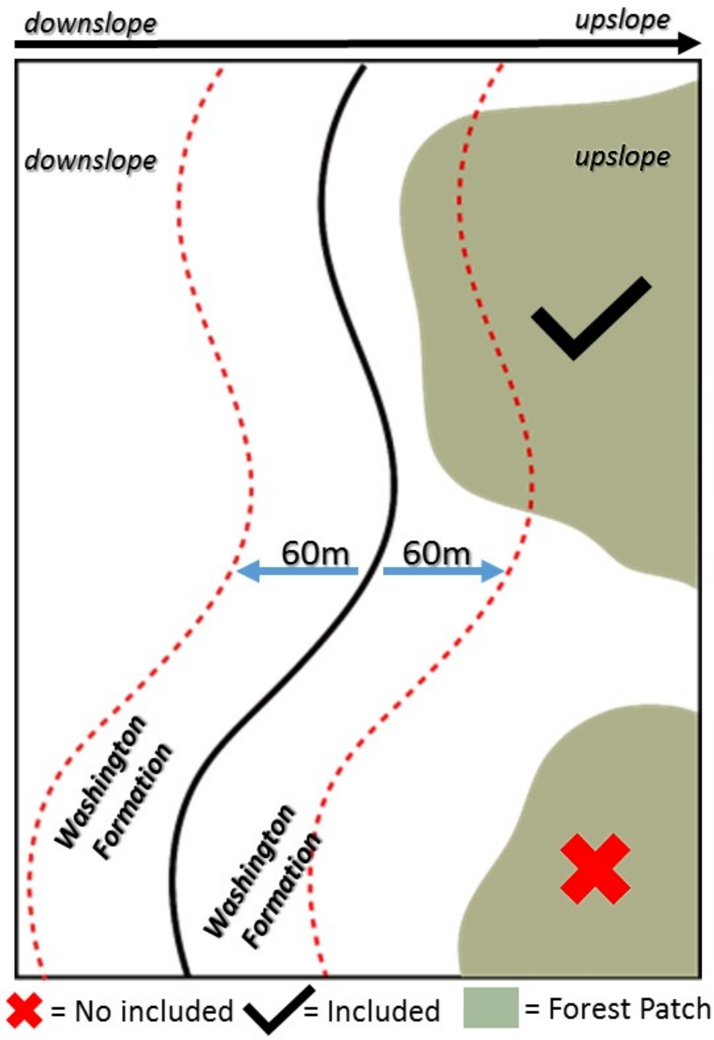

Figure 4-17: Method of selecting forest patches potentially influenced by the upper limestone boundary of the Washington formation. A 60m buffer on each side of the Washington formation upper boundary is indicated by the red dashed lines.

subsidence. The upper limestone member (e.g. rock type) of the Washington Formation is 15 – 60 cm thick and weathers easily when exposed to water (Newport 1973). Longwall mine subsidence may create new or enhance existing flow paths within this limestone, and enhance ground water drainage in areas near the limestone. For example, 170 of the 317 consistently dry areas are within 60 meters of limestone upper boundary of the Washington Formation. All but 16 of the 170 consistently dry areas contacting the Washington formation are located over the Bailey and pre-2002 mined areas, with 95 dry areas located over the pre-2002 patch area and 75 located over the Bailey patch area (Figure 4-16). The high prevalence of the consistently dry areas in close proximity to the upper boundary of the Washington Formation in mined areas indicates an important interaction among bedrock geology, longwall mine subsidence, and canopy moisture dynamics.

4.5 IMPLICATIONS

The patterns of canopy moisture in this study reveal previously uncharacterized hydrological impacts that follow longwall mine subsidence. Overall, canopy moisture dynamics of forest patches located in areas with a history of longwall mine subsidence are relatively drier than forests located in areas without longwall mine subsidence. These results indicate areas where longwall mining had occurred over 20 years ago, had the highest dry pixel proportions and was were relatively drier than the rest of the study area, contradicting conceptual models of self-healing. Further, the distinct patterns in canopy moisture on LMS impacted hillslopes suggests evidence of impacts to existing fracture networks changing shallow groundwater flow crucial to hillslope hydrologic regimes. Specifically, variation in the hillslope position of persistently wet and dry canopy areas when compared with mining histories indicates interactions among LMS, bedrock geology, and landscape characteristics (e.g. slope) that has reconfigured shallow groundwater flow paths for extended periods.

Though longwall mining impacts remain poorly characterized in high relief regions, this study identifies patterns of canopy moisture across broad spatial scales that may explain important changes to ground and soil hydrology following LMS. These otherwise difficult to detect changes elucidate previously unknown relationships between forest canopy moisture, landscape characteristics, and longwall mine subsidence.

4.6 BIBLIOGRAPHY

Anon. 2016. "NOAA National Center for Environmental Information." Retrieved (http://www.ncdc.noaa.gov/).

Bell, FG, TR Stacey, and DD Genske. 2000. "Mining Subsidence and Its Effect on the Environment: Some Differing Examples." Environmental Geology 40(1–2):135–52.

Bernhardt, Emily S. and Margaret a Palmer. 2011. "The Environmental Costs of Mountaintop Mining Valley Fill Operations for Aquatic Ecosystems of the Central Appalachians." Annals of the New York Academy of Sciences 1223:39–57. Retrieved January 26, 2014 (http://www.ncbi.nlm.nih.gov/pubmed/21449964).

Beyer, H. L. 2012. "Geospatial Modeling Environment (Version 0.7. 2.1)."

Bian, Zheng-fu, Hai-xia Zhang, and Shao-gang Lei. 2011. "Analyses of Environmental Impacts of Underground Coal Mining in an Arid Region Using Remote Sensing and GIS." Journal of Coal Science and Engineering (China) 17(4):363–71.

Bian, Zhengfu et al. 2008. "Integrated Method of RS and GPS for Monitoring the Changes in the Soil Moisture and Groundwater Environment due to Underground Coal Mining." Environmental Geology 57(1):131–42. Retrieved January 16, 2014 (http://link.springer.com/10.1007/s00254-008-1289-x).

Booth, C. J. 2006. "Groundwater as an Environmental Constraint of Longwall Coal Mining." Environmental Geology 49(6):796–803. Retrieved February 1, 2014 (http://link.springer.com/10.1007/s00254-006-0173-9).

Elsworth, D. and J. Liu. 1995. "Topographic Influence of Longwall Mining on Ground-Water Supplies." Ground Water (33.5).

Fry, J. et al. 2011. "Completion of the 2006 National Land Cover Database for the Conterminous United States." PE&RS 77(9):858–64.

Getis, Arthur and J. K. Ord. 1992. "The Analysis of Spatial Association." Geographical Analysis 24(3):189–206.

Holla, L. 1997. "Ground Movement Due to Longwall Mining in High Relief Areas in New South Wales, Australia." International Journal of Rock Mechanics and Mining Science 34(5):775–87.

Homer, C. G. et al. 2015. "Completion of the 2011 National Land Cover Database for the Conterminous United States-Representing a Decade of Land Cover Change Information." Photogrammetric Engineering and Remote Sensing 81(5):345–54.

Iannacchione, A. et al. 2008. "The Effects of Subsidence Resulting from Underground Bituminous Coal Mining on Surface Structures and Features and on Water Resources, 2003 to 2008." 3rd Act 54 Report 2.

Kelly, Michael, Xun Luo, and Stuart Craig. 2002. "Integrating Tools for Longwall Geomechanics Assessment." International Journal of Rock Mechanics and Mining Sciences 39(5):661–76.

Kozar, Mark D. and Kurt J. Mccoy. 2012. "Use of Modflow Drain Package for Simulating Inter-Basin Transfer of Groundwater in Abandoned Coal Mines." Journal American Society of Mining and Reclamation 1(1):27–43.

Kozar, Mark D., Kurt J. McCoy, James Q. Britton, and Blake M.Jr. Bascombe. 2012. Hydrogeology, Groundwater Flow, and Groundwater Quality of an Abandoned Underground Coal-Mine. Morgantown, WV.

Li, Jianwei, Changyou Liu, and Tong Zhao. 2016. “Effects of Gully Terrain on Stress Field Distribution and Ground Pressure Behavior in Shallow Seam Mining.” International Journal of Mining Science and Technology. Retrieved (http://linkinghub.elsevier.com/retrieve/pii/S2095268615002190).

Li, Wang, Mu Yan, Zhang Qingfeng, and Zhang Xingchang. 2013. “Groundwater Use by Plants in a Semi-Arid Coal-Mining Area at the Mu Us Desert Frontier.” Environmental Earth Sciences 69:1015–24.

Liu, Xuesheng, Yunliang Tan, and Jianguo Ning. 2015. “The Height of Water-Conducting Fractured Zones in Longwall Mining of Shallow Coal Seams.” Geotechnical and Geological Engineering 693–700. Retrieved (http://dx.doi.org/10.1007/s10706-015-9851-2).

Masek, JG et al. 2006. “A Landsat Surface Reflectance Data Set for North America, 1990-100.” IEEE Geoscience and Remote Sensing Letters 3:68–72.

Matetic, R. J., J. Liu, and D. Elsworth. 1995. Modeling the Effects of Longwall Mining on the Ground Water System.

McCoy, Kurt J. and Mark D. Kozar. 2007. Relation of Chlorofluorocarbon Ground-Water Age Dates to Water Quality in Aquifers of West Virginia Scientific Investigations Report 2006-5221 Relation of Chlorofluorocarbon Ground-Water Age Dates to Water Quality in Aquifers of West Virginia. Reston, Virginia.

Newport, Thomas G. 1973. Water Resources Report 35 Summary: Ground-Water Resources of Westmoreland County, Pennsylvania.

Palmer, M. A. et al. 2010. “Mountaintop Mining Consequences.” Science 327:148–49.

Pechanec, Vilem, Ales Vavra, Martina Hovorkova, Jan Brus, and Helena Kilianova. 2014. “Analyses of Moisture Parameters and Biomass of Vegetation Cover in Southeast Moravia.” International Journal of Remote Sensing 35(3):967–87. Retrieved (http://www.tandfonline.com/doi/abs/10.1080/01431161.2013.875236).

Peng, S. S. 2008. Coal Mine Ground Control. 3rd ed. Morgantown, WV: University, West Virginia.

Sheets, Charlynn J. and Mark D. Kozar. 2000. Ground-Water Quality in the Appalachian Plateaus, Kanawha River Basin, West Virginia. Charleston, WV.

Tonsor, Stephen J. et al. 2013. The Effects of Subsidence Resulting from Underground Bituminous Coal Mining. Retrieved (http://www.dep.pa.gov/PublicParticipation/CitizensAdvisoryCouncil/Issue-Areas/Pages/Act54.aspx#.V0iAKPkrK70).

Wang, Lingli and John J. Qu. 2009. “Satellite Remote Sensing Applications for Surface Soil Moisture Monitoring: A Review.” Frontiers of Earth Science in China 3(2):237–47. Retrieved January 16, 2014 (http://link.springer.com/10.1007/s11707-009-0023-7).

Wickham, J. D., K. H. Riitters, T. G. Wade, M. Coan, and C. Homer. 2007. “The Effect of Appalachian Mountaintop Mining on Interior Forest.” Landscape Ecology 22(2):179–87.

Wyrick, Granville G. and James W. Borchers. 1981. Hydrologic Effects of Stress-Relief Fracturing In an Appalachian Valley. Alexandria, VA.

Zegre, Nicolas P., Andrew J. Miller, Aaron Maxwell, and Samuel J. Lamont. 2014. “Multiscale Analysis of Hydrology in a Mountaintop Mine-Impacted Watershed.” Journal of the American Water Resources Association 50(5):1257–72.

5.0 CONCLUSIONS AND SYNTHESIS

Humans depend on forest systems to maintain the health and safety of urban environments. However, human impacts on forests through urbanization and industrialization, impacts that degrade forest benefits, occur across broad spatial scales. Therefore, to document forest response to urbanization, a multiple scale analytical framework is essential. This dissertation addressed significant challenges in our ability to detect human impacts on forests, predict changes in landslide risks following the loss of urban forests, and understand the coupling between hydrologic change and forest change in urban and industrial systems.

The role of forests in urban hydrological processes has an extensive literature, but impacts of urban hydrological change on forests remain poorly documented (Pfeil-McCullough et al. 2015; Livesley et al. 2016). Chapter 2 characterizes forest transformation in Pittsburgh, PA since European settlement (and subsequent urbanization) through a comparison of pre-settlement forests to three surveys of contemporary forests. Comparisons between historic and contemporary forests revealed shifts in species type within the urban datasets assumed to arise from soil moisture preferences (i.e., wetland indicator species (WIS) designation). Specifically, shifts in WIS distributions toward higher proportions of species preferring both wetter and drier conditions relative to the historic dataset, indicate more spatial heterogeneity in modern soil moisture. Further, these shifts are observed at unexpected landscape positions. For example, trees that prefer wetter soil conditions are present near ridges, areas that are expected to be well drained and therefore drier. Shifts in WIS categories also varied with the forest history (i.e., parks, urban woodlands, or street trees), confirming urban hydrology, management, and spatial constraints interact to influence patches of urban forests differently. Overall, shifts in forest species suggest that urbanization-driven hydrological change creates new landscape conditions that ultimately change the spatial distribution of tree species and therefore the mix of species in urban forests. However, even with major changes in species composition between historic and contemporary forests, there was surprising consistency in the soil moisture preferences of the trees in the forest. So while urbanization can increase heterogeneity in hydrological processes, the functional traits of historic forests are persistent and continue to influence contemporary forests.

These urban forests are especially important in cities with topographic relief, as vegetation is a primary control on slope stability (Ekanayake and Phillips 2002; Pfeil-McCullough et al. 2015). Chapter 3 exposes a fundamental truth in spatial patterns of trees in urban systems: they often coincide with hillslope positions that are too steep to develop. Therefore, they add important stability to hillslopes and rapid tree loss can be particularly devastating to urban systems. Increases in landslide susceptibility were predicted in Pittsburgh based on several scenarios of ash loss to the emerald ash borer (EAB), a bark beetle that rapidly kills ash trees. Chapter 3 expands on available urban forestry tools (e.g. iTree, (Davey Resource Group 2012)) by applying a hillslope stability model (SINMAP) to predict spatially explicit changes in urban landslide susceptibility following EAB losses. This model provides the means to predict changes in landslide susceptibility following tree loss (e.g., other forest pathogens such as the Asian longhorn beetle) and increase the understanding of urban forest function and its role in slope stability.

Finally, urbanization impacts forests in many ways, including forests far outside the city. Chapter 4 reveals previously uncharacterized impacts of longwall mine subsidence (LMS) to forest health. Though LMS impacts are detectable at small spatial scales, hydrological changes are difficult to assess at the broad spatial scales over which longwall mining occurs. By using readily available Landsat imagery and hot spot analysis tools, declines in forest canopy moisture were detected over longwall mines as mining progressed through time. Specifically, the results indicate that areas where longwall mining had occurred two decades ago were relatively drier than the rest of the study area, contradicting conceptual models of “self-healing” (the assumption that the hydrological impacts overlying LMS recover within 4-5 years following subsidence (Iannacchione et al. 2008)). The distinct patterns in canopy moisture on LMS impacted hillslopes provides evidence documenting how LMS impacts interact with existing hydrological flow paths to reroute shallow groundwater flow crucial to hillslope hydrologic regimes. The results of this chapter provide new insight into longwall mining impacts in high relief areas, particularly important but hard to measure changes to soil moisture following subsidence.

Hydrological processes and forest ecosystems are closely linked, allowing for the use of forests as a proxy for hydrological change following the urbanization and industrialization of southwestern Pennsylvania. This relationship between forests and hydrology allows assessment of difficult to detect urban hydrological changes at broad spatial scales. This dissertation advances our ability to characterize changes in soil moisture patterns and forest function at the landscape scale. Results from this dissertation will ultimately allow improvements in the management and protection of both trees and water resources in urban systems and beyond.

5.1 BIBLIOGRAPHY

Davey Resource Group 2012. Pittsburgh Urban Forest Master Plan: A Roadmap for the Effective Management of Our Urban Forest. , p. 78. Available at: http://treepittsburgh.org/urban-forest-master-plan.

Ekanayake, J.C. and Phillips, C.J. 2002. Slope stability thresholds for vegetated hillslopes: a composite model. Canadian Geotechnical Journal 39(4), pp. 849–862.

Pfeil-McCullough, E., Bain, D.J., Bergman, J. and Crumrine, D. 2015. Emerald ash borer and the urban forest: Changes in landslide potential due to canopy loss scenarios in the City of Pittsburgh, PA. The Science of the Total Environment 536, pp. 538–545.